STUDIES ON THE TREATMENT OF WASTEWATERS CONTAINING Cr^{6+} WITH IRONOXIDE-SILICA COMPOSITE MATERIALS PREPARED BY DIFFERENT METHODS

A dissertation submitted in partial fulfillment of the requirements for the degree of M.Phil. in Chemistry

By

Biplob Kumer Deb
Registration No. 100703207P
Roll No. 100703207P
Session: October,2007

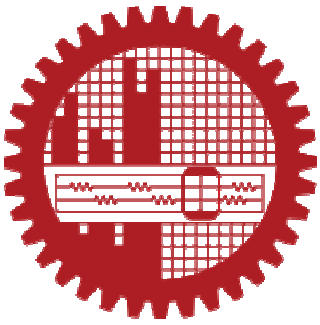

Physical Chemistry Research Laboratory
Department of Chemistry
BANGLADESH UNIVERSITY OF ENGINEERING AND TECHNOLOGY,
DHAKA. Bangladesh.
June,2012.

CANDIDATE'S DECLARATION

It is hereby declared that this thesis or any part of it has not been submitted elsewhere for the award of any degree or diploma.

.....

(Signature of the student)

Biplob Kumer Deb.

Name of the candidate

Bangladesh University of Engineering and Technology, BUET, DHAKA .
Department of Chemistry

Certification of Thesis

A thesis on

STUDIES ON THE TREATMENT OF WASTEWATERS CONTAINING Cr^{6+} WITH IRONOXIDE-SILICA COMPOSITE MATERIALS PREPARED BY DIFFERENT METHODS

SUBMITTED BY
BIPLOB KUMER DEB
Roll No. : 100703207P, Session : October 2007

has been accepted as satisfactory in partial fulfillment of the requirements for the degree of Master of Philosophy (M.Phil) in Chemistry on June 09, 2012

Board of Examiners

1. **Dr. Md. Rafique Ullah**
   Professor
   Department of Chemistry,
   BUET, Dhaka
   (Supervisor)
2. **Dr. Mohammad Yousuf Ali Mollah**
   Professor
   Department of Chemistry
   University of Dhaka.
   (Co-Supervisor)
3. **Dr. Shakila Rahman**
   Professor & Head
   Department of Chemistry, BUET, Dhaka.
4. **Dr. Al Nakib Chowdhury**
   Professor
   Department of Chemistry, BUET, Dhaka.
5. **Dr. Omar Ahmed**
   Professor
   Department of Chemistry
   University of Dhaka.

Dedicated
To
My Beloved Parents

Acknowledgements

I am pleased to express my deep sense of gratitude and sincere appreciation to my reverend supervisor Professor Md. Rafique Ullah, M.Sc.(Chittagong), Ph.D. (India), Department of Chemistry, Bangladesh University of Engineering and Technology and co-supervisor Professor Mohammad Yousuf Ali Mollah, M.Sc. (Dhaka), Ph.D. (Macquari, Australia), Department of Chemistry, University of Dhaka, Bangladesh for their supervision and guidance at every stage of this study.

I am especially grateful to Dr. Shakila Rahman, Chairman, Department of Chemistry, Bangladesh University of Engineering and Technology, Dhaka for allowing me to undertake this research in the Department of Chemistry of BUET.

I wish to thank Professor Dr. Al-Nakib Chowdhury, Department of Chemistry, Bangladesh University of Engineering and Technology, Dhaka for his help and valuable suggestions during the research work.

My heartiest thanks to Professor Wahab Khan, Department of Chemistry, Bangladesh University of Engineering and Technology, Dhaka for his help in taking FT-IR and valuable guidance .

I sincerely thank Fr. Benjamin Costa, C.S.C., Principal, Notre Dame College, Dhaka for permission to carry out my research work , without which I could not complete my thesis work. I am thankful to Mr. A.C. Das Talukdar, ex-Chairman, Department of Chemistry, Notre Dame College, Dhaka for his support .

I am deeply grateful to my colleagues, Mr. Sanjit Kumar Guho, Mr. Promod Allen Gomes , Mr. Sushil Ekka , Mr. Bodruzzaman and Mr. Mahmud for their support and encouragement .

I would gratefully remember loving younger brothers Anup, Sohel and Ramakrishna for their help and valuable suggestions throughout my work.

A few words of acknowledgements will never be sufficient to express my deepest sense of gratitude to my wife Rakhi for her continuous inspiration and mental support during this research work. My heartfelt thanks to my family members also.

Biplob Kumer Deb.

TABLE OF CONTENTS

List of Tables

List of Figures

Abstract

Chromium is found in many forms, but Cr(VI) is known to be carcinogenic to humans. It is important to ensure the removal of Chromium (VI) from aqueous solutions and industrial effluents.

Among the known methods for removing chromium from aqueous solutions, adsorption is an important method based on the ability of some porous materials to bind chromium to their surfaces. In order to improve the efficiency of this process a variety of new synthetic materials have been investigated.

In the present work a novel method for preparing Fe_2O_3-SiO_2 composite materials is presented. Iron (III) oxide was prepared by electrochemical method. SiO_2 was prepared by acid hydrolysis of the tetraethylorthosilicate (TEOS). A relatively slow rate of hydrolysis of the TEOS occurred during the process, which resulted in larger silica particles with a narrower size distribution.

This study shows the influence of the type of silica matrix on the structure, size, and distribution of the Fe_2O_3 particles in the Fe_2O_3-SiO_2 systems. The gels were annealed at 550°C in order to consolidate the matrices. The structural characterization of the synthesised materials was performed by X-ray diffraction, FT-IR, Scanning Electron Microscopy (SEM), EDS and DTA/TGA analysis. The present study introduces a good alternative method for Cr (VI) removal from aqueous solutions by adsorption, allowing the development of newer, lower operational cost, and more efficient technology than other processes already in use. Adsorption was found to be dependent on pH and initial concentration of Cr(VI) solution. Results of adsorption studies suggest that pristine iron

oxide and silicon (IV) oxide removes 72.10% and 24.73% respectively. The iron oxide – silicon (IV) oxide composite, prepared in this work, removes 93.88% Cr(IV) from aqueous solution. Therefore, it can be concluded that iron oxide – silicon (IV) oxide composite is a potential adsorbent for adsorption of Cr(VI) from aqueous solution. Studies of the sorption kinetics show that equilibrium adsorption was attained in 20 minutes depending on other experimental conditions. The kinetic data justified Lagergren first-order kinetic equation. Adsorption isotherm study showed that the results fulfilled the Langmuir Model of adsorption isotherm.

Introduction

1.1 Wastewater

Water is an invaluable resource. It is essential for all living organism. It is known that 3/4th of the surface of the earth is covered with water (**Figure 1.1**).

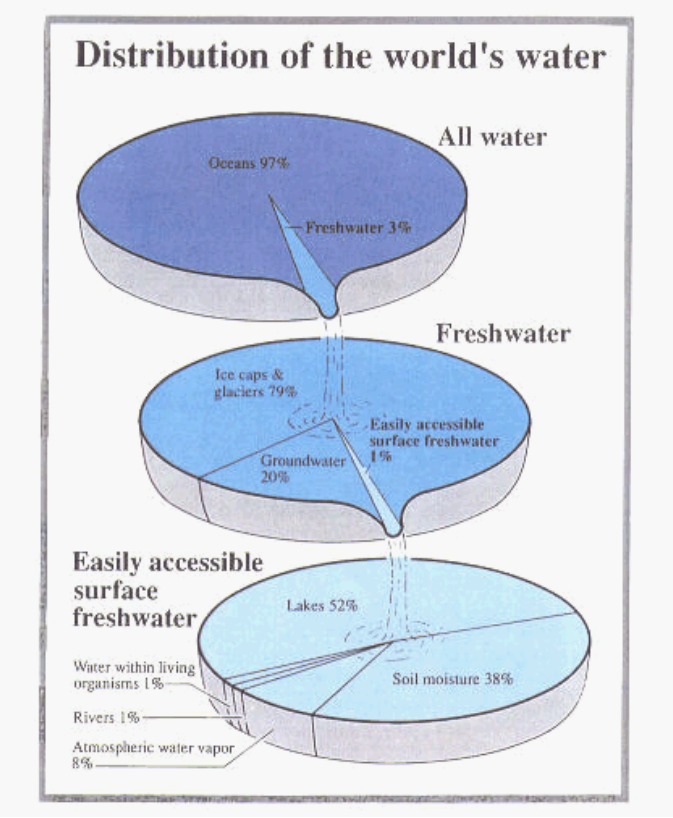

Figure 1.1: Distribution of the world's water

Only 3% of this water is freshwater and 1% of which is easily accessible surface freshwater. The remaining 20% is groundwater and 79% covers ice caps and glaciers. With growing population and increasing industrialization this easily accessible 1% water is constantly being polluted.

The polluted water , also known as wastewater , indicates a combination of one or more of : domestic effluent consisting of black water (excreta, urine and faecal sludge) and grey water (kitchen and bathing wastewater); water from commercial establishments

and institutions, including hospitals; industrial effluent, storm water and other urban run-off; agricultural, horticultural and aquaculture effluent, either dissolved or as suspended matter[1]. Wastewater may also refer to any water that is utilized in an agricultural facility and is no longer considered fit for human consumption. Groundwater that is contaminated due to a leaking septic tank or agents such as insecticide, petroleum products, blood, or cleaning liquids can also be referred as wastewater.

The quality of wastewater can be determined by studying the following physical parameters[2] :

Temperature (which affects rates of chemical and biochemical reactions)

Viscosity

Solubility of gases

Odour

Colour

Solids

The chemical quality of wastewater can be determined by studying the following[2]:

pH

Alkalinity

Chlorides

Various forms of nitrogen

Phosphorous

Sulfur

Heavy metals

Toxic substances

Gases

Above all, tests like BOD, COD, and TOC (which are used to estimate the organic content either directly or indirectly as oxygen consumed by organic matter).

1.2 Origin of wastewater[2]

Wastewater or sewage can come from :

- Human waster (faeces, used toilet paper or wipes, urine, or other bodily fluids), also known as black water, usually from lavatories;
- Cesspit leakage;
- Septic tank discharge;
- Sewage treatment plant discharge;
- Washing water (personal, clothes, floors, dishes, etc.), also known as grey water or sullage;
- Rainfall collected on roofs, yards, hard-standings, etc. (generally clean with traces of oils and fuel);
- Groundwater infiltrated into sewage;
- Surplus manufactured liquids from domestic sources (drinks, cooking oil, pesticides, lubricating oil, paint, cleaning liquids, etc.);
- Urban rainfall runoff from roads, car parks, roofs, sidewalks, or pavements (contains oils, animal fæces, litter, fuel or rubber residues, metals from vehicle exhausts, etc.);
- Seawater ingress (high volumes of salt and micro-biota);

- Direct ingress of river water (high volumes of micro-biota);
- Direct ingress of manmade liquids (illegal disposal of pesticides, used oils, etc.);
- Highway drainage (oil, de-icing agents, rubber residues);
- Storm drains (almost anything, including cars, shopping trolleys, trees, cattle, etc.);
- Black water (surface water contaminated by sewage);
- Industrial waste
- Industrial site drainage (silt, sand, alkali, oil, chemical residues);
- Industrial cooling waters (biocides, heat, slimes, silt);
- Industrial process waters;
- Organic or bio-degradable waste, including waste from abattoirs, creameries, and ice cream manufacture;
- Organic or non bio-degradable/difficult-to-treat waste (pharmaceutical or pesticide manufacturing);
- extreme pH waste (from acid/alkali manufacturing, metal plating);
- Toxic waste (metal plating, cyanide production, pesticide manufacturing, etc.);
- Solids and Emulsions (paper manufacturing, foodstuffs, lubricating and hydraulic oil manufacturing, etc.);
- Agricultural drainage, direct and diffuse.

1.3 Wastewater constituents[2]

The composition of wastewater varies widely. This is a partial list of what it may contain:

- Water (> 95%) which is often added during flushing to carry waste down a drain;
- Pathogens such as bacteria, virus, prions and parasitic worms;
- Non-pathogenic bacteria;

- Organic particles such as faeces, hairs, food, vomit, paper fibers, plant material, humus, etc.;
- Soluble organic material such as urea, fruit sugars, soluble proteins, drugs, pharmaceuticals, etc.;
- Inorganic particles such as sand, grit, metal particles, ceramics, etc.;
- Soluble inorganic material such as ammonia, road-salt, sea-salt, cyanide, hydrogen sulphide, thiocyanates, thiosulphates, etc.;
- Animals such as protozoa, insects, arthropods, small fish, etc.;
- Macro-solids such as sanitary napkins, nappies/diapers, condoms, needles, children's toys, dead animals or plants, etc.;
- Gases such as hydrogen sulfide, carbon dioxide, methane, etc.;
- Emulsions such as paints, adhesives, mayonnaise, hair colourants, emulsified oils, etc.;
- Toxins such as pesticides, poisons, herbicides etc.
- Heavy metals: Municipal wastewater also contains a variety of potentially toxic elements such as arsenic, cadmium, chromium, copper, lead, mercury, zinc, etc.

1.4 Surface Water Pollution in Bangladesh[3,4,5,6,7]

Bangladesh has about 230 small and large rivers, and a large chunk of the country's 140 million people depend on them for a living and for transportation. Surface water occurs in rivers, lakes, ponds and floodplains. It has been the source of water supply since the dawn of civilization. But intense human activities have been polluting these readily available sources. Surface water used to be the primary source of water supply in Bangladesh, but it is no longer the case. Surface water in Bangladesh is extensively polluted by sources

such as industrial and urban wastes, agrochemicals and sewerage wastes and seawater intrusion. Surface water bodies are extensively used for disposal of untreated industrial wastes and this is one of the main sources of pollution. The Buriganga is a typical example of serious surface water contamination. Apart from industrial sources, surface water in the country is also extensively contaminated by human faeces as sanitation in general is poor. Agrochemicals are extensively used in the country causing pollution of surface water. Due to withdrawal of water from the Ganges, sea water intrudes a long way inside the coastline which causes river water pollution by salinity. A World Bank study said four major rivers near Dhaka -- the Buriganga, Shitalakhya, Turag and Balu -- receive 1.5 million cubic metres of waste water every day from 7,000 industrial units in surrounding areas and another 0.5 million cubic meters from other sources[3(b)].Unabated encroachment that prevents the free flow of water, dumping of medicinal waste and waste of river passengers have compounded the problem, making the water unusable for humans and livestock. There are also other minor sources that contaminate surface water extensively.

Industrial discharges along with municipal and urban wastes are creating special problems that completely destroy the microbial-based systems of decomposition. About 7,000 large and medium industries and 24,000 small industries are operating in Bangladesh which discharge effluents directly to the rivers or nearby canal or waterbed without any regard to environment. A recent study, jointly done by the World Bank and the Institute of Water Modelling (IWM, BUET), shows the pollution level in the Buriganga, Shitalakshya, Balu and most parts of the Turag so high that simply no living

organism can survive in their waters[8]. A review of the surface water pollution of different rivers of Bangladesh is discussed below:

Pollution in Buriganga River: The once mighty Buriganga river, which flows by Dhaka, is now one of the most polluted rivers in Bangladesh because of rampant dumping of industrial and human waste. Dhaka City is very densely populated and considered to be one of the ten 'Mega Cities' of the world. However, only a small fraction of the total wastewater being generated in the city is treated. Consequently, the amount of untreated wastes, both domestic and industrial, being released into the Buriganga is tremendous and is increasing day by day. The river is seriously polluted by discharge of industrial effluents into river water, indiscriminate throwing of household, clinical, pathological & commercial wastes, and discharge of fuel and human excreta. In fact, the river has become a dumping ground of all kinds of solid, liquid and chemical waste of bank-side population. These activities on the Buriganga have caused narrowing of the river and disruption of its normal flow of water. The water of the river has become so polluted that all fish have died, and increasing filth and human waste have turned it like a black gel. Even rowing across the river is now difficult for bad smells. People, living near the rivers, use the water because they are unaware of the health risks and also having no other alternative. This causes incidents of water borne and skin diseases. Located in the capital city of Bangladesh, Dhaka, the densely populated Hazaribagh tanning industrial zone constitutes 90% of the total 270 tanneries in the country. Approximately15000 m^3 of untreated chemical wastes are discharged to the low-lying areas, natural canals and other water bodies such as the Buriganga and Turag rivers, which are major sources of water supply for agricultural, livestock and fishing activities[9]. Chrome tanning is the most

common type of tanning where large amounts of chrome powder and liqueur are used[10] . Furthermore, several other studies have been undertaken describing the pollution state of the Hazaribagh area[11] .

A study on the ecotoxicological characterization of tannery wastes of Bangladesh[12] shows that the degree of environmental hazard in this particular area of Hazaribagh is high. It was suggested that elevated concentrations of heavy metals may be posing a considerable risk to the ecosystem surrounding the tanneries. It has been previously suggested that the presence of chromium in the environment can cause detrimental human and environmental effects[13] . This study provides biological evidence that the tannery wastewater of the area of Hazaribagh exhibits detrimental impacts on broad aquatic and land organisms, which in turn destruct the ecosystem.

About 12 sq. km area of Hazaribag and adjacent area are full of offensive odors of various toxic Chemicals: hydrogen sulphide, ammonia, poisonous chlorine and several nitrogen based gases to mention a few. According to an expert, ‘‘an average of 19 cubic liter water containing more than 300 different chemical compounds is being discharged daily from these industries.” The relative acidity or alkalinity of this liquid toxic waste flown through the drainage system has been observed as between 1-14 not only that, traces of chemical elements also remain. Detergent increases the pH level in water.

According to a recent estimate, about 70,000 tons of raw hides and skins are processed in these tanneries every year polluting the environment and the quantity of untanned solid wastes namely raw trimming, we lime fleshing, pelt trimming generated in these tanneries is estimated to be 28,000 tons. Statistics provided by various sources suggest

that a big tannery of the Hazaribagh area releases 2,500 gallons of chemicals wastes each day, polluting the city's air in addition to contaminating the water of the river Buriganga. Effluents and solid waste generated at different steps of leather processing trekking through the low-lying area of Hazaribagh contaminated by chromium, the old wounds take a longer time to heal. Long term chromium contamination may cause cancer. Laboratory tests carried out by DOE (Department of Environment) shows that chromium, a carcinogenic agent, has seeped into the aquifer at some places of Hazaribagh flow into the Buriganga River. Liquid waste is contaminating the waters of the Buriganga River on the surface as well as the ground water resource base. During the lean season, the Buriganga River turns deadly for fish and other sub aquatic organisms. When solid waste and effluents run into the river, the Biological Oxygen Demand (BOD) in the water rises, creating oxygen is calamitous for the sub aqueous life. Among others, effluents of tannery factories lower the dissolved oxygen (DO) content of the river water below the critical level of four milligrams per liter.

Sitalakhya River: Besides wastes from Dhaka urban population, the river Sitalakhya, receives untreated industrial wastes from urea fertilizer plants, textile mills and other industries. The principal polluting agent in the region is the Urea Fertilizer Factory of Ghorasal and the concentration of ammonia dissolved in water has increased over time causing fish-kills. The waters of Sitalakhya river are so stinky and polluted that hardly any fish or other aquatic life form could survive there[3(b)].

Balu River: The River near Tongi (15 miles north of Dhaka) receives untreated effluents from industries such as textiles, lead batteries, pulp and paper, pharmaceuticals, paints, detergents, iron and steel, rubber etc.

Turag River: The waters of this river is affected by industrial effluents and wastewater. The waters are also affected by municipal sewage disposal contamination, agro chemicals and large amount of suspended sediments carried by upstream flow. A study, jointly done by the World Bank and IWM of BUET , showed that the oxygen levels were 0.27 ppm and 0.63ppm in the Turag in Tongi before and after the monsoon respectively[9].

Bhairab/Rupsa Rivers: The principal industries of Khulna (south-east of Bangladesh) are jute mills, oil mills, newsprint mills, cable, shipyards, tobacco, match factories, hardboard and others dispose molasses, starch, oil, sodium-sulphide, ethane, lissapol, soda ash, dye, sulphuric acid, salicylic acid, lime, ammonium sulphide, and chrome etc. A few studies at Bhairab River show a very alarming water quality data (Nov.-April 1988-89) - conductivity a 390-9500 Micro-mhos/cms, total solid 260-3500 mg/L, TDS 260-3200 mg/L. The pollution aspects of Bhairab and Rupsa Rivers is very critical – the Rupsa River does not receive continuous flow of fresh water from the parent river, on the other hand, the Bhairab River, being subject to tides, has marked backwater effects which reduce the purification capacity of the river. Some 300 industries are located in and around Khulna City currently discharge huge amount of liquid waste into the river Bhairab. These pollutants may be contributing to the “top dying” disease of the tress in the Sunderbans in addition to causing serious damage to both freshwater and marine ecosystems[3(d)].

Karnaphuli River: The polluting industries of Chittagong, the second largest city of Bangladesh, are 19 tanneries, 26 textile mills, 1 oil refinery, 1 TSP plant, 1 DDT plant, 2 chemical complexes, 5 fish processing units, 1 urea fertilizer factory, 1 asphalt bitumen plant, 1 steel mill, 1 paper mill (solid waste disposal hourly 1450 m^3), 1 rayon mill

complex, 2 cement factories, 2 pesticide manufacturing plants, 4 paint and dye manufacturing plants, several soap and detergent factories and a number of light industrial units directly discharge untreated toxic effluent into Karnaphuli river. Even 1.5 lakh litre of crude waste from the tannery industries and 35 tons of China clay, four tons of fibres from KPM and Karnaphuli Rayon Mills are dumped into the river and directly falls into the coastal and marine water every day[3(e)]. The amount of waste dumped into the river Karnaphuli would have turned it into a dead river many years ago, but it is still alive because of its tidal flow. From the survey of effluents from different industries, it has been found that the discharge is generally composed of organic and inorganic wastes. The organic wastes are the effluents from the tanneries, fish processing units, degradable wood chips, pulps and untreated municipal and sewage (about 40,000 kg BOD daily) etc. The inorganic wastes are chemicals used by the industries such as various acids, bleaching powder, lissapol, hydrogen peroxide, alkali, salts, lime, dyes, pigments, aluminium-sulphate and heavy metals etc. The DDT factory and fertilizer factory disposing of DDT, toxic chemicals and heavy metals to the Karnaphuli River and ultimately to the Bay of Bengal. Some survey shows that about 220 ppm of chromium, 0.3-2.9 ppm of cadmium, 0.05-0.27 ppm of mercury, 0.5-21.8 ppm of lead entering river and sea water much higher than allowable limits and extremely alarmingly to aquatic flora and fauna and through food chains to human beings. It may be mentioned that Bangladesh obtain table salt from solar drying of sea water and consequently increasing pollution of sea water which will create a serious national health hazard situation.

The organic pollutants are both biodegradable and non-biodegradable in nature. The biodegradable organic components degrade water quality during decomposition by

depleting dissolved oxygen. The non-biodegradable organic components persist in the water system for a long time and pass into the food chain . Inorganic pollutants are mostly metallic salts, and basic and acidic compounds. These inorganic components undergo different chemical and biochemical interactions in the river system, and deteriorate water quality[14].

1.5 Sources of Chromium in wastewater

Chromium does not occur freely in nature. The main chromium mineral is chromite. Chromium compounds can be found in waters only in trace amounts. Wastewater usually contains about 5 ppm of chromium. The element and its compounds can be discharged in surface water through various industries. For example, it is applied for metal surface refinery and in alloys. Stainless steel consists of 12-15% chromium. Chromium metal is applied worldwide in amounts of approximately 20,000 tons per year. The major sources of chromium in wastewater are-

(i) The metal industry mainly discharged trivalent chromium.

(ii) Hexavalent chromium in industrial wastewaters mainly originates from tanning and painting.

(iii) Chromium compounds are applied as pigments, and 90% of the leather is tanned by means of chromium compounds.

(iv) Chromium may be applied as a catalyser, in wood impregnation, in audio and video production and in lasers.

(v) Chromite is the starting product for inflammable material and chemical production.

(vi) Chromium may be present in domestic waste from various synthetic materials.

(vii) Through waste incineration it may spread to the environment when protection is insufficient.

(viii) In nuclear fission the ^{51}Cr isotope is released, and this can be applied for medical purposes.

1.6 Chromium in the environment

Chromium exists in food, air, water and soil, mostly in the Cr (III) form. It is only as a result of human activities that substantial amounts of Cr (VI) are present in the environment. Cr (III) is comparatively insoluble while Cr (VI) is quite soluble and is readily leached from soil to groundwater or surface water.

1.7 Environmental effects of chromium[15]

There are several different kinds of chromium that differ in their effects upon organisms. Chromium enters into air, water and soil in the chromium(III) and chromium(VI) form through natural processes and human activities[16]. Chromium is a dietary requirement for a number of organisms. This however only applies to trivalent chromium. Hexavalent chromium is very toxic to flora and fauna[17].

Chromium in phosphates used as fertilizers may be an important source of Cr in soil, water and some foods[17] .The main human activities that increase chromium(VI) concentrations are chemical, leather and textile manufacturing, electro painting and other chromium(VI) applications in the industry[18,19]. These applications will mainly increase concentrations of chromium in water. Chromium water pollution is not regarded one of the main and most severe environmental problems, although discharging chromium

polluted untreated wastewater in rivers has caused environmental disasters in the past. Chromium is largely bound to floating particles in water.

Chromium (VI) compounds are toxic at low concentrations for both plants and animals. The mechanism of toxicity is pH dependent. These compounds are more mobile in soils than chromium (III) compounds, but are usually reduced to chromium (III) compounds within a short period of time, reducing mobility. Soluble chromates are converted to insoluble chromium (III) salts and consequently, availability for plants decreases. This mechanism protects the food chain from high amounts of chromium. Chromate mobility in soils depends on both soil pH and soil sorption capacity, and on temperature. The guideline for chromium in agricultural soils is approximately 100 ppm. Chromium naturally has four stable isotopes and eight unstable isotopes. The ^{51}Cr, which is applied for diagnosis purposes, has an average degree of radioactivity.

Chromium is not known to accumulate in the bodies of fish, but high concentrations of chromium, due to the disposal of metal products in surface waters, can damage the gills of fish that swim near the point of disposal[20]. In animals, chromium can cause respiratory problems, a lower ability to fight disease, birth defects, infertility and tumor formation[21].Adverse effects of Cr to sensitive species have been documented at 10.0 ug/L (ppb) of Cr(VI) and 30.0 ug/L of Cr(III) in freshwater and 5.0 ug/L of Cr(VI) in saltwater and to, wildlife, 5.1 and 10.0 mg of Cr(VI) and Cr(III), respectively, per kilogram of diet (ppm).

Environmental effects of Chromium have been extensively reviewed[16,17,18,19,21,22,23,24,25] . These authorities agreed that Cr is used widely in domestic

and industrial products and the some of its chemical forms, primarily hexavalent chromium and trivalent chromium are toxic. Reports from Europe, Scandinavia, Asia and North America all emphasize the high incidence of lung cancer and other respiratory diseases among the workers involved in the manufacture of chromates. Others document that land dumping of wastes from chromate production and electroplating operations have been responsible for groundwater contamination that discharge of Cr wastes into streams and lakes has caused damage to aquatic ecosystem and accidental poisoning of livestock ; and that large amounts of Cr(VI) and Cr(III) are reintroduced into the environment as sewage and solid wastes by the disposal of consumer products containing chromium.

Chromium toxicity to aquatic biota is significantly influenced by abiotic variables such as hardness, temperature, pH, and salinity of water and biological factors such as species, life stage and potential differences in sensitive of local populations[19] .In both freshwater and marine environments, hydrolysis and precipitation are the most important processes that determine the fate and effects of Chromium, whereas adsorption and bioaccumulation are relatively minor[19] . Ciavatta, et al.[26] reported that toxicity of chromium (III) to mammals and aquatic organisms appears to be lower compared to Cr(VI) due to lower solubility of its compounds.

Hexavalent chromium is well known for its high toxicity[27].Since hexavalent chromium species are classified as carcinogens, mutagens, dermatogens in biological systems[28], its species pose severe threat to public health and environment if discharged without adequate treatment[29]. USEPA recommends that the levels of chromium in water

should be reduced to 0.1 mgL^{-1} [30] The maximum permitted Cr(VI) in the U.K. is currently set up at 50 μgdm^{-3} with Cr(III) set as 1000 μgdm^{-3} [31] . For compliance with this limit, it is imperative for industries to reduce the chromium in their effluents to an acceptable level before discharging into municipal sewers.

1.8 Human Exposure of Chromium

People can be exposed to chromium through breathing, eating or drinking and through skin contact with chromium or chromium compounds. The level of chromium in air and water is generally low. In drinking water the level of chromium is usually low as well, but contaminated well water may contain the dangerous chromium(VI); hexavalent chromium. The human body contains approximately 0.03 ppm of chromium. Daily intake strongly depends upon feed levels, and is usually approximately 15-200 µg, but may be as high as 1 mg. Chromium uptake is 0.5-1%, in other words very small. For most people eating food that contains chromium(III) is the main route of chromium uptake, as chromium(III) occurs naturally in many vegetables, fruits, meats, yeasts and grains. Various ways of food preparation and storage may alter the chromium contents of food. When food is stored in steel tanks or cans, chromium concentrations may rise.

The placenta is the organ with the highest chromium amounts. Trivalent chromium is an essential trace element for humans. Together with insulin it removes glucose from blood, and it also plays a vital role in fat metabolism. But the uptake of too much chromium(III) can cause health effects as well, for instance skin rashes.

1.9 Health Effect of Chromium[15]

Chromium(VI) is a danger to human health[32], mainly for people who work in the steel and textile industry. People who smoke tobacco also have a higher chance of exposure to chromium.

Chromium(VI) is known to cause various health effects. When it is a compound in leather products, it can cause allergic reactions, such as skin rash[33] . After breathing it in chromium(VI) can cause nose irritations and nosebleeds. Other health problems that are caused by chromium(VI) are:

- Skin rashes
- Upset stomachs and ulcers
- Respiratory problems
- Weakened immune system
- Kidney and liver damage
- Alteration of genetic material
- Lung Cancer
- Death

Effects on the cardiovascular, respiratory, gastrointestinal, hematological, hepatic and renal systems are observed in humans who die after ingestion of large amounts of Chromium (VI)[33]. Ellis et al. 1982 reported that a 22 month old boy died of cardiopulmonary arrest after ingesting an unknown amount of sodium dichromate. Ingestion by humans of Cr(VI) in drinking water or diet has been shown to have chronic

effects like leukocytosis and immature neutrophils[34] . According to the World Health Organization (WHO) drinking water guidelines, the maximum allowable limit for total chromium is 0.05 mg/L. A cross sectional epidemiological studies have been conducted on villagers in China who consumed water from wells contaminated with 20 ppm Cr(VI) were experienced oral ulcer, diarrhea, abdominal pain, indigestion and vomiting[34] . Chromium is not listed under Proposition of 65 [35] as a chemical known to the state to cause reproductive or developmental harm.

The health hazards associated with exposure to chromium are dependent on its oxidation state. The metal form (chromium as it exists in this product) is of low toxicity. The hexavalent form is toxic. Adverse effects of the hexavalent form on the skin may include ulcerations, dermatitis, and allergic skin reactions. Inhalation of hexavalent chromium compounds can result in ulceration and perforation of the mucous membranes of the nasal septum, irritation of the pharynx and larynx, asthmatic bronchitis, bronchospasms and edema. Respiratory symptoms may include coughing and wheezing, shortness of breath, and nasal itch.

Carcinogenicity- Chromium and most trivalent chromium compounds have been listed as having inadequate evidence for carcinogenicity in experimental animals. There is sufficient evidence for carcinogenicity in experimental animals for the following hexavalent chromium compounds; calcium chromate, chromium trioxide, lead chromate, strontium chromate, and zinc chromate. Occupational exposures to chromium (VI) in the dichromate production industry over a period from the 1930s to the 1980s has been shown in numerous epidemiological studies to be correlated with increased risk of

respiratory cancers (cancers of the lungs and respiratory tract)[33] . Thus Cr(VI) is a known human carcinogen by the inhalation route[33,36,37].International Agency for Research on Cancer (IARC) has listed chromium metal and its trivalent compounds within Group 3 (The agent is classifiable as to its carcinogenicity to humans)[38]. In the same year, American Conference of Governmental International Hygienists (ACGIH) has classified chromium metal and trivalent chromium compounds as A4, (Confirmed human carcinogen) [39].Because of the epidemiological evidence, and because chromium (VI) is converted to Chromium(III) in the gastric environment, some reviewers doubt that chromium(VI) would be carcinogenic by the oral route[40]. The reduction of chromium(VI) to chromium(III) in the gastric environment would not preclude the possibility that chromium (VI) could produce tumors in the stomach. Others have argued strongly that chromium(VI) should be regarded as carcinogenic by the oral route. Costa (1997)[41] reviewed evidence that supports the conclusion that hexavalent chromium is taken up by the GI tract and transported to all tissues of the body. He also reviewed epidemiological evidence that exposure to hexavalent chromium causes increased risk of cancer in bone, prostate, stomach and other organs.

1.10 Basic Chemistry of Chromium[15]

Chromium, which was discovered by Louis Vaquelin in 1797, is the 24th element in the periodic table and it is found in about 0.0122% of the Earth's crust. It is named after the Greek word "c*hroma*," meaning color. This element produces many beautifully colored compounds, as well as a wide array of colored solutions. When Chromium (Cr) is in the crystalline form, it is a steel-gray,lustrous,hard metal . It is characterized by an atomic weight of 51.996, an atomic number of 24, a density of 7.14, a melting point of

1900^0C and a boiling point of 2642^0C. Naturally four Chromium isotopes occurs. They are Cr-50(4.3%), Cr-52(83.8%), Cr-53(9.6%) and Cr-54(2.4%) . There are eight manmade isotopes. Elemental Chromium is very stable but is not usually found pure in nature.

Trivalent (+3) and hexavalent (+6) oxidation states are frequently observed in nature but Chromium can exist in oxidation states ranging from -2 to +6. The most important forms of Chromium are +3 and +6 because the +2,+4 and +5 forms are unstable and are rapidly converted to +3, which in turn is oxidized to +6[17,18,19]. In soil and natural water, the stable forms of chromium ,Chromium (III) and Chromium (VI) , are observed.

Most compounds prepared from chromite ore contain chromium in the more stable +3 and +6 states. Chromium is in one of these two oxidation states in all the important chromium compounds. Due to low membrane permeability and non-corrosive property, the toxicity of trivalent chromium to mammals is low . There is a little tendency for chromium(III) to bio-magnify in food chain in the inorganic form. However, different accumulation tendencies are shown by the organo-trivalent chromium compounds .

Hexavalent Chromium, Cr(VI)

Hexavalent chromium, also known as chromium 6, is a heavy metal that is commonly found at low levels in drinking water. In dilute to moderately strong solutions, the main species of Cr(VI) are chromic acid (H_2CrO_4), bichromate ($HCrO_4^-$) and chromate (CrO_4^{2-}) . The acid-base relationships are : $H_2CrO_4 = HCrO_4^- + H^+$ $pK_a = 0.7$

$$HCrO_4^- = CrO_4^{2-} + H^+ \qquad pK_a = 6.5$$

Hence in waters , in the natural pH range , nearly all hexavalent chromium is bichromate or chromate or both anions. At low pH and at very high pH , total Cr(VI) is a dimer of chromate (the dichromate ion) forms: $2\ HCrO_4^- = Cr_2O_7^{2-} + H_2O$

In industrial use, hexavalent chromium is often supplied as a dichromate salt such as $K_2Cr_2O_7$. In highly concentrated solutions (e.g., an electroplating bath) $Cr_2O_7^{2-}$ is an important species. Cr(VI) species are typically quite soluble over a wide pH range, which allows them to be easily transported, both in natural waters and into organisms exposed to the ions.

1.11 Diphenyl carbazide (DPC) and its complex formation with Cr(VI) [15]

Octahedral complexes are formed by Cr(VI) with ligands. In this study, 1,5 diphenyl carbazide (DPC) is used as ligand. Cr(VI) in solution complexes very strongly with diphenyl carbazide (DPC) and the complex has a strong pink colour. By constructing a molecular model of the ligand and positioning it around a suitable 6-branched element, the following complex is made (**Figure 1.2)**

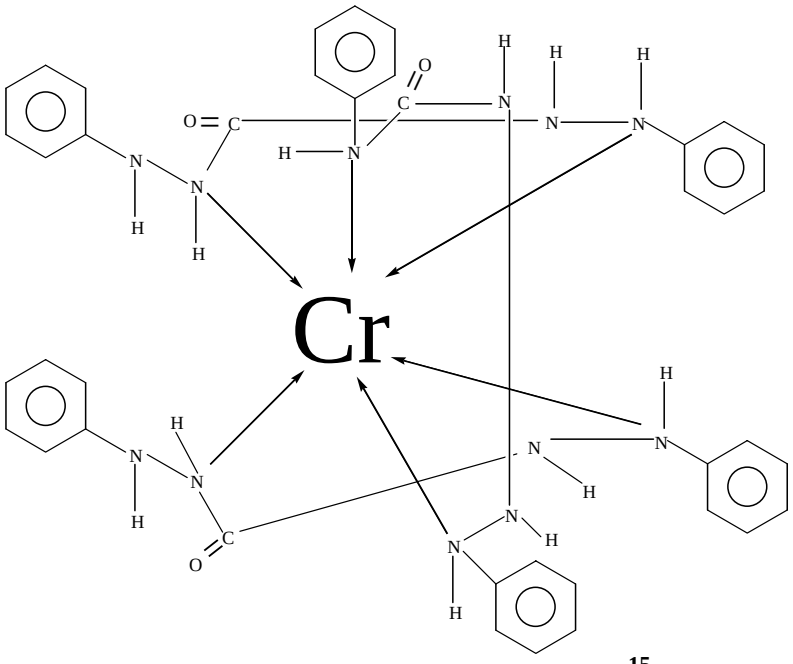

Figure 1.2 : Model for Cr(VI) -DPC complex[15]

The **Figure 1.2** shows that three of the DPC ligands can be joined to the central Chromium. This complex is extremely stable. A second structure has also been proposed (shown in **Figure 1.3**) with the chromium being "sandwitched" between the delocalized rings on the primary benzene rings. The apparent conflicts between the two theories for the structure are due to one version being borne out of models (as in **Figure 1.2**) while the second is as a result of the use of x-ray diffraction techniques, which gave the second results. The colour of the compound is due to electron transfer, rather than d orbital shifts.

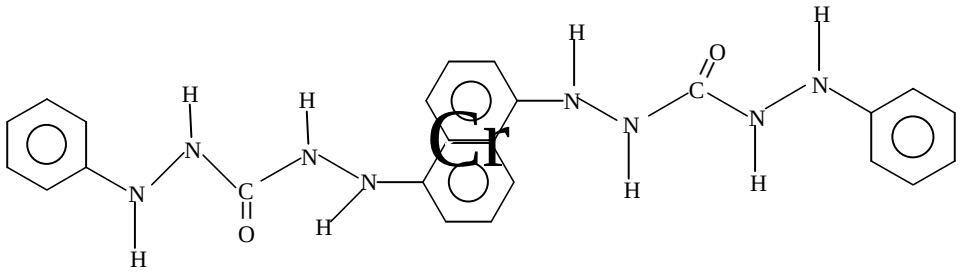

Figure 1.3 : Structure of Cr(VI) -DPC complex from X-ray Diffraction[15]

1.12 Methods of treatment of Wastewater and their Disposal[42]

Satisfactory disposal of wastewater, whether by surface, subsurface methods or dilution, is dependent on its treatment prior to disposal. Adequate treatment is necessary to prevent contamination of receiving waters to a degree which might interfere with their best or intended use, whether it be for water supply, recreation, or any other required purpose.

Wastewater treatment consists of applying known technology to improve or upgrade the quality of a wastewater. Usually wastewater treatment will involve collecting the wastewater in a central, segregated location (the Wastewater Treatment Plant) and subjecting the wastewater to various treatment processes. Most often, since large volumes of wastewater are involved, treatment processes are carried out on continuously flowing wastewaters (continuous flow or "open" systems) rather than as "batch" or a series of periodic treatment processes in which treatment is carried out on parcels or "batches" of wastewaters. While most wastewater treatment processes are continuous flow, certain operations, such as vacuum filtration, involving as it does, storage of sludge, the addition of chemicals, filtration and removal or disposal of the treated sludge, are routinely handled as periodic batch operations.

Wastewater treatment can also be organized or categorized by the nature of the treatment process operation being used; for example, physical, chemical or biological. Examples of these treatment steps are shown below. A complete treatment system may consist of the application of a number of physical, chemical and biological processes to the wastewater.

Some Physical, Chemical and Biological Wastewater Treatment Methods

Physical : Physical methods include processes where no gross chemical or biological changes are carried out and strictly physical phenomena are used to improve or treat the wastewater. Examples are:

(i) **Sedimentation** (Clarification) : Sedimentation is one of the most common physical treatment processes that is used to achieve treatment. In the process of sedimentation, physical phenomena relating to the settling of solids by gravity are allowed to operate. Usually this consists of simply holding a wastewater for a short period of time in a tank under quiescent conditions, allowing the heavier solids to settle, and removing the "clarified" effluent. Sedimentation for solids separation is a very common process operation and is routinely employed at the beginning and end of wastewater treatment operations.

(ii) **Screening** : To remove larger entrained objects and sedimentation

(iii) **Aeration** : Physically adding air, usually to provide oxygen to the wastewater.

(iv) **Filtration** : Here wastewater is passed through a filter medium to separate solids. An example would be the use of sand filters to further remove entrained solids from a treated wastewater.

(v) **Flotation and Skimming** : Permitting greases or oils, for example, to float to the surface and skimming or physically removing them from the wastewaters is often carried out as part of the overall treatment process.

(vi) Degasification

(vii) **Equalization** : In certain industrial wastewater treatment processes strong or undesirable wastes are sometimes produced over short periods of time. Since such "slugs" or periodic inputs of such wastes would damage a biological treatment process, these wastes are sometimes held, mixed with other wastewaters, and gradually released, thus eliminating "shocks" to the treatment plant. This is call equalization.

Chemical : Chemical treatment consists of using some chemical reaction or reactions to improve the water quality.

(i) **Chlorination** : Probably the most commonly used chemical process is chlorination. Chlorine, a strong oxidizing chemical, is used to kill bacteria and to slow down the rate of decomposition of the wastewater.

(ii) **Ozonation :** This process involves with the killing of bacteria by using ozone.

(iii) **Neutralization** : A chemical process commonly used in many industrial wastewater treatment operations is neutralization. Neutralization consists of the addition of acid or base to adjust pH levels back to neutrality. Since lime is a base it is sometimes used in the neutralization of acid wastes.

(iv) **Coagulation** : Coagulation consists of the addition of a chemical that, through a chemical reaction, forms an insoluble end product that serves to remove substances from the wastewater. Polyvalent metals are commonly used as coagulating chemicals in wastewater treatment and typical coagulants would include lime (that can also be used in neutralization), certain iron containing compounds (such as ferric chloride or ferric sulfate) and alum (aluminum sulfate).

(v) **Adsorption**: Certain processes may actually be physical and chemical in nature. The use of activated carbon to "adsorb" or remove organics, for example, involves both chemical and physical processes.

(vi) **Ion Exchange** : Processes such as ion exchange, which involves exchanging certain ions for others, are not used to any great extent in wastewater treatment.

Biological : Biological treatment methods use microorganisms, mostly bacteria, in the biochemical decomposition of wastewaters to stable end products. More microorganisms, or sludge's, are formed and a portion of the waste is converted to carbon dioxide, water and other end products. Generally, biological treatment methods can be divided into aerobic and anaerobic methods, based on availability of dissolved oxygen.

(A) ***Aerobic***

(i) Activated Sludge Treatment Methods

(ii) Trickling Filtration

(iii) Oxidation Ponds

(iv) Lagoons

(v) Aerobic Digestion

(B) ***Anaerobic***

(i) Anaerobic Digestion

(ii) Septic Tanks

(iii) Lagoons

1.13 Technologies applied to remove chromium from wastewater

Many manufacturing processes, such as those used by the electroplating, leather tanning, and textile industries produce wastewaters containing chromium. The US Environmental Protection Agency has established standards that require the destruction of chromates prior to discharge to avoid the potential risks of surface and drinking water contamination. The US EPA has designated the following treatment methods as Best Available Technology (BAT) for removing chromium from water.

Hexavalent Chromium Removal Treatment Technologies[43]

(A) . Ion exchange

Among the physicochemical methods developed for chromium removal from wastewater, ion exchange is becoming a popular method that has received much attention in recent years[43] . Ion exchange is an exchange of ions between two electrolytes or between an electrolyte solution and a complex. This technology removes chromium ions from the aqueous phase by replacing them with the anion present in the ion exchange resin. As contaminated water is passed through the resin, contaminant ions are exchanged for other ions such as chlorides or hydroxides in the resin.

Resins are classified based on the type of functional group they contain: Cationic Exchangers: - Strongly acidic – functional groups derived from strong acids e.g., R-SO_3H (sulfonic). - Weakly acidic – functional groups derived from weak acids, e.g., R-COOH (carboxylic).Anionic Exchangers: - Strongly basic – functional groups derived from quaternary ammonia compounds, R_3N-OH. - Weakly basic - functional groups derived from primary and secondary amines, R-NH_3OH or RR'NH_2OH. About 100% removal of

Cr (VI) was achieved in the studies (Sapari et al. 1996). Its advantages over other processes are the recovery of the metal's value, high selectivity, less sludge volume produced and the ability to meet strict discharge specifications. Its limitations are high operating costs compared to other treatment systems. There can be incomplete removal of the chromium from the salt solution

(B) . Chemical Precipitation :(Coagulation and Flocculation)

Wastewater discharge compliance is also achieved by reducing hexavalent chromium to trivalent chromium with precipitation to chromium hydroxide, a non-toxic substance. Coagulation and/or filtration technology consists of decreasing the pH level (as low as 4 or 5) and increasing the feed rate of a chemical coagulant combined with mechanical flocculation to allow fine suspended and some dissolved solids to clump together (flock). There are a variety of coagulants available (e.g. aluminum sulfate, ferric chloride, ferric sulphate, poly aluminum chloride, etc.), and the choice of one depends on water quality, contaminant removal requirements and cost. The majority of the flock and other suspended solids are removed by settling and easily separated and disposed of.

The remaining suspended particles are removed by filtration using multimedia filters. Water passes through the filtration media bed and the suspended solids are captured in the bed. This continues until the bed has reached a maximum solids loading. The flow is reversed causing bed expansion and release of the captured solids.

The removal of chromium can be accomplished by the addition of ferrous sulphate and lime. Ferrous ion first reduces hexavalent chromium to trivalent chromium by simultaneous oxidation of ferrous ion to ferric. The resulting forms can be precipitated as

hydroxides by lime. Chromium is precipitated as hydroxide: $Cr^{3+} + 3OH^- \rightarrow Cr(OH)_3$. The process requires addition of other chemicals, which finally leads to the generation of a high water content sludge, the disposal of which is cost intensive. Its efficiency is affected by low pH and the presence of other salts (ions) and is ineffective in removal of the metal ions at low concentration[44,45].

(C). Adsorption and Biosorption

Adsorption and Biosorption can be defined as accumulation of liquid or gas phase on the surface of a solid phase. The material that adsorbs is called adsorbent and the substance getting adsorbed is called adsorbate. A variety of natural and synthetic materials has been used as Cr(VI) sorbents, including activated carbons, biological materials, zeolites, chitosan, and industrial wastes[43] .Adsorption may be physical adsorption or chemical adsorption or a combination of both. Adsorbent materials have negatively charged ligands that can form complexes with metal ion via electrostatic interactions. If we have to remove soluble material from the solution phase, but the material is neither volatile nor biodegradable, we often employ adsorption processes[45].Biosorption is a property of certain types of inactive, dead, microbial biomass to bind and concentrate heavy metals from even very dilute aqueous solutions[46].It is particularly the cell wall structure of certain algae, fungi and bacteria which was found responsible for this phenomenon. The advantages of biosorption process are that these are cost effective, technically feasible and eco-friendly. This method suffers from low adsorption capacity and less intensity of biosorption.

(D). Reverse Osmosis

Reverse osmosis is a filtration process that is often used for water. It works by using pressure to force a solution through a membrane[45,47], retaining the solute on one side and allowing the pure solvent to pass to the other side. This is the reverse of the normal osmosis process, which is the natural movement of solvent from an area of low solute concentration, through a membrane, to an area of high solute concentration when no external pressure is applied .

A semi permeable membrane, like the membrane of a cell wall or a bladder, is selective about what it allows to pass through, and what it prevents from passing. These membranes in general pass water very easily because of its small molecular size; but also prevent many other contaminants from passing by trapping them. Water will typically be present on both sides of the membrane, with each side having a different concentration of dissolved minerals. Since the water with the less concentrated solution seeks to dilute the more concentrated solution, water will pass through the membrane from the lower concentration side to the greater concentration side. Eventually, osmotic pressure will counter the diffusion process exactly, and an equilibrium will form. The semi permeable membrane can be fabricated by a variety of materials in a way to support a high trans membrane pressure. Generally membranes made up of polyamide are used . The reverse osmosis, for the treatment of chromium containing effluent, technique has been successfully used in the treatment of electroplating rinse waters, not only to meet effluent discharge standards, but also to recover concentrated metal salt solutions for reuse. Demerits are high priced

equipment and/or expensive monitoring system, high energy requirement, sludge generation.

(E). Electro dialysis

Electro dialysis is an electro membrane process in which ions are transported through ion permeable membranes from one solution to another under the influence of a potential gradient. The electrical charges on the ions allow them to be driven through the membranes fabricated from ion exchange polymers. Applying a voltage between two end electrodes generates the potential field required for this. Since the membranes used in electro dialysis have the ability to selectively transport ions having positive or negative charges. The ion permeable membranes used in electro dialysis are essentially sheets of ion-exchange resins. They usually also contain other polymers to improve mechanical strength and flexibility. The resin component of a cation-exchange membrane would have negatively charged groups chemically attached to the polymer chains (e.g. styrene/divinylbenzene copolymers). Polymer chains forms anion permeable membranes, which are selective to transport of negative ions, because the fixed $-NR_3^+$ groups repel positive ions. The recovery percentage of Chromium is quite good, the chromium concentration is not high enough to be recycled to the tanning process. Other problems with electro dialysis are high capital and operating costs involved and the requirement of highly trained human resources. The fouling and scaling of membranes is another drawback which can be controlled to an extent by employing flushing step.

(F) . Photo-catalysis

Photo-catalysis over a semiconductor oxide such as TiO_2 is initiated by the absorption of a photon with energy equal to, or greater than the band gap of the semiconductor producing electron-hole (e-/h+) pairs. Oxidation of water by the hole produces the hydroxyl radical (•OH). Similarly O_2 radical also formed.• OH radicals rapidly attack pollutants in solution. The oxidation pathway is not yet fully understood. But OH radical can be formed in two different manners. Cr (VI) will be reduced to Cr (III).And precipitated out. Photo-catalysis has large capability for the removal of trace metals[48] . The drawback of this method is that of being slow compared with traditional methods but it has the advantage not leaving toxic by product or sludge to be disposed.

1.14 Adsorption technique and removal of Cr (VI) using composite material

The Cr(VI), appear to be one of the major heavy metal pollutants globally in this century. Cr(VI), derived from industrial wastewater, is highly toxic and present a serious threat to human health and environment. Various techniques for Cr(VI) removal has been studied widely and has attracted the attention of more scientists. Comparisons of different techniques are very difficult because of inconsistencies in the data presentation. Cr(VI) removal was evaluated at different conditions, such as pH, initial chromium concentration, temperature, ratios. Various chromium-contaminated water such as ground water, drinking water, tannery wastewater, electroplating wastewater, and synthetic industrial wastewater were used. This makes comparisons more complicated and difficult to pursue. Each methods has its own merits and limitations. The versatility, simplicity, cost effectiveness and technical feasibility are a few factors that must be considered while

selecting a particular method. High cost and technical complications are the problem associated with Reverse osmosis and electro dialysis. Ion exchange is also comparatively costly whereas chemical precipitation leads to sludge generation and involve high capital costs. Photo-catalysis process is still in the development stage. Coagulation and filtration produce solid residue (sludge) containing compounds whose final destination is generally land filling with related high costs and still a possibility of ground water contamination. Adsorption offers significant advantages like low cost, availability, profitability, easy of operation and efficiency, in comparison with conventional methods (such as membrane filtration or ion exchange) especially from economical and environmental points of view .

Adsorption is relatively new practice for the removal of chromium. It has been a useful tool for controlling the extent of metal pollution. Different types of adsorbents and their performance in Cr(VI) removal were studied[43,49]. Activated carbons are expensive and can remove a few milligrams of metal ions per gram of activated carbon[50], Chitosan are Nonporous sorbent; the sorption capacity depends on the origin of the polysaccharide and the degree of N-acetylation and requires chemical modification to improve its performance (Udaybhaskar et al. 1990). Biosorbents are sensitivity to operating conditions like pH and ionic strength and requires large amount of biosorbent[51]. Inorganic membrane are costly and also have low surface area[52]. Chromium removal from wastewater by adsorption process with composite materials are simple, more efficient and economically viable. Thus in the present study, hexavalent chromium from wastewater is removed by using iron oxide- SiO_2 composite material prepared by different methods.

1.15 Composite Material[53]

1.15.1 Definition

Composite material is a material composed of two or more distinct phases (matrix phase and dispersed phase) and having bulk properties significantly different form those of any of the constituents. The primary phase, having a continuous character, is called matrix. It holds the dispersed phase and shares a load with it. The second phase (or phases) is embedded in the matrix in a discontinuous form is called dispersed phase, which is usually stronger than the matrix, therefore it is sometimes called reinforcing phase.

Composites are a unique class of materials made from two or more distinct materials that when combined are better (stronger, tougher, and/or more durable) than each would be separately. The different materials work together to give the composite unique properties, but within the composite you can easily tell the different materials apart – they do not dissolve or blend into each other.

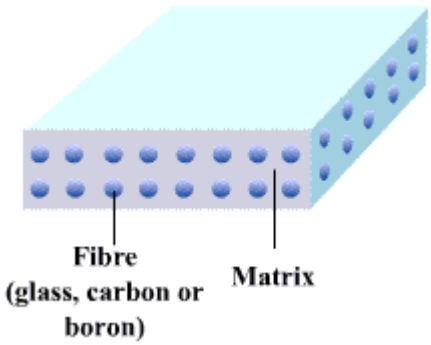

Figure 1.4 : Basic construction of a composite material

In composite materials, the components can be physically identified and exhibit an interface between one another. The most common composite is the fibrous composite consisting of reinforcing fibers embedded in a binder, or matrix materials.

1.15.2 Constituents of a composite

The individual materials that make up composites are called *constituents*. Most composites have two constituents: **a binder or *matrix***, and a ***reinforcement or filler*.**

Matrix

The matrix is the component that holds the filler together to form the bulk of the material. It usually consists of various epoxy type polymers but other materials may be used. Matrix keeps the reinforcement in a set place. The binder also protects the reinforcement, which may be brittle or breakable, as in the case of the long glass fibers used in conjunction with plastics to make fiberglass.

Reinforcement

The reinforcements or filler is the material that has been impregnated in the matrix to lend its advantage (usually strength) to the composite. The fillers can be of any material such as carbon fiber, glass bead, sand, or ceramic. Reinforcement improves the overall mechanical properties of the matrix. The reinforcement is usually much stronger and stiffer than the matrix, and gives the composite its good properties .

When designed properly, the new combined material exhibits better surface area than would each individual material. Generally, composite materials have excellent adsorbing ability combined with good porosity, making them versatile in a wide range of situations.

1.15.3 Classification[54]

Actually the production of composites is an attempt to copy nature. Wood is a composite of cellulose fibers cemented together with lignin. This kind of composite is called natural composites. And for man-made composites, there are two classification systems of composite materials. One of them is based on the matrix material (metal, ceramic, polymer) and the second is based on the material structure.

Classification based on matrix material : With respect to the matrix constituent composite materials are of three types:

Organic Matrix Composites (OMCs) : The term organic matrix composite is generally assumed to include two classes of composites, namely Polymer Matrix Composites (PMCs) and carbon matrix composites commonly referred to as carbon-carbon composites. Polymer Matrix Composites (PMC's) are the most common . Also known as FRP - Fiber Reinforced Polymers - these materials use a polymer-based resin as the matrix, and a variety of fibers such as glass and carbon as the reinforcement. Polymer Matrix Composites are composed of a matrix from thermoset [Unsaturated Polyester (UP), Epoxiy (EP)] or thermoplastic [Polycarbonate (PC), Polyvinylchloride, Nylon, Polystyrene] and embedded glass, carbon, steel or Kevlar fibers (dispersed phase).

For example "fibreglass", the first successful modern composites, is one of the polymer matrix composites. It is used for making boat hulls, storage tanks, pipes, and car components.

Metal Matrix Composites (MMCs) : Metal Matrix Composites are composed of a metallic matrix (aluminum, magnesium, iron, cobalt, copper) and a dispersed ceramic (oxides, carbides) or metallic (lead, tungsten, molybdenum) phase. MMC's are increasingly found in the mobile industry.

Ceramic Matrix Composites (CMCs): Ceramic Matrix Composites are composed of a ceramic matrix and embedded fibers of other ceramic material (dispersed phase). Ceramic Matrix Composites are used in very high temperature environments.

1.15.4 Properties of composite materials[15]

Superior and unique mechanical and physical properties can be provided by a composite, because it combines the most desirable properties of its constituents while suppressing their least desirable properties. The example is , a glass-fiber reinforced plastic combines the high strength of thin glass fibers with the ductility and chemical resistance of plastic; the brightness that the glass fibers have when isolated is not a characteristic of the composite.

Some other attractive properties can be shown by the composites, such as high thermal or electrical conductivity and a low coefficient of thermal expansion. Also, depending on how the fibers are oriented or interwoven within the matrix, composites can be fabricated that have structural properties specifically tailored for a particular structural use. The most important distinguishing characteristics of a composite are its geometrical features and the fact that its performance is the collective behaviour of its constituents. A composite material can vary in composition, structure and properties from one point to

the next inside the material. Surface , catalytic , photocatalytic and elastic properties are also observed for some of the prepared metal oxide composites.

1.15.5 The importance of composites

Composites have properties, which could not be achieved by either of the constituent materials alone. We can see that composites are becoming more and more important as it can help to improve our quality of life. Composites are put into service in flight vehicles, automobiles, boats, pipelines, buildings, roads, bridges, and dozens of other products. Researchers are finding ways to improve other qualities of composites so they may be strong, lightweight, long-lived, and inexpensive to produce. Different materials are suitable for different applications.

1.15.6 Disadvantages of composite material

Although composite materials have certain advantages over conventional materials, composites also have some disadvantages. The common one is the high manufacturing costs. However, as improved manufacturing techniques are developed, it will become possible to produce composite materials at higher volumes and at a lower cost than is now possible. Most composites use thermoset matrices that can't be reshaped. Some of the associated disadvantages of advanced composites are as follows:

a). High cost of raw materials and fabrication.

b). Reuse and disposal may be difficult.

However, proper design and material selection can circumvent many of the above disadvantages.

1.15.7 Nanocomposites[55]

Nanocomposite materials formed by metallic or oxide particles dispersed in polymer, ceramic or vitreous matrices have important application in areas such as catalysis and electronics. An interesting class of nanocomposite materials is formed by nanometer sized magnetic particles dispersed in insulating matrix. These nanocrystalline particles have a high surface/volume ratio, leading to magnetic properties different from those of bulk materials. Such properties are also highly dependent on the particle size distribution as well as on the aggregation of particles when compared to different production methods. Sol-gel process has proved to be an efficient method to prepare ultra-fine particles dispersed in different matrices and, particularly, to produce thin film. Through this method, a good control of the sample morphology, texture, structure, and chemical composition can be attained by carefully monitoring the preparation parameters. The use of an inorganic matrix allows narrow dispersion of particle size, and homogeneous distribution.

Nanocomposites are composites in which at least one of the phases shows dimensions in the nanometer range (1 nm = 10^{-9}m)[56]. Nanocomposite materials have emerged as suitable alternatives to overcome limitations of micro composites and monolithic, while posing preparation challenges related to the control of elemental composition and stoichiometry in the nanocluster phase. They are reported to be the materials of 21st century in the view of possessing design uniqueness and property combinations that are not found in conventional composites. The general understanding of these properties is yet to be reached[57], even though the first inference on them was reported as early as 1992[58].

The general class of nanocomposite organic/inorganic materials is a fast growing area of research. Significant effort is focused on the ability to obtain control of the nanoscale structures via innovative synthetic approaches. The properties of nano-composite materials depend not only on the properties of their individual parents but also on their morphology and interfacial characteristics.

The inorganic components can be three-dimensional framework systems such as zeolites, two-dimensional layered materials such as clays, metal oxides, metal phosphates, and chalcogenides. Experimental work has generally shown that virtually all types and classes of nanocomposite materials lead to new and improved properties when compared to their macro composite counterparts. Therefore, nanocomposites promise new applications in many fields such as mechanically reinforced lightweight components, non-linear optics, battery cathodes and Ionic, nano-wires, sensors and other systems. The general class of organic/inorganic nanocomposites may also be of relevance to issues of bio-ceramics and biomineralization in which *in-situ* growth and polymerization of biopolymer and inorganic matrix is occurring. Finally, lamellar nanocomposites represent an extreme case of a composite in which interface interactions between the two phases are maximized. Since the remarkable properties of conventional composites are mainly due to interface interactions, the materials dealt with here could provide good model systems in which such interactions can be studied in detail using conventional bulk sample (as opposed to surface) techniques. Inorganic layered materials exist in great variety. They possess well defined, ordered intra lamellar space potentially accessible by foreign species. This ability enables them to act as matrices or hosts for polymers, yielding interesting hybrid nano-composite materials.

1.15.8 General method of preparation of iron oxide-SiO_2 composite

Nowadays, the attention of many scientists is focused on the development of new methods for synthesis and stabilization of composite materials, especially nanoparticles. Moreover, special attention is paid to monodispersed and stable particles formation. Different metals, metal oxides, sulfides, polymers, core-shell and composite nanoparticles can be prepared using a number of synthetic techniques, which are broadly classified into three categories, namely, physical methods, chemical methods and electro-chemical methods.

Chemical techniques involves (i) Chemical vapor deposition (ii) vapor-phase synthesis: (iii) Hydrothermal synthesis (iv) Sol-gel technique (v) Sonochemical technique (vi) Micro emulsion technique and (vii) Wet-chemical Process.

Physical methods involves – (i) Laser ablation (ii) Sputtering (iii) Spray route pyrolysis and (iv) Inert Gas condensation.

Nanostructured composites can also be synthesized by electrochemical method. The electrochemical method has been used for the synthesis of an array of nanomaterials such as metals, inorganic composites, conducting polymer fibers or tubes, nanotubes and nanofibers etc. In this method, nanostructured materials are allowed to deposit on the electrode from different electrolytic solution. Depending on the precursor of the element to be deposited, electrodes of various types were used. [59,60]

General method of Chemical Synthesis[15]

A widely used chemical process is the oxidative polymerization. Various oxidizing agents, such as potassium dichromate, ammonium persulphate, ferric chloride, hydrogen peroxide etc. are used in these processes. Persulphate is the most commonly

used oxidant and its ammonium salt was preferred to the potassium counterpart because of its better solubility in water. A colloidal solution of silica is used for the polymerization. During dispersion polymerization, a monomer, soluble in the reaction medium is converted into polymer, which is insoluble under those conditions. In this approach the silica particles act as colloidal substrate having high surface area the resulting nanocomposite particles are stable colloidal dispersions, which consist of micro aggregates of silica particles "glued" together by the conducting polymer component.

Conventional chemical polymerization techniques have been successfully applied by various research groups for the preparation of sterically stabilized particles of electrically conducting polymers.

In this research, we focused our attention on the preparation of iron oxide –silica composites by Sol-Gel method and we attempted to synthesize the iron oxide-silica composite following the Sol-Gel method. We used tetraethylorthosilicate (TEOS) as the precursor of silicon (IV) oxide and iron oxide was prepared by electrochemical method.

MariaZaharescu et al[61] prepared iron oxide-silica composite by Sol-Gel method. The reagents employed were tetraethoxysilane (TEOS)(Merck) as a precursor to silicon (IV) oxide and $FeSO_4.7H_2O$ as a precursor to iron oxide, absolute ethyl alcohol as solvent ammonia as catalyst and water for hydrolysis. They reported that the iron oxide-silica composite was prepared as follows:

(i) the iron oxide was generated during the Sol-Gel process

(ii) the SiO_2 matrix was initially obtained and iron oxide was formed by thermal treatment after impregnation of soluble Fe^{2+} salt in the previously processed matrix;

(iii) magnetite powder prepared by wet chemical method were mixed with Sol-Gel solution, being embedded into SiO_2 based matrix after gelation.

They characterized the synthesized iron oxide-silica composite by XRD,DTA/TG techniques and reported that materials with high porosity and nano-sized oxides content could be prepared by Sol-Gel method.

Silicon (IV) oxide of iron oxide-silica composite synthesized by Sol-Gel method provides a high surface area, which enables the composite to act as a good sorbent material.

Clapsaddle et al. [62] synthesized silicon oxide in an iron (III) oxide matrix by Sol-Gel method. In the synthesis, iron oxide precursor, iron(III) chloride ($FeCl_3.6H_2O$) was mixed with a silica precursor, tetraethylorthosilicate(TEOS) in ethanol and gelled using an organic epoxide. The composition of the resulting materials was varied from Fe/Si (mol/mol)=1-5 by adjusting the amount of silica precursor added to the $FeCl_3.6H_2O$ solution. They reported that the synthesis method they presented is general for the synthesis of several other metal oxide/silicon oxide nanocomposite materials.

R. Predoi et al [63] synthesized nanocomposites Fe_xO_y-SiO_2, with an iron content of 3 wt.% by the Sol-Gel method starting from tetraethoxysilane (TEOS) and methyltrietoxysilane (MTEOS) precursors as the SiO_2 sources. This original method produces large quantities of amorphous gels that are thermally treated at 550ºC and 1000ºC as the final step of the synthesis. The average diameter of iron particles in the nano-composite materials can be controlled by the iron concentration and thermally treatment. The dried gel was treated at increasing temperatures, and the samples were characterized by transmission electron microscopy (TEM), IR-spectroscopy and magnetic

measurements. The result indicates that the formation and the stability of the iron oxide phases are strongly affected by the precursors used as the SiO_2 sources.

1.15.9 Application[15]

Composites have acquired a leading position in the development of new materials. Due to some miraculous properties, composites have widen research arena in Chemistry. The nanocomposite particles are important in two ways. Firstly, the silica component enables facile functionalisation at the particle surface. Secondly, the intense black colour, which is an intrinsic property of the conducting polymer component (in this case polypyrrole), eliminates the need to use an extrinsic dye to achieve the visual agglutination test. In principle, this increases the sensitivity of the test, allowing lower analyte concentrations to be detected.

Nanocoposte materials like Zeolites are micro porous, aluminosilicate minerals commonly used as commercial adsorbents. These materials are also known as *molecular sieve* – they contain tiny pores of a precise and uniform size that are useful as adsorbent for gases and liquids. Due to these characteristics, zeolite has found wide applications in adsorption, catalysis, and the removal of heavy metal ions from industrial wastewaters. Composite materials prepared by different method can be used for the removal of different heavy metals from wastewater. Thus we can use composite materials for environmental applications.

1.16 The Sol-Gel Method[2,64]

The sol-gel process is very long known since the late 1800s. The versatility of the technique has been rediscovered in the early 1970s when glasses where produced without high temperature melting processes. This made possible the organic modification of silicon compounds (ORMOSIL), which cannot withstand high temperatures. The interest in sol-gel processing can be traced back in the mid-1980s with the observation that the hydrolysis of tetraethyl orthosilicate (TEOS) under acidic conditions led to the formation of SiO_2 in the form of fibers and monoliths. Sol-gel research grew to be so important that in the 1990s more than 35,000 papers were published worldwide on the process. [65,66,67]

Definition

The **sol-gel** process is a wet-chemical technique widely used in the fields of materials science and ceramic engineering. Such methods are used primarily for the fabrication of materials (typically metal oxides) starting from a colloidal solution (*sol*) that acts as the precursor for an integrated network (or *gel*) of either discrete particles or network polymers. Typical precursors are metal alkoxides and metal salts (such as chlorides, nitrates and acetates), which undergo various forms of hydrolysis and polycondensation reactions.

Process

In this chemical procedure, the 'sol' (or solution) gradually evolves towards the formation of a gel-like diphasic system containing both a liquid phase and solid phase whose morphologies range from discrete particles to continuous polymer networks. In the case

of the colloid, the volume fraction of particles (or particle density) may be so low that a significant amount of fluid may need to be removed initially for the gel-like properties to be recognized. This can be accomplished in any number of ways. The simplest method is to allow time for sedimentation to occur, and then pour off the remaining liquid. Centrifugation can also be used to accelerate the process of phase separation.

Removal of the remaining liquid (solvent) phase requires a drying process, which is typically accompanied by a significant amount of shrinkage and densification. The rate at which the solvent can be removed is ultimately determined by the distribution of porosity in the gel. The ultimate microstructure of the final component will clearly be strongly influenced by changes imposed upon the structural template during this phase of processing.

Afterwards, a thermal treatment, or firing process, is often necessary in order to favor further polycondensation and enhance mechanical properties and structural stability via final sintering, densification and grain growth. One of the distinct advantages of using this methodology as opposed to the more traditional processing techniques is that densification is often achieved at a much lower temperature.

The precursor sol can be either deposited on a substrate to form a film (e.g., by dip coating or spin coating), cast into a suitable container with the desired shape (e.g., to obtain monolithic ceramics, glasses, fibers, membranes, aero gels), or used to synthesize powders (e.g., micro spheres, nanospheres). The sol-gel approach is a cheap and low-temperature technique that allows for the fine control of the product's chemical composition. Even small quantities of dopants, such as organic dyes and rare earth

elements, can be introduced in the sol and end up uniformly dispersed in the final product. It can be used in ceramics processing and manufacturing as an investment casting material, or as a means of producing very thin films of metal oxides for various purposes. Sol-gel derived materials have diverse applications in optics, electronics, energy, space, (bio)sensors, medicine (e.g., controlled drug release), reactive material and separation (e.g., chromatography) technology.

Preparation of metal oxides using sol-gel routes proceeds by three basic steps: 1) partial hydrolysis of metal alkoxides to form reactive monomers, 2) condensation of these monomers to form colloid-like oligomers (sol formation), 3) additional hydrolysis to promote polymerization and cross-linking leading to a three-dimensional matrix (gel formation).

Monomer Formation (Partial Hydrolysis)

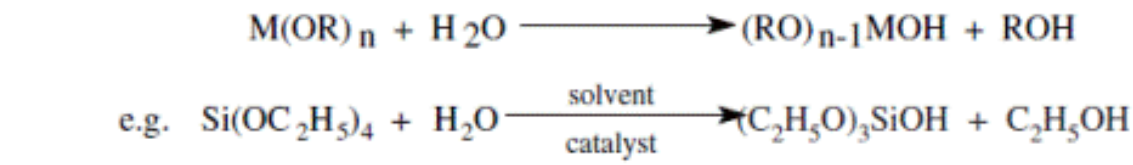

Sol Formation (Polycondensation)

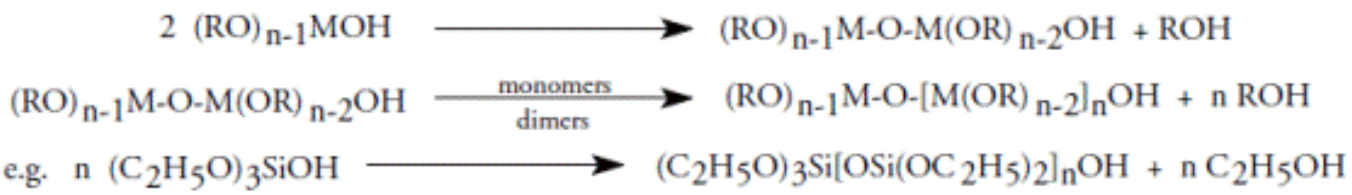

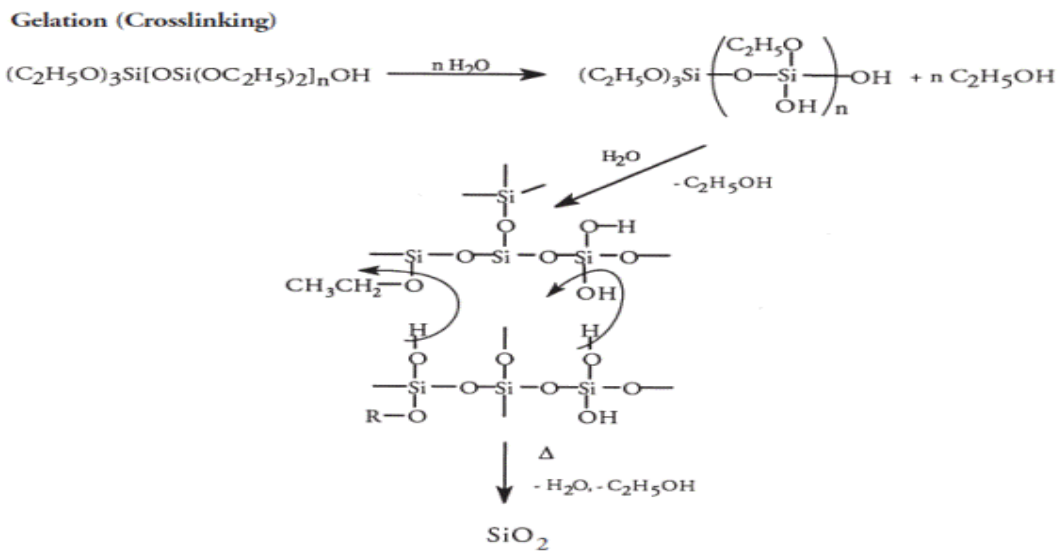

Applications

The applications for sol gel-derived products are numerous[68]

Nanoscale powders: Ultra-fine and uniform ceramic powders can be formed by precipitation. These powders of single and multiple component compositions can be produced on a nanoscale particle size for dental and biomedical applications. Composite powders have been patented for use as agro chemicals and herbicides. Powder abrasives, used in a variety of finishing operations, are made using a sol-gel type process. One of the more important applications of sol-gel processing is to carry out zeolite synthesis.

Advantages

The sol-gel technique offers a low-temperature method for synthesizing materials that are either totally inorganic in nature or both inorganic and organic. The process, which is based on the hydrolysis and condensation reaction of organometallic compounds in alcoholic solutions, offers many advantages for the fabrication of coatings, including excellent control of the stoichiometry of precursor solutions, ease of compositional modifications, customizable microstructure, ease of introducing various functional groups

or encapsulating sensing elements, relatively low annealing temperatures, the possibility of coating deposition on large area substrates, and simple and inexpensive equipment. Within the past several years, a number of developments in precursor solutions, coating processes and equipment have made the sol-gel technique even more widespread.

1.17 Adsorption[2,69]

1.17.1 Definition

The phenomenon of attracting and retaining the molecules of a substance on the surface of a liquid or a solid resulting in the higher concentration of the molecules on the surface is called Adsorption. The substance thus adsorbed on surface is called Adsorbate and the substance on which it is adsorbed is called Adsorbent.

Alternately, adsorption is the process through which a substance, originally present in one phase, is removed from that phase by *accumulation at the interface* between that phase and a separate (solid) phase. In principle adsorption can occur at any solid fluid interface. The driving force for adsorption is the reduction in interfacial (surface) tension between the fluid and the solid adsorbent as a result of the adsorption of the adsorbate on the surface of the solid. The most important factors affecting adsorption are:

- *Surface area of adsorbent* : Larger sizes imply a greater adsorption capacity.
- *Particle size of adsorbent* : Smaller particle sizes reduce internal diffusional and mass transfer limitation to the penetration of the adsorbate inside the adsorbent (i.e., equilibrium is more easily achieved and nearly full adsorption capability can be attained).

- *Contact time or residence time*: The longer the time the more complete the adsorption will be. However, the equipment will be larger.
- *Solubility of solute (adsorbate) in liquid (wastewater)*: Substances slightly soluble in water will be more easily removed from water (i.e., adsorbed) than substances with high solubility. Also, non-polar substances will be more easily removed than polar substances since the latter have a greater affinity for water.
- *Affinity of the solute for the adsorbent (carbon)*: The surface of activated carbon is only slightly polar. Hence non-polar substances will be more easily picked up by the carbon than polar ones.
- *Number of carbon atoms*: For substances in the same homologous series a larger number of carbon atoms is generally associated with a lower polarity and hence a greater potential for being adsorbed (e.g., the degree of adsorption increases in the sequence formic-acetic-propionic-butyric acid).
- *Size of the molecule with respect to size of the pores* : Large molecules may be too large to enter small pores. This may reduce adsorption independently of other causes.
- *Degree of ionization of the adsorbate molecule*: More highly ionized molecules are adsorbed to a smaller degree than neutral molecules.
- *pH* : The degree of ionization of a species is affected by the pH (e.g., a weak acid or a weak basis). This, in turn, affects adsorption.
- *Nature of gas being Adsorb* : Higher the critical temp. of gas, greater is the among of that gas adsorbed.
- *Temperature* : Adsorption decreases with increase in temperature and vice - versa.

- *Pressure* : Adsorption of a gas increase with increase of pressure because on applying pressure gas molecules comes close to each other.

1.17.2 Causes of Adsorption

Adsorption arises at the surface of solids as a result of presence of unbalanced forces at the surface. These forces develop either during the crystallization of solids or by virtue of the presence of unpaired electron in d-orbital.

1.17.3 Characteristics of Adsorption

1. It is specific and selective in nature.

2. It is accompanied by decrease in the free energy of the system. When G becomes zero, Adsorption equilibrium is established.

3. Adsorption is spontaneous process therefore change in free energy (G) for the process is negative.

According to Gibb's Helmhotz equation :

$G = H - TS$

G = -Ve ; H = -Ve (it is exothermic process) And S is -Ve because adhering of gas molecules to the surface lowers the randomness.

1.17.4 Types of Adsorption[70]

1.17.4.A Physical Adsorption :

Physisorption, also called physical adsorption, is a process in which the electronic structure of the atom or molecule is barely perturbed upon adsorption[71]. The weak bonding of physisorption is due to the induced dipole moment of a nonpolar adsorbate interacting with its own image charge in the polarizable solid.

Some features which are useful in recognizing physisorption include:

(a) the phenomenon is a general one and occurs in any solid/fluid system, although certain specific molecular interactions may occur, arising from particular geometrical or electronic properties of the adsorbent and/or adsorptive;

(b) evidence for the perturbation of the electronic states of adsorbent and adsorbate is minimal;

(c) the adsorbed species are chemically identical with those in the fluid phase, so that the chemical nature of the fluid is not altered by adsorption and subsequent desorption;

(d) the energy of interaction between the molecules of adsorbate and the adsorbent is of the same order of magnitude as, but is usually greater than, the energy of condensation of the adsorptive;

(e) the elementary step in physical adsorption from a gas phase does not involve an activation energy. Slow, temperature dependent, equilibration may however result from rate-determining transport processes;

(f) in physical adsorption, equilibrium is established between the adsorbate and the fluid phase. In solid/gas systems at not too high pressures the extent of physical adsorption increases with increase in gas pressure and usually decreases with increasing temperature. In the case of systems showing hysteresis the equilibrium may be metastable;

(g) under appropriate conditions of pressure and temperature, molecules from the gas phase can be adsorbed in excess of those in direct contact with the surface (multilayer adsorption or filling of micro pores).

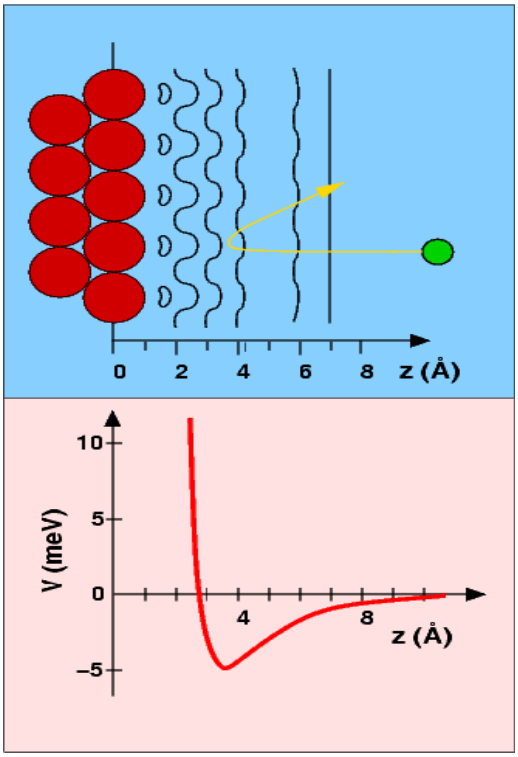

Figure 1.5 : Example of Physisorption: He-Metal interaction[69(d)]

1.17.4.B Chemical Adsorption :

Chemisorption is a sub-class of adsorption, driven by a chemical reaction occurring at the exposed surface. A new chemical species is generated at the adsorbent surface (e.g. corrosion, metallic oxidation). The strong interaction between the adsorbate and the substrate surface creates new types of electronic bonds - ionic or covalent, depending on the reactive chemical species involved[72] .It is characterised by:

- An activation energy for the chemical reaction that takes place only in a monolayer
- A high enthalpy change/ temperature gain, indicating an exothermic chemical reaction: -20 kJ/mol >ΔH> -200 kJ/mol

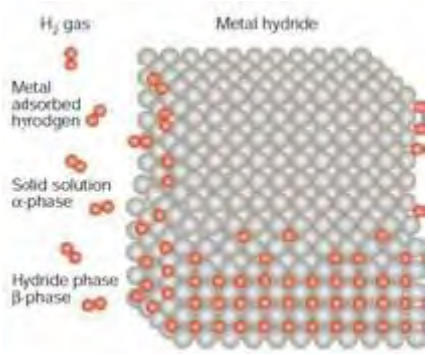

Figure 1.6 : Illustration of Chemisorption[69(d)]

Due to specificity, the nature of chemisorption can greatly differ from system to system, depending on the chemical identity and the surface structure. When a gas is held on the surface of solid by forces similar to those of a chemical bond, the type of

adsorption is called chemical adsorption or chemisorptions. It is also known as Langmuir adsorption.

1.17.5 Adsorption on solid liquid interface[15]

There is a competition between the solute and solvent molecules for adsorption in the case of adsorption from solution. If the solute is adsorbed more than the solvent, i.e., the concentration of solute is less in the bulk, the adsorption is termed as positive adsorption. But if it is more in the bulk than in the interface, then negative adsorption results.

If the solute is a strong electrolyte, the cations and the anions are not likely to adsorb equally, particularly at low concentration. In general one of the ions depending on the nature of the adsorbent is preferently adsorbed and the surface will acquire electric charge accordingly.

The extent of adsorption is greatly influenced by the lyophobicity of compound. The higher is the solvophobicity greater is the adsorption and vice versa. Adsorption from solution is also influenced by the pH of the solution. The change of ionic strength of the medium also alters the mode of adsorption.

In case of adsorption from solution, the effects of solvent on solution can not be neglected. Especially, when the surface is polar. For very dilute solutions and for low solubility of solute, the measurement of change in concentration of solution resulting from adsorption gives a very responsible isotherm for solute.

1.17.6 Adsorption equilibrium[15]

The adsorbed solute tends to desorb into the solution during the adsorption from solution as the adsorption continues. At one stage, equal amount of solute is adsorbed and

desorbed simultaneously. Eventually, the rate of adsorption and the rate of desorption will attain an equilibrium. This is called adsorption equilibrium and the corresponding time at which such equilibrium is achieved is known as the equilibrium time, t_e. The knowledge of equilibrium time is necessary for adsorption which controls the adsorption capacity.

The position of equilibrium is the characteristics of the following factors:

a) the entire system, b) the adsorbate, c) the adsorbent, d) the solvent, e) temperature, f) pH and g) ionic strength.

To investigate the mechanism of adsorption, the study of amount adsorbed at constant temperature using different concentration of adsorbate is mostly chosen. A number of mathematical expressions have been developed to give quantitative relationship between the amount adsorbed with equilibrium concentration of the solution. The amount adsorbed from solution at equilibrium is a function of temperature and equilibrium concentration of adsorbate, i.e. $x/m = f(C_e T)$

where, x/m = mass of adsorbate adsorbed per gram of adsorbent in $molg^{-1}$

C_e = equilibrium concentration (M) of the solution; T = Absolute temperature (K)

1.17.7 Adsorption Isotherm[2, 69-74]

Adsorption is usually described through isotherms, that is, the amount of adsorbate on the adsorbent as a function of its pressure (if gas) or concentration (if liquid) at constant temperature. In the process of adsorption, adsorbate gets adsorbed on adsorbent.

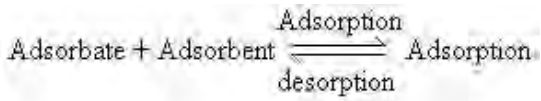

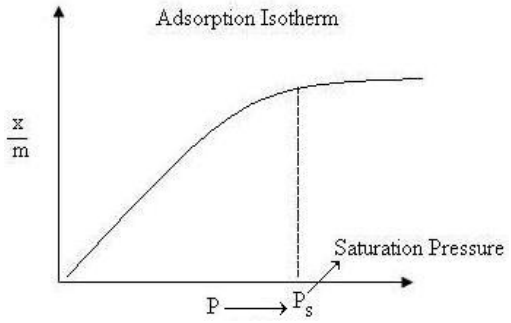

Figure 1.7: Basic Adsorption Isotherm[69(b)]

1.17.7.A Freundlich Adsorption Isotherm

In 1909, Freundlich gave an empirical expression representing the isothermal variation of Adsorption of a quantity of gas adsorbed by unit mass of solid adsorbent with pressure.

$$\frac{x}{m} = kP^{\frac{1}{n}}$$

This equation is known as Freundlich Adsorption Isotherm or Freundlich Adsorption equation.

Where x is the mass of the gas adsorbed on mass m of the adsorbent at pressure p and k, n are constants whose values depend upon adsorbent and gas at particular temperature.

Explanation of Freundlich Adsorption equation:

At low pressure, extent of adsorption is directly proportional to pressure (raised to power one).

$$\frac{x}{m} \propto P^1$$

At high pressure, extent of adsorption is independent of pressure (raised to power zero).

$$\frac{x}{m} \propto P^0$$

Therefore at intermediate value of pressure, adsorption is directly proportional to pressure raised to power 1/n .Here n is a variable whose value is greater than one.

$$\therefore \frac{x}{m} \propto P^{\frac{1}{n}}$$

Using constant of proportionality, k, also known as adsorption constant we get

$$\frac{x}{m} = kP^{\frac{1}{n}}$$

The above equation is known as Freundlich adsorption equation.

Plotting of Freundlich Adsorption Isotherm:

As per Freundlich adsorption equation $\frac{x}{m} = kP^{\frac{1}{n}}$

Taking log both sides of equation, we get, $\log\left(\frac{x}{m}\right) = \log k + \frac{1}{n}\log p$

The equation above equation is comparable with comparable with equation of straight line, y = m x + c where, m represents slope of the line and c represents intercept on y axis. Plotting a graph between log(x/m) and log p, we will get a straight line with value of slope equal to 1/n and log k as y-axis intercept.

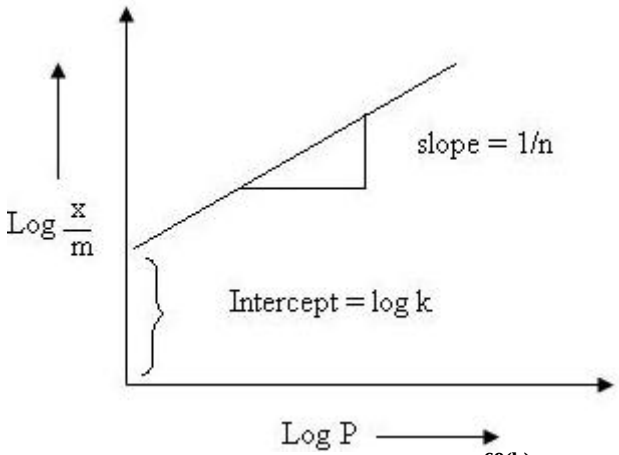

Figure 1.8: log(x/m) vs. log p graph[69(b)]

The Freundlich Adsorption Isotherm is mathematically expressed as

$$x/m = Kp^{1/n}$$

It is also written as

$$log(x/m) = logk + (1/n)logp$$

Or $x/m = Kc^{1/n}$

It is also written as

$$log(x/m) = logk + (1/n)logc$$

Where, x = mass of adsorbate ; m = mass of adsorbent ; p = Equilibrium pressure of adsorbate ; c = Equilibrium concentration of adsorbate in solution.

K and n are constants for a given adsorbate and adsorbent at a particular temperature.

At high pressure 1/n = 0 Hence extent of adsorption is independent of pressure.

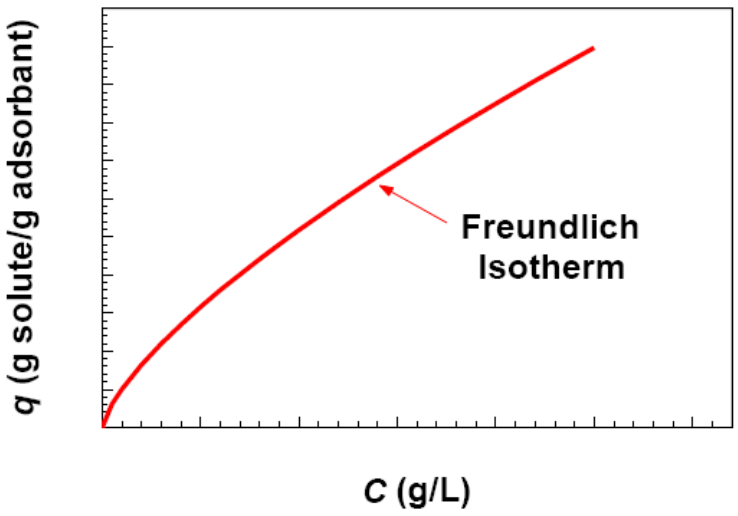

Figure 1.9 : Example of the Freundlich isotherm, showing the amount adsorbed, q , as a function of equilibrium concentration in the solution, c (e.g., in g/L)[69(e)].

Limitation of Freundlich Adsorption Isotherm:

Experimentally it was determined that extent of adsorption varies directly with pressure till saturation pressure Ps is reached. Beyond that point rate of adsorption saturates even after applying higher pressure. Thus Freundlich Adsorption Isotherm failed at higher pressure.

1.17.7.B Langmuir Adsorption Isotherm

In 1916, Irving Langmuir published an isotherm for gases adsorbed on solids, which retained his name. It is an empirical isotherm derived from a proposed kinetic mechanism. This isotherm was based on five assumptions[73]:

1. The surface containing the adsorbing sites is perfectly flat plane with no corrugations (assume the surface is homogeneous) .
2. The adsorbing gas adsorbs into an immobile state.
3. All sites are equivalent.
4. Each site can hold at most one molecule of A (mono-layer coverage only).
5. There are no interactions between adsorbate molecules on adjacent sites.

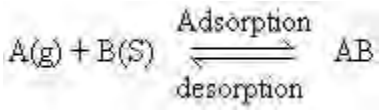

Where A(g) is unadsorbed gaseous molecule, B(s) is unoccupied metal surface and AB is Adsorbed gaseous molecule.

Based on his theory, he derived Langmuir Equation which depicted a relationship between the number of active sites of the surface undergoing adsorption and pressure.

$$\theta = \frac{KP}{1 + KP}$$

Where θ the number of sites of the surface which are covered with gaseous molecule, P represents pressure and K is the equilibrium constant for distribution of adsorbate between the surface and the gas phase . At lower pressure, KP is so small, that factor (1+KP) in denominator can almost be ignored. So Langmuir equation reduces to

$$\theta = KP$$

At high pressure KP is so large, that factor (1+KP) in denominator is nearly equal to KP. So Langmuir equation reduces to

$$\theta = \frac{KP}{KP} = 1$$

Langmuir adsorption equation can be written as (for liquid adsorbate)

$$Q = \frac{K_a C}{1 + K_a C}$$

Where, $Q = Q_m$ = for a complete monolayer, K_a= a coefficient ; C_e = concentration in the fluid. Taking reciprocals and rearranging:

$$\frac{Ce}{Q} = \frac{1}{K_a Q_m} + \frac{Ce}{Q_m}$$

A plot of C_e/Q versus C_e should indicate a straight line of slope $1/Q_m$ and an intercept of $1/K_aQ_m$. The graph shows data points and lines to both Fraundlich and Langmuir equation.

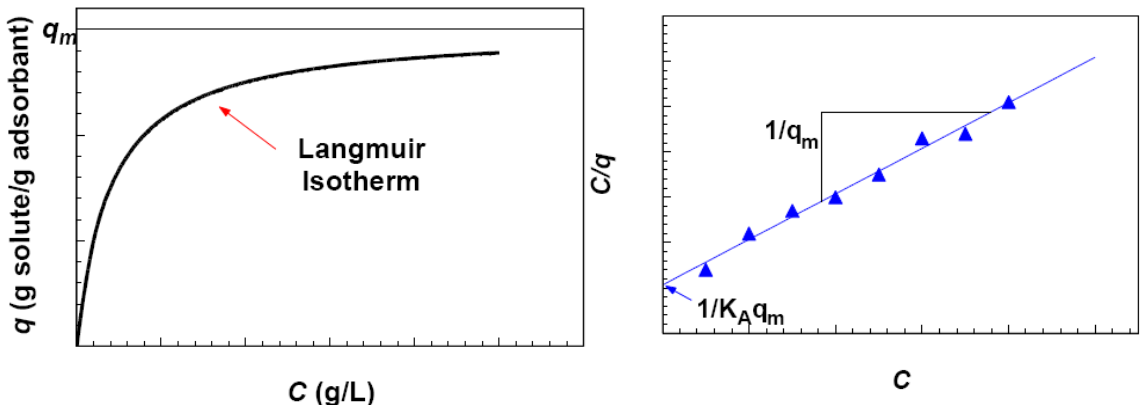

Figure 1.10: (a) Langmuir Isotherm ; (b) Determination of parameters in Langmuir isotherm[69(e)]

Limitations of Langmuir Adsorption Equation

1. The adsorbed gas has to behave ideally in the vapor phase. This condition can be fulfilled at low pressure conditions only. Thus Langmuir Equation is valid under low pressure only.
2. Langmuir Equation assumes that adsorption is monolayer. But, monolayer formation is possible only under low pressure condition. Under high pressure condition the assumption breaks down as gas molecules attract more and more molecules towards each other. *BET theory* proposed by Brunauer, Emmett and Teller explained more realistic multilayer adsorption process.
3. Another assumption was that all the sites on the solid surface are equal in size and shape and have equal affinity for adsorbate molecules i.e. the surface of solid if homogeneous. But we all know that in real solid surfaces are heterogeneous.
4. Langmuir Equation assumed that molecules do not interact with each other. This is impossible as weak force of attraction exists even between molecules of same type.

5. The adsorbed molecules has to be localized i.e. decrease in randomness is zero ($\Delta S = 0$).This is not possible because on adsorption liquefaction of gases taking place, which results into decrease in randomness but the value is not zero.

1.16.7.C BET adsorption Isotherm

In 1938, Brunauer, Emmett and Teller[74] derived the first isotherm for multilayer adsorption. It assumes a random distribution of sites that are empty or that are covered with by one monolayer, two layers and so on, as illustrated alongside.

Figure 1.11: Brunauer's model of multilayer adsorption, that is, a random distribution of sites covered by one, two, three, etc., adsorbate molecules[2].

The BET equation is given as

$$V_{total} = \frac{V_{mono} C \left(\frac{P}{P_0}\right)}{\left(1-\frac{P}{P_0}\right)\left(1+C\left(\frac{P}{P_0}\right)-\frac{P}{P_0}\right)}$$

The another form of BET equation is

$$\frac{P}{V_{total}(P-P_0)} = \frac{1}{V_{mono} C} + \frac{c-1}{V_{mono} C}\left(\frac{P}{P_0}\right)$$

Where V_{mono} be the adsorbed volume of gas at high pressure conditions so as to cover the surface with a unilayer of gaseous molecules,

$$\frac{K_1}{K_L}$$

the ratio is designated C. K_1 is the equilibrium constant when single molecule adsorbed per vacant site and K_L is the equilibrium constant to the saturated vapor liquid equilibrium.

It is important that many unusual adsorption isotherms are fitted well by the BET equation. This is to be expected when there are three coefficients to manipulate.

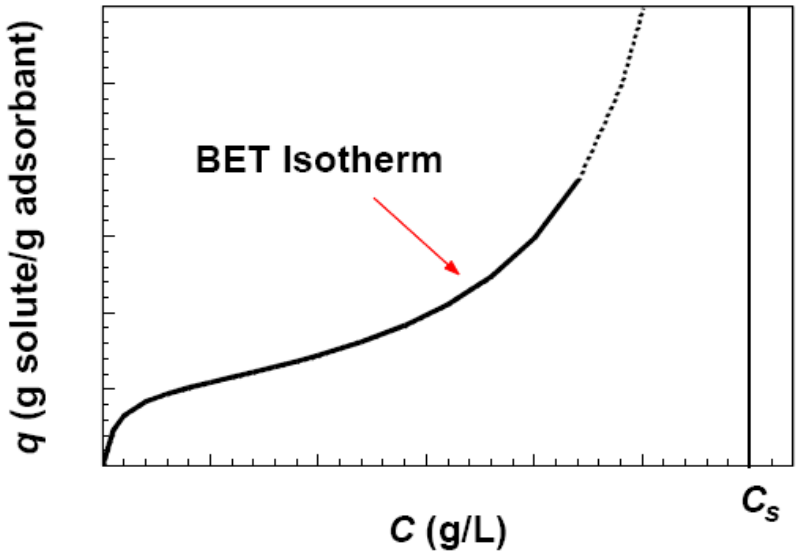

Figure 1.12 : BET isotherm [69(e)]

1.17.7.D. Type of Adsorption Isotherm

Five different types of adsorption isotherm and their characteristics are explained below.

Type I Adsorption Isotherm

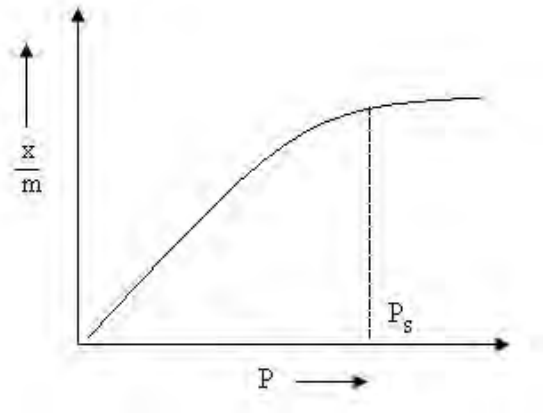

Figure 1.13 : Type I Adsorption Isotherm[69(b)]

- The above graph depicts Monolayer adsorption and can be easily explained using Langmuir Adsorption Isotherm.
- If BET equation, when $P/P_0 << 1$ and $c >> 1$, then it leads to monolayer formation and Type I Adsorption Isotherm is obtained.
- Examples of Type-I adsorption are Adsorption of Nitrogen (N_2) or Hydrogen (H_2) on charcoal at temperature near to -180^0C.

Type II Adsorption Isotherm

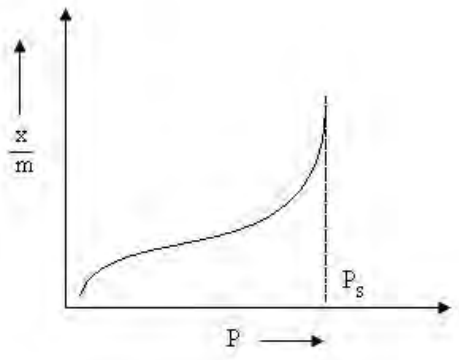

Figure 1.14: Type II Adsorption Isotherm[69(b)]

- Type II Adsorption Isotherm shows large deviation from Langmuir model of adsorption.
- The intermediate flat region in the isotherm corresponds to monolayer formation.
- In BET equation, value of C has to be very large in comparison to 1.
- $\Delta H^0_{del} > \Delta H^0_{vapl}$
- Examples of Type-II adsorption are Nitrogen (N_2 (g)) adsorbed at -195^{0}C on Iron (Fe) catalyst and Nitrogen (N_2 (g)) adsorbed at -195^{0}C on silica gel.

Type III Adsorption Isotherm

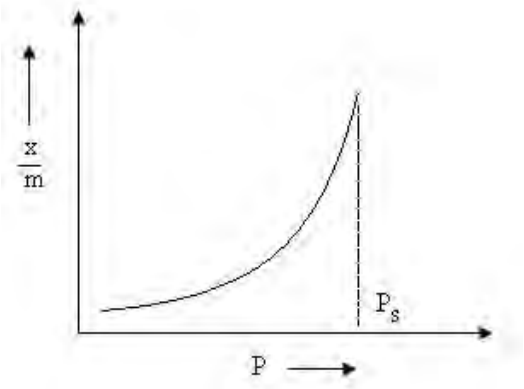

Figure 1.15 : Type III Adsorption Isotherm[69(b)]

- Type III Adsorption Isotherm also shows large deviation from Langmuir model.
- In BET equation value if C <<< 1 Type III Adsorption Isotherm obtained.
- This isotherm explains the formation of multilayer.
- There is no flattish portion in the curve which indicates that monolayer formation is missing.
- Examples of Type III Adsorption Isotherm are Bromine (Br_2) at 79^{0}C on silica gel or Iodine (I_2) at 79^{0}C on silica gel.

Type IV Adsorption Isotherm

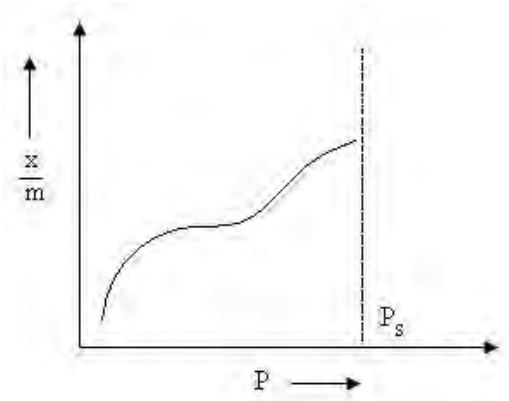

Figure 1.16 : Type IV Adsorption Isotherm[69(b)]

- At lower pressure region of graph is quite similar to Type II. This explains formation of monolayer followed by multilayer.
- The saturation level reaches at a pressure below the saturation vapor pressure .This can be explained on the basis of a possibility of gases getting condensed in the tiny capillary pores of adsorbent at pressure below the saturation pressure (P_S) of the gas.
- Examples of Type IV Adsorption Isotherm are of adsorption of Benzene on Iron Oxide (Fe_2O_3) at 50^0C and adsorption of Benzene on silica gel at 50^0C.

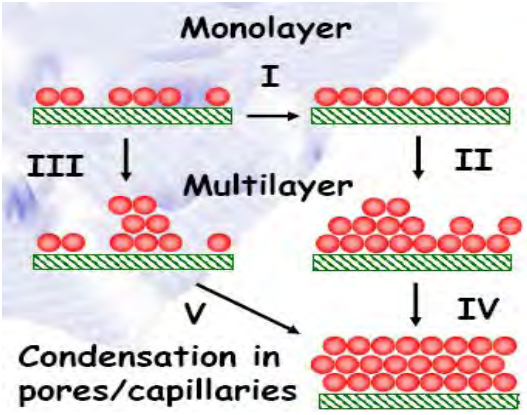

Figure 1.17 : Nature of adsorption isotherm[69(f)]

Type V Adsorption Isotherm

- Explanation of Type V graph is similar to Type IV.
- Example of Type V Adsorption Isotherm is adsorption of Water (vapors) at 100^0C on charcoal.

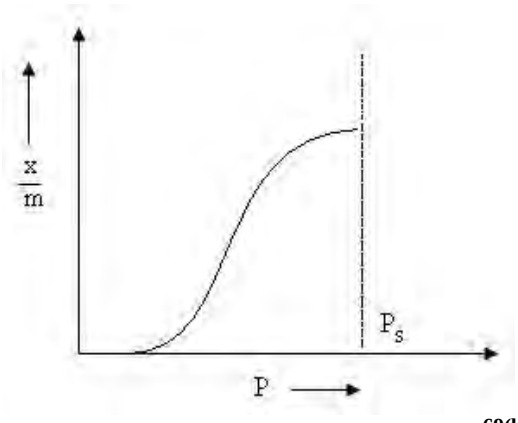

Figure 1.18: Type V Adsorption Isotherm[69(b)]

1.17.8 Application of Adsorption

1. In preserving vacuum : In Dewar flasks activated charcoal is placed between the walls of the flask so that any gas which enter in to the annular space either due to glass imperfection or diffusion through glass is adsorbed.

2. In gas masks : All gas masks are devices containing suitable adsorbent so that the poisonous gases present in the atmosphere are preferentially absorbed and the air for breathing is purified.

3. In clarification of sugar : Sugar is decolorized by treating sugar solution with charcoal powder. The later adsorbs the undesirable colours present.

4. In softening of hard water : The use of ion exchangers for softening of hard water is based upon the principle of competing adsorption just as in chromatography.

5. In removing moisture from air in the storage of delicate instruments : Such instruments which may be harmed by contact with the moist air, are kept out of contact with moisture using silica gel.

6. In Adsorption indicator : Various dyes, which owe their use to adsorption, have been introduced as indicator particularly in precipitation titration. For example, KBr is easily titrated with $AgNO_3$ using eosin as indicator.

1.17.9 Adsorption kinetics-the rate of adsorption[15, 75]

The rate of adsorption, R_{ads}, of a molecule onto a surface can be expressed in the same manner as any kinetic process. For example, when it is expressed in terms of the partial pressure of the molecule in the gas phase above the surface:

$$R_{ads} = k' P^{x};$$

where x = kinetic order ; k' = rate constant ; P = partial pressure

If the rate constant is expressed in an Arrhenius form, then we obtain a kinetic equation of the form : $R_{ads} = A \exp (-E_a / RT). P^{x}$

where E_a is the *activation energy for adsorption,* and A the *pre-exponential (frequency) factor*.

It is much more informative, however, to consider the factors controlling this process at the molecular level .

The rate of adsorption is governed by

1. the rate of arrival of molecules at the surface
2. the proportion of incident molecules which undergo adsorption

i.e. we can express the rate of adsorption (per unit area of surface) as a product of the incident molecular flux, *F*, and the sticking probability, *S* .

$$R_{ads} = S \,.\, F \qquad [\text{molecules m}^{-2}\ \text{s}^{-1}\ ]$$

The flux of incident molecules is given by the Hertz-Knudsen equation

$$\text{Flux,}\ \ F = P / (2\pi mkT)^{1/2} \qquad [\ \text{molecules m}^{-2}\ \text{s}^{-1}\ ]$$

Where, P = gas pressure [N m^{-2}] ; m = mass of one molecule [kg] ; T = temperature [K]

The sticking probability is clearly a property of the adsorbate / substrate system under consideration but must lie in the range $0 < S < 1$; it may depend upon various factors - foremost amongst these being the existing coverage of adsorbed species (θ) and the presence of any activation barrier to adsorption. In general, therefore,

$$S = f\,(\theta \exp\,(\,-E_a / RT\,))\ .$$

where, once again, E_a is the activation energy for adsorption and $f(\theta)$ is some, as yet undetermined, function of the existing surface coverage of adsorbed species.

Combining the equations for *S* and *F* yields the following expression for the rate of adsorption :

$$R = \frac{f(\theta).P}{\sqrt{2\pi mkT}} \exp(-E_a / RT)$$

The above equation indicates that the rate of adsorption is expected to be first order with regard to the partial pressure of the molecule in the gas phase above the surface.

It should be recognised that the activation energy for adsorption may itself be dependent upon the surface coverage, i.e. $E_a = E(\theta)$.

If it is further assumed that the sticking probability is directly proportional to the concentration of vacant surface sites (which would be a reasonable first approximation for non-dissociative adsorption) then $f(\theta)$ is proportional to $(1-\theta)$; where, in this instance, θ is the fraction of sites which are occupied (i.e. the Langmuir definition of surface coverage).

1.18 Characterization techniques

1.18.1 Principle of FT-IR[2, 76]

Infrared spectroscopy is an important technique in organic chemistry. It is an easy way to identify the presence of certain functional groups in a molecule. Also, one can use the unique collection of absorption bands to confirm the identity of a pure compound or to detect the presence of specific impurities.

FT-IR spectroscopy has been a workhorse technique for materials analysis in the lab for over 70 years. An IR spectrum represents a fingerprint of a sample with absorption peaks which correspond to the frequencies of vibrations between the bonds of the atoms making up the material. Because each different material is a unique combination of atoms, no two compounds produce the same IR spectrum. Therefore, IR spectroscopy can result in a positive identification (qualitative analysis) of every different kind of material. In addition, the size of the peaks in the spectrum is a direct indication of the amount of material present. With intuitive software algorithms, infrared is an excellent tool for quantitative analysis.

Figure 1.19: Basic components of FT-IR[76(a)]

The basic components of an FTIR are shown schematically in **Figure 1.19**. The infrared source emits a broad band of different wavelength of infrared radiation. The IR radiation goes through an interferometer that modulates the infrared radiation. The interferometer performs an optical inverse Fourier transform on the entering IR radiation. The modulated IR beam passes through the gas sample where it is absorbed to various extents at different wavelengths by the various molecules present. Finally the intensity of the IR beam is detected by a detector, which is a liquid-nitrogen cooled MCT (Mercury-Cadmium-Telluride) detector in the case of the Temet GASMET FTIR CR-series. The detected signal is digitised and Fourier transformed by the computer to get the IR spectrum of the sample gas.

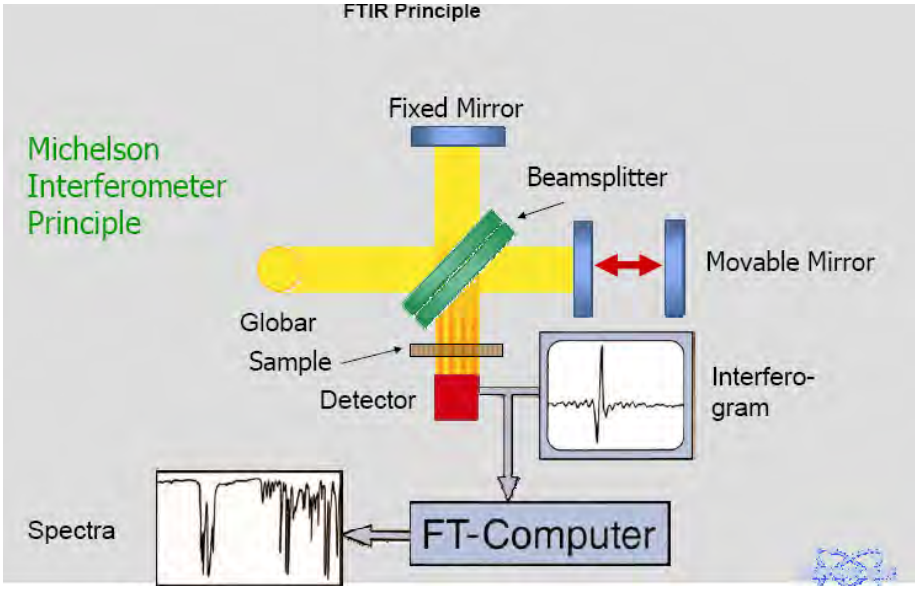

Figure 1.20: Michelson Interferometer

The unique part of an FTIR spectrometer is the interferometer. A Michelson type plane mirror interferometer is displayed in **Figure 1.20.** Infrared radiation from the source is collected and collimated (made parallel) before it strikes the beam splitter. The beam splitter ideally transmits one half of the radiation, and reflects the other half. Both transmitted and reflected beams strike mirrors, which reflect the two beams back to the beam splitter. Thus, one half of the infrared radiation that finally goes to the sample gas has first been reflected from the beam splitter to the *moving* mirror, and then back to the beam splitter. The other half of the infrared radiation going to the sample has first gone through the beam splitter and then reflected from the *fixed* mirror back to the beam splitter. When these two optical paths are reunited, interference occurs at the beam splitter because of the optical path difference caused by the scanning of the moving mirror.

The optical path length difference between the two optical paths of a Michelson interferometer is two times the displacement of the moving mirror. The interference signal measured by the detector as a function of the optical path length difference is called the interferogram. A typical interferogram produced by the interferometer is shown in **Figure 1.21.**The graph shows the intensity of the infrared radiation as a function of the displacement of the moving mirror. At the peak position, the optical path length is exactly the same for the radiation that comes from the moving mirror as it is for the radiation that comes from the fixed mirror.

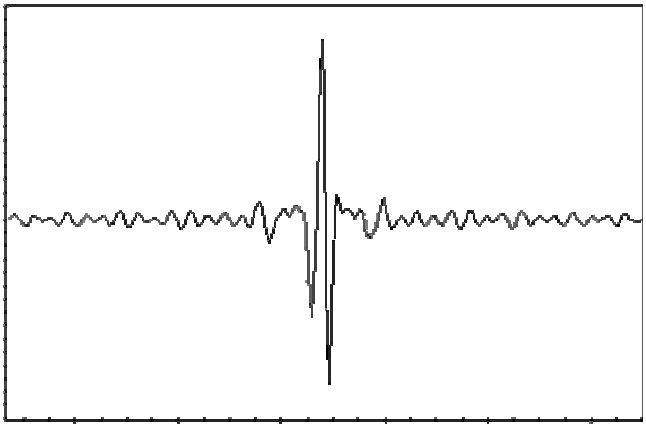

Figure 1.21: A typical interferogram[76(a)]

The spectrum can be computed from the interferogram by performing a Fourier transform. A mathematical function called a Fourier transform allows us to convert an intensity-vs.-time spectrum into an intensity-vs.-frequency spectrum.

The Fourier transform:

$$A(r) = \sum X(k) \exp\left(-2\pi \frac{irk}{N}\right)$$

A(r) and X(k) are the frequency domain and time domain points, respectively, for a spectrum of N points.

1.18.2 Principle of X-ray Diffractometer (XRD)[2, 77]

X-ray diffraction (XRD) is one of the most powerful technique for qualitative and quantitative analysis of crystalline compounds. The technique provides information that cannot be obtained any other way. The information obtained includes types and nature of crystalline phases present, structural make-up of phases, degree of crystallinity, amount of amorphous content, micro strain & size and orientation of crystallites.

When a material (sample) is irradiated with a parallel beam of monochromatic X-rays, the atomic lattice of the sample acts as a three dimensional diffraction grating causing the X-ray beam to be diffracted to specific angles. The diffraction pattern, that includes position (angles) and intensities of the diffracted beam, provides several information about the sample and are discussed below:

- Angles are used to calculate the interplanar atomic spacing (d- spacing). Because every crystalline material will give a characteristic diffraction pattern and can act as a unique 'fingerprint', the position (d) and intensity (I) information are used to identify the type of material by comparing them with patterns for over 80,000 data entries in the database, complied by the Joint Committee for Diffraction Standards (JCDS).By this method, identification of any crystalline compounds, even in a complex sample, can be made.
- The position (d) of diffracted peaks also provides information about how the atoms are arranged within the crystalline compound (unit cell size or lattice parameter). The intensity information is used to assess the type and nature of atoms. Determination of lattice parameter helps understand extent of solid solution (complete or partial substitution of one element for another, as in some alloys) in a sample.
- Width of the diffracted peaks is used to determine crystallite size and micro-strain in the sample.
- The 'd' and 'I' from a phase can also be used to quantitatively estimate the amount of that phase in a multi-component mixture.

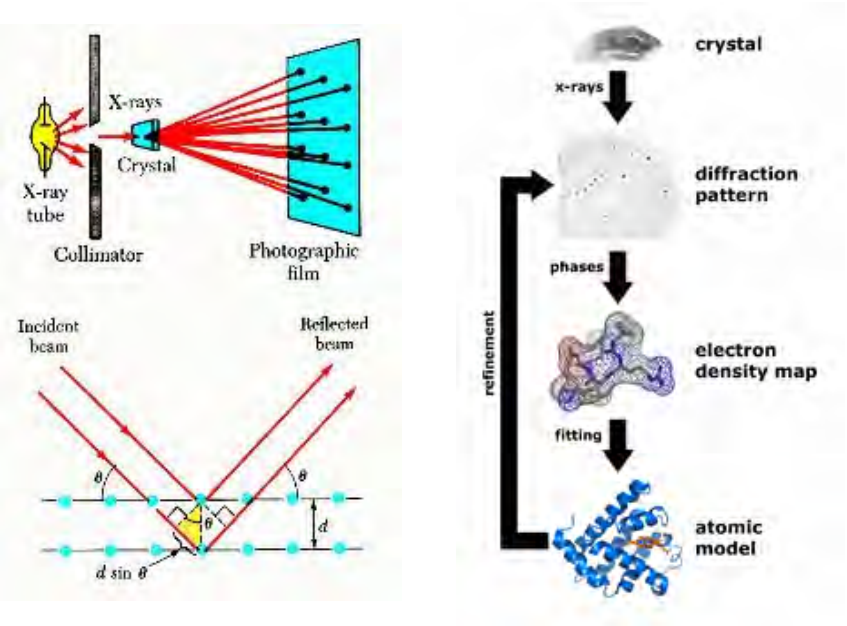

Figure1.22: Workflow for solving the structure of a molecule by X-ray crystallography[2,77].

As mentioned earlier, XRD can be used not only for qualitative identification but also for quantitative estimation of various crystalline phases. This is one of the important advantage of the important advantage of X-ray diffraction technique. Several methods have been proposed and successfully used to quantify crystalline phases in mixtures. They include external standard methods, the reference-intensity-ratio (RIR) method, chemical methods and the whole pattern fitting Rietveld method. Of the available methods, the Rietveld method is probably the most accurate and reliable method. The Rietveld method is a whole-pattern fitting least squares refinement technique and has been successfully used for quantification and characterization of inorganic and organic compounds It has also been used for crystal structure refinement, to determine size and strain of crystallites.

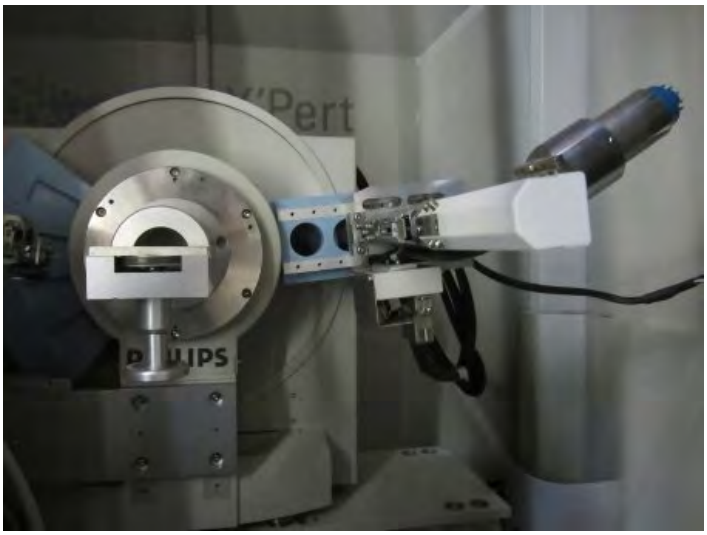

Figure1.23: X-ray diffractiometer

1.18.3 Principle of Scanning Electron Microscope (SEM) [2, 78]

A typical SEM instrument, showing the electron column, sample chamber, EDS detector, electronics console, and visual display monitors. The scanning electron microscope (SEM) uses a focused beam of high-energy electrons to generate a variety of signals at the surface of solid specimens. The signals that derive from electron-sample interactions reveal information about the sample including external morphology (texture), chemical composition, and crystalline structure and orientation of materials making up the sample. In most applications, data are collected over a selected area of the surface of the sample, and a 2-dimensional image is generated that displays spatial variations in these properties. Areas ranging from approximately 1 cm to 5 microns in width can be imaged in a scanning mode using conventional SEM techniques (magnification ranging from 20X to approximately 30,000X, spatial resolution of 50 to 100 nm). The SEM is also capable of performing analyses of selected point locations on the sample; this approach is especially useful in qualitatively or semi-quantitatively determining chemical compositions (using EDS), crystalline structure, and crystal orientations (using EBSD).

The scanning electron microscope (SEM) enables the investigation of specimens with a resolution down to the nanometer scale. Here an electron beam is generated by an electron cathode and the electromagnetic lenses of the column and finally swept across the surface of a sample (**Fig.1.24**). The path of the beam describes a raster which is correlated to a raster of gray level pixels on a screen. As a consequence the magnification is simply computed by the ratio of the image width of the output medium divided by the field width of the scanned area.

Figure 1.24 : Scanning electron microscope

The main signals which are generated by the interaction of the primary electrons (PE) of the electron beam and the specimen's bulk are secondary electrons (SE) and backscattered electrons (BSE) and furthermore X rays. They come from an interaction

volume in the specimen which differs in diameter according to different energies of the primary electrons (typically between 200 eve and 30 keg). The SE come from a small layer on the surface and yield the best resolution, which can be realized with a scanning electron microscope. The well known topographical contrast delivers micrographs which resemble on conventional light optical images.

The BSE come from deeper regions of the investigated material thus giving a lower resolution. The typical compositional contrast gives material specific information since the signal is brighter for regions of a higher middle atomic number of the investigated area. As a byproduct of the image giving signals X-rays are produced. They result from ionization processes of inner shells of the atom leading to electromagnetic radiation. The characteristic X-rays give information about the chemical composition of the material. The methods energy dispersive X-ray spectroscopy (EDS) and wavelength dispersive X-ray spectroscopy (WDS) enable the detection of chemical elements from Boron to Uranium in a qualitative and even quantitative manner. They differ in the energy resolution (the energy values are correlated to the line energy of a special chemical element) in the processing and in time of measurement.

In the conventional scanning electron microscope, which operates in high vacuum, the specimen has to be electrically conductive or has to be coated with a conductive layer (e.g. Carbon, Gold etc.).

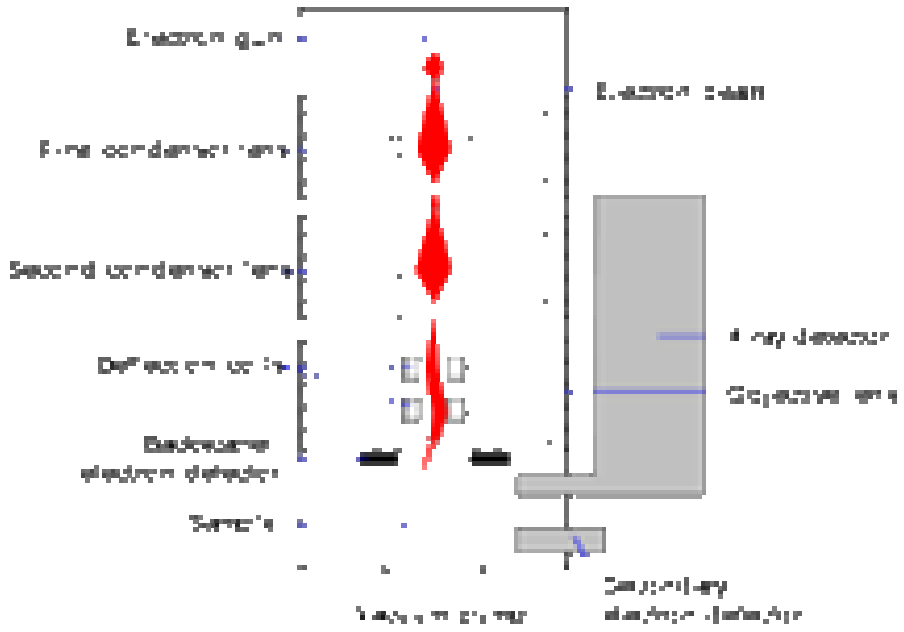

Figure1.25 : Schematic diagram of a SEM[2]

Essential components of all SEMs include the following:

- Electron Source ("Gun")
- Electron Lenses
- Sample Stage
- Detectors for all signals of interest
- Display / Data output devices
- Infrastructure Requirements:
    - Power Supply
    - Vacuum System
    - Cooling system
    - Vibration-free floor
    - Room free of ambient magnetic and electric fields

SEMs always have at least one detector (usually a secondary electron detector), and most have additional detectors. The specific capabilities of a particular instrument are critically dependent on which detectors it accommodates.

1.18.4 Principle of Differential Thermal Analysis (DTA) [79]

Both Differential Thermal Analysis (DTA) and Differential Scanning Calorimetry (DSC) are concerned with the measurement of energy changes in materials. They are thus the most generally applicable of all thermal analysis methods, since every physical or chemical change involves a change in energy.

DTA is the older technique. The principle of the "classical" arrangement is readily explained with reference to the following figures.

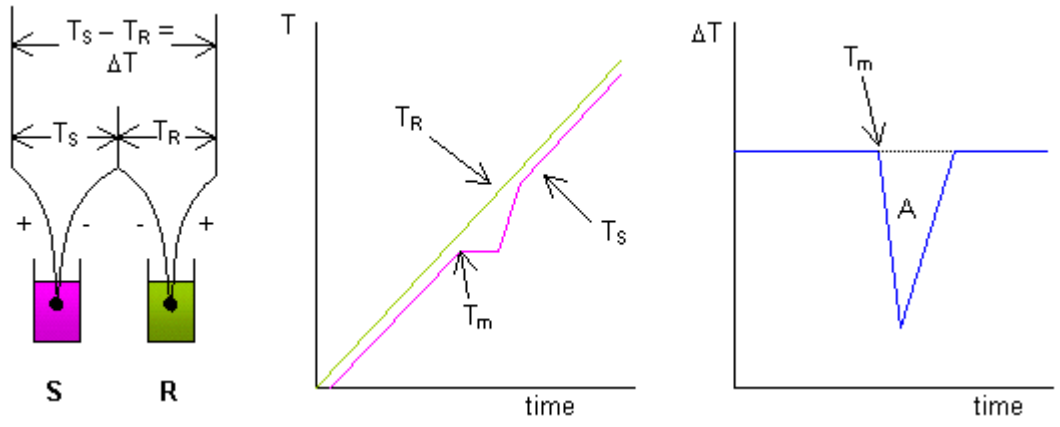

Figure 1.26: Illustration of principles of DTA[79 (a)]

S and **R** are containers holding the Sample and an inert Reference material. In these are thermocouples measuring their respective temperatures. By connecting the thermocouples in opposition, the difference in temperature (Delta T) is also measured. If

S and **R** are heated at the same rate, by placing them in the same furnace, their temperatures will rise as in the middle figure. $\mathbf{T_R}$ rises steadily, as the reference material is chosen to have no physical or chemical transitions. $\mathbf{T_S}$ also rises steadily in the absence of any transitions, but if for instance the sample melts, its temperature will lag behind $\mathbf{T_R}$ as it absorbs the heat energy necessary for melting. When melting is complete, steady heating is resumed. The right-hand figure shows the DTA curve - a plot of Delta T against time, or more usually, sample temperature. The curve shows an endothermic (heat-absorbing) peak. If an exothermic (heat-producing) event had occurred, the curve would show a peak in the opposite direction. The area **A** on the curve is proportional to the heat of the reaction:

$$\Delta H = K.A = K\int \Delta T.dt$$

The constant **K** comprises many factors, including the thermal properties of the sample, and varies with temperature. The generation of quantitative data using the "classical" arrangement above is laborious.

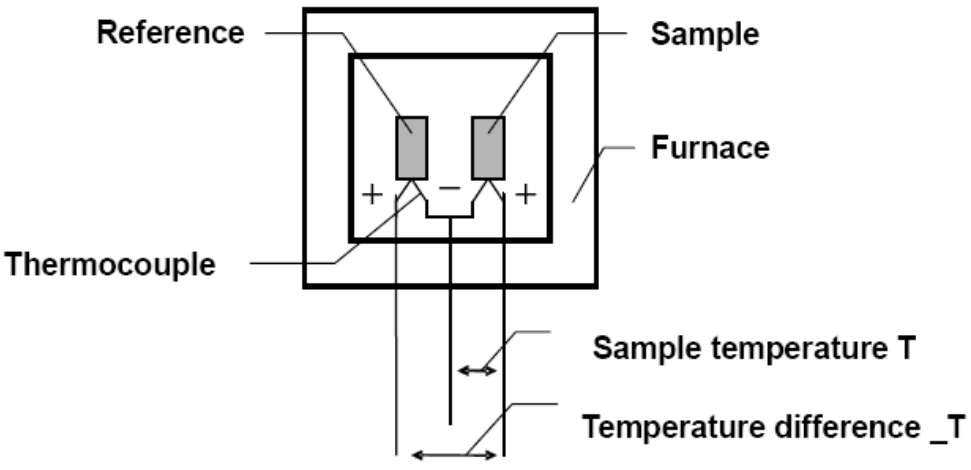

Figure 1.27 : DTA device structure[79(c)]

Nowadays the thermocouples are rarely, if ever in the sample itself, but are placed below the container, which has the effect of reducing the influence of sample properties on the area of the DTA peak. With such designs, it is easier to determine the variation in **K** with temperature, and quantitative data are more readily obtained. DTA instruments are still valuable, particularly at higher temperatures (>1000^{0}C), or in aggressive environments.

1.18.5 Principle of Thermo gravimetric Analysis (TGA) [2, 15]

The diagram shows the configuration of a device that conducts TG and DTA measurements simultaneously with a horizontal scale in a differential structure. The respective balance beams for the sample and the reference are placed in the furnace, mass is measured with drive coils sensitivity-calibrated for the sample and the reference independently, and the difference in mass is output as TG signal.

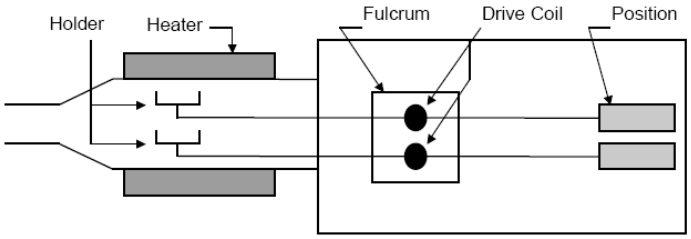

Figure 1.28 : Horizontal Differential TG-DTA Device Structure[79(c)]

By conducting mass measurements differentially, effects of beam expansion, convection and effects of buoyancy are cancelled and high sensitivity thermal mass measurement is achieved. By measuring with independent drive coils for the sample and reference, TG baseline drift(baseline movement due to temperature change) can be adjusted easily and electrically. Also, thermocouple is placed directly below the respective holders for the sample and reference, measuring sample temperature while outputting DTA signal simultaneously.

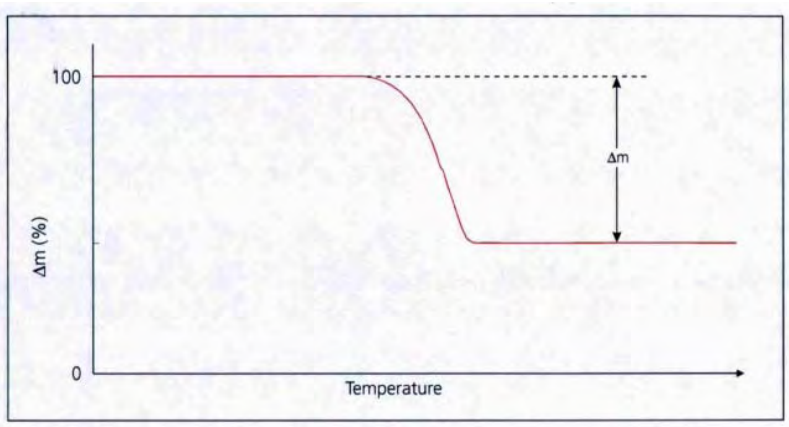

Figure 1.29 : Step of weight loss with increasing temperature[79 (b)]

In this technique changes in the mass of a sample are studied while the sample is subjected to a controlled temperature program. Most often a linear increase in temperature is followed but isothermal studies can be carried out, when changes in sample mass with time are noted. TGA is inherently quantitative, and therefore an extremely powerful thermal technique, but gives no direct chemical information. The ability to analyze the volatile products during a weight loss is of great value.

Careful calibration for temperature is important, especially for kinetic studies. Various means are available for temperature calibration, which is not a trivial matter, though reproducibility is often more important than absolute accuracy. Weight calibration is readily achieved using standard weights.

1.18.6 Principle of Atomic Absorption Spectrophotometer (AAS)[2]

Atomic absorption spectroscopy (AAS) is a spectro-analytical procedure for the qualitative and quantitative determination of chemical elements employing the absorption of optical radiation (light) by free atoms in the gaseous state. In analytical chemistry the

technique is used for determining the concentration of a particular element (the analyte) in a sample to be analyzed. AAS can be used to determine over 70 different elements in solution or directly in solid samples. Atomic absorption spectrometry was first used as an analytical technique, and the underlying principles were established in the second half of the 19th century by Robert Wilhelm Bunsen and Gustav Robert Kirchhoff, both professors at the University of Heidelberg, Germany. The modern form of AAS was largely developed during the 1950s by a team of Australian Chemists. They were led by Sir Alan Walsh at the CSIRO (Commonwealth Scientific and Industrial Research Organization), Division of Chemical Physics, in Melbourne, Australia.

The technique makes use of absorption spectrometry to assess the concentration of an analyte in a sample. It requires standards with known analyte content to establish the relation between the measured absorbance and the analyte concentration and relies therefore on Beer-Lambert Law. In short, the electrons of the atoms in the atomizer can be promoted to higher orbitals (excited state) for a short period of time (nanoseconds) by absorbing a defined quantity of energy (radiation of a given wavelength). This amount of energy, i.e., wavelength, is specific to a particular electron transition in a particular element. In general, each wavelength corresponds to only one element, and the width of an absorption line is only of the order of a few picometers (pm), which gives the technique its elemental selectivity. The radiation flux without a sample and with a sample in the atomizer is measured using a detector, and the ratio between the two values (the absorbance) is converted to analyte concentration or mass using Beer-Lambert Law.

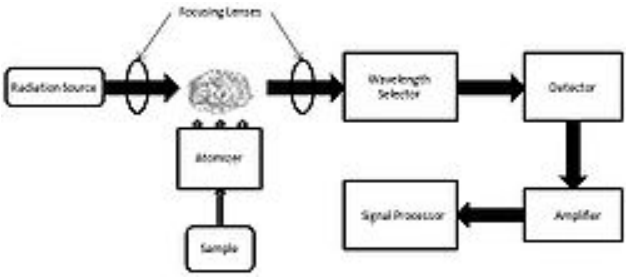

Figure 1.30 : Atomic absorption spectrometer block diagram[2]

The basic instrument for atomic absorption requires a light source, an atom source, a monochrometer to isolate the specific wavelength of light, a detector, some electronics to treat the signal, and a data display. The light source is usually a hollow cathode lamp.

Figure 1.31 : Atomic absorption spectrophotometer

Atomic spectroscopy has experienced remarkable growth and diversity in the past few years, making it more difficult for analysts to keep up with developments in the field. Atomic spectroscopy is not one but three techniques: 1) atomic absorption, 2) atomic emission, and 3) atomic fluorescence. The first two are the most common and widely used techniques. The linear relationship between the amount of light absorbed or emitted and the amount of species of interest is called the Beer-Lambert Law. It can be used to

find unknown concentrations by measuring the light emitted or absorbed.

1.19 Review of Background Literature[15]

A review of the current developments in the area of treatment of wastewater by composite materials prepared by different method is represented in this section. Present research is focused on the treatment of wastewater containing chromium (VI) with silica coated iron oxide composite material prepared by different methods and hence a detailed review is presented on core-shell (coated) composites. Review of the literature reveals that considerable volume of research have been carried out to develop coated composites and their applications on waste water treatment for removal of hexavalent chromium .

Gang et al.[26] studied removal of Cr(VI) by modified poly(4-vinyl pyridine) (PVP)-coated silica gel. Their research involved the synthesizing of a reactive polymer, long alkyl quarternized poly(4-vinyl pyridine) (PVP) and coating it on the surface of silica gel to produce a granular sorbent . The sorbent was used to remove Cr(VI) from water. Batch experiments were conducted to determine the kinetics, sorption isotherm, pH effects and influence of other ions on the chromium adsorption onto the coated silica gel. The research demonstrated that the synthesized PVP-coated silica gel (referred to as coated gel) could successfully remove Cr(VI) from solution. The adsorption of Cr(VI) by the coated gel was strongly influenced by the pH. The maximum sorption occurred at about pH 4.5-5.5 under the test conditions. The removal efficiency was 100% when the initial Cr(VI) concentration was 2.5 mg/L using 2.5 g/L of coated gel at pH 5.0. The concentration of Cr(VI) had a pronounced effect on the rate of sorption. They also

reported that compared to ion exchange, the sorption kinetics of Cr(VI) were fast and equilibrium sorption data fitted the Langmuir isotherm model.

Albino et al (2006) [80] reported that aniline formaldehyde condensate (AFC) coated silica gel for removal of Cr(VI) from wastewater by considering the effects of various parameters like reaction pH, dose of AFC coated silica gel, initial Cr(VI) concentration and aniline to formaldehyde ratio in AFC synthesis. The optimum pH for total chromium [Cr(VI) and Cr(III)] adsorption was observed as 3. Total chromium adsorption was second order and equilibrium was achieved within 90–120 min. Aniline to formaldehyde ratio of 1.6:1 during AFC synthesis was ideal for chromium removal. Total chromium adsorption followed Freundlich's isotherm with adsorption capacity of 65 mg/g at initial Cr(VI) 200 mg/L. Total chromium removal was explained as combinations of electrostatic attraction of acid chromate ion by protonated AFC, reduction of Cr(VI) to Cr(III) and bond formation of Cr(III) with nitrogen atom of AFC. Almost 40–84% of adsorbed chromium was recovered during desorption by NaOH, EDTA and mineral acids.

Sangkorn Kongjao et al (2007) [81] studied removal of chromium from tannery wastewater by electro precipitation technique in a batch electrochemical membrane reactor. This reactor, having a total capacity of 1 liter, was separated into two compartments (anodic and cathode compartments) by using an anionic membrane. A stainless steel sheet with the square holes having total surface area of 0.0215 m^2 and a Ti/RuO_2 grid was used as the cathode and anode, respectively. The results indicated that the optimum condition for removal of chromium from tannery wastewater was found at

the current density of 60.5 A/m^2 at initial pH of 4.5. At this condition, more than 98% of chromium was removed within 60 min. Some organic pollutants contained in wastewater such as oil and grease, color and the level of biochemical oxygen demand (BOD), chemical oxygen demand (COD) and total kjeldahl nitrogen (TKN) were also markedly reduced.

Bailey et al. [82] prepared a new adsorbent media consisting of iron oxide coated onto sand surface. The oxide coating was made by adding a solution of ferric salt and base to a mixture of sand and applying various heating protocols. Depending on solution pH, the media can be made to adsorb either cationic or anionic elements. In the work, the media was used to collect hexavalent chromium from a synthetic waste stream. The effluent contained 20 mg/L Cr(VI), and better than 99% removal was achieved consistently. The chromium (VI) removed by sorption to the sand was concentrated at least forty fold using a relatively low pH regeneration process. Regeneration at pH 9.5 was slower than when a 1.0 $moldm^{-3}$ NaOH solution was used, but the media appears to have a longer working life when the less alkaline solution was employed.

Borai et. al.(2007)[83] studied the removal of chromium species from wastewater by using mixed silica and alumina hosted carboxylate oxide. The experimental work was developed to improve the physical and chemical characteristics of the prepared mesoporous SiO_2–Al_2O_3 mixed oxides via a sol–gel process. The effective key parameter on the properties of the materials was achieved by the addition of carboxylate functional group such as Alph-hydroxyl isobutyric acid (AHIBA) during the gelation process and prior the calcinations step. Better performance of these carboxylate resins were attributed

to the complexing ability of the carboxylate groups toward polyvalent chromium species which was added to the normal sorption properties of the oxides. Introduction of Al and Si salts together to form mixed oxide modified the way of their substitution in the hosting resin than when they were separately added. The data revealed that mesoporous materials with very narrow pore diameter distribution (micron-sized) and high surface area were obtained. The surface areas and pore size distributions were mainly depend on SiO_2 content. Systematic investigations were carried out on the set of the prepared mixed oxides with different porosity, cross-linking degree and exchange loading to find out the best sorbent for chromium removal.

A fast and efficient method for the removal of hexavalent chromium from aqueous solutions was studied by **Mansoor Anbia et. Al. (2011)** [84] . In this study, removal of chromium (VI) from aqueous solution by as synthesized MCM-48 adsorbent was studied. Cetyltrimethylammonium bromide (CTAB) was used as a cationic template for the synthesis of MCM-48. The extent of adsorption was investigated as a function of solution pH, agitation speed, contact time, adsorbent and adsorbate concentrations, reaction temperature and supporting electrolyte (sodium chloride). Langmuir and Freundlich isotherms were used to model the adsorption equilibrium data. The adsorption of Cr (VI) was found to be maximum at pH values in the range of 1–3. The yielded maximum adsorption capacity of 153.8 mg/g at initial concentration of 800 (mg/L) was well predicted by the Langmuir isotherm. Compared to the various adsorbents reported in the literature, the surfactant-containing material prepared in this study showed promise for practical applications.

The adsorption of chromium compounds from solutions by a composite of polyaniline/poly ethylene glycol (PANi/PEG) was investigated by **Samani et al.(2010)**[85] . Experiments were conducted in batch mode under various operational conditions including agitation time, solution pH, PANi/PEG dose and initial concentration of chromium salts. Results showed that concentration of PEG at synthesizing stage has a significant effect on the capacity of produced composite for removal of chromium. Morphologically, PANi/PEG composite was closely dependent on the concentration of PEG. Maximum removal of hexavalent chromium was experienced when 2g/L of PEG was used in synthesis of PANi/PEG. Removal of hexavalent chromium by PANi/PEG composite included surface adsorption and reduction reaction. The optimum pH was 5 and the equilibrium time for hexavalent chromium removal was about 30 min. Investigation of the isothermal characteristics showed that chromium adsorption by PANi/PEG composite was in high accordance with Langmuir's isotherm.

Gupta,V.K., et. al(2011) [86] showed the chromium removal process by using multiwall carbon nanotubes (MWCNTs) /nano-iron oxide composites . The process involves combination of the magnetic properties of iron oxide with adsorption properties of carbon nanotubes. In the study, the adsorption features of (MWCNTs) with the magnetic properties of iron oxides have been combined in a composite to produce a magnetic adsorbent. Composites of MWCNT/nano-iron oxide were prepared, and were characterized by X-ray diffraction (XRD), field emission scanning electron microscope (FESEM) and Fourier transform infrared spectroscopy (FTIR). XRD suggests that the magnetic phase formed was maghemite and/or magnetite. FESEM image shows nano-

iron oxides attached to a network of MWCNTs. The adsorption capability of the composites was tested in batch and fixed bed modes. The composites have demonstrated a superior adsorption capability to that of activated carbon. The results also showed that the adsorptions of Cr(III) on the composites was strongly dependent on contact time, agitation speed and pH, in the batch mode; and on flow rate and the bed thickness in the fixed bed mode. Along with the high surface area of the MWCNT's, the advantage of the magnetic composite was that it can be used as adsorbent for contaminants in water and can be subsequently controlled and removed from the medium by a simple magnetic process.

Veera M. Boddu et.al(2003) [87] used Chitosan biosorbent for the removal of hexavalent chromium. The composite, chitosan biosorbent was prepared by coating chitosan, a glucosamine biopolymer, onto ceramic alumina. The composite bioadsorbent was characterized by high-temperature pyrolysis, porosimetry, scanning electron microscopy, and X-ray photoelectron spectroscopy. Batch isothermal equilibrium and continuous column adsorption experiments were conducted at 25 °C to evaluate the biosorbent for the removal of hexavalent chromium from synthetic as well as field samples obtained from chrome plating facilities. The effect of pH, sulfate, and chloride ion on adsorption was also investigated. The biosorbent loaded with Cr(VI) was regenerated using 0.1 M sodium hydroxide solution. A comparison of the results of the present investigation with those reported in the literature showed that chitosan coated on alumina exhibits greater adsorption capacity for chromium(VI). Further, experimental equilibrium data were fitted to Langmuir and Freundlich adsorption isotherms, and values

of the parameters of the isotherms are reported. The ultimate capacity obtained from the Langmuir model was 153.85 mg/g chitosan.

Eisazadeh, H. (2007) [88] showed the chromium removal efficiency of the polyaniline-polyvinyl alcohol composites. In this article, the preparation of polyaniline and its composites as adsorbents were discussed and the capability of separating chromium from industrial waste water was studied. The results were compared with anthracite and cation exchangers such as purolite-302 and amberjet. The observations indicated that the purolite and amberjet have the most chromium removal percentage. Also the role of polyaniline and its composite as adsorbents were studied. The results show that the percentage of chromium removal has increased in polyaniline/poly(vinyl alcohol) composite. Furthermore, the adsorption percentage was related to the surface morphology, type of adsorbents, and their weight ratios.

Synthesis, characterization and studies of the efficiency of chromium removal from wastewater by hydrotalcite-like compounds (HLC) with Mg/Al =2 was studied by **N. Guti´errez et. al (2009)** [89] . Hydrotalcite-like compounds are also known as layered double hydroxides. The general formula of HLC can be expressed as [M(II)1¡*x*M(III)*x*(OH)2]*x*+ A*n*¡ *x*=*n*; where M(II) was a divalent metal ion, M(III) was a trivalent metal and A was an anion that occupy the interlayer region of these crystalline materials. These anions were exchanged according to the affinity scale reported by Miyata. The hydrotalcite-like compounds were commonly prepared by co-precipitation of metallic salts in alkaline medium at constant pH . With the purpose of modifying the textural properties of the HLC, these substances were synthesized by the sol - gel method . In the study, HLC with Mg/Al =2 were synthesized by the sol-gel method, with the

purpose of modifying their thermal and textural properties and determine their sorption capacity for Cr (VI). Additionally, the HLC was heated at 350±C and the product was also used as a sorbent for Chromium (VI). The maximum chromium (VI) uptake by hydrotalcite-like compounds and its heated product were 100 and 125 mg of Cr (VI)/g, respectively.

Sharma Y.C., et al (2009) [90] showed the chromium removal efficiency by using the adsorbent, iron nanoparticle. Nanoparticles of iron were prepared by sol–gel method. The characterisation of the nanoparticles was carried out by XRD and TEM analysis. Batch experiments were adopted for the adsorption of Cr(VI) from its solutions. The effect of different important parameters such as contact time and initial concentration, pH, adsorbent dose, and temperature on removal of chromium was studied. The removal of chromium increased from 88. 5% to 99.05% by decreasing its initial concentration from 15 to 5mgL^{-1} at optimum conditions. Removal of Cr(VI) was found to be highly pH dependent and a maximum removal (100%) was obtained at pH 2.0. The process of removal was governed by first and pseudo-second-order kinetic equations and their rate constants were determined. The process of removal was also governed by intra particle diffusion. Values of the thermodynamic parameters viz. $\Delta G°$, $\Delta H°$, and $\Delta S°$ at different temperatures were determined. Adsorption results indicate that nano iron particles can be effective for the removal of chromium from aqueous solutions.

A. P. Carnizello et al (2009) [91] showed Takovite−Aluminosilicate Nanocomposite as Adsorbent for Removal of Cr(III) and Pb(II) from Aqueous Solutions. This work reports on the application of a takovite−aluminosilicate nanocomposite, synthesized by a co-precipitation procedure, as adsorbent for the removal of Cr(III) and Pb(II) from aqueous

solutions. Experimental studies to determine the maximum fixation capacities, the adsorption isotherms, and the affinity order of the adsorption process were carried out. The sorption of Pb(II) ions was fast, and the equilibrium was reached within 20 min, while 180 min was necessary for the equilibrium to be reached in the case of Cr(III) ions. The adsorption kinetics of cations was studied in terms of pseudo-first-order and pseudo-second-order kinetics. The Freundlich and Sips isotherm models have also been applied to the equilibrium adsorption data. The takovite−aluminosilicate nanocomposite material had excellent textural properties and was used as an efficient adsorbent of Cr(III) and Pb(II) cations.

Removal of Chromium (VI) from water by using Lanthanum based Hybrid Materials was studied by **Langkam, Johny (2011)** [92].Cr (VI) was removed from water by a synthesized Lanthanum based hybrid material as adsorbent. The removal of fluoride was 98.50 % at optimum condition from the synthetic solution having initial Cr(VI) concentration of 100 mg/L The extend of adsorption was investigated as a function of solution pH, contact time, adsorbent concentration, reaction temperature . Langmuir and Freundlich isotherm were used to construct the adsorption equilibrium data.

Application of Cellulose-Clay Composite Biosorbent toward the Effective Adsorption and Removal of Chromium from Industrial Wastewater was studied by **Santhana et al (2012)**[93]. An effective methodology for the detoxification of chromium using cellulose-montmorillonite composite material as the adsorbent was reported here. The interaction of surfactant modified sodium montmorillonite (NaMMT) with cellulose biopolymer was followed by the subsequent adsorption of Cr(VI) from aqueous solution as bichromate anion onto the surface of the biocomposite material. The composite

adsorbent was characterized comprehensively using Fourier transform infrared spectroscopy (FT-IR), Energy dispersive X-ray spectrometry (EDX), X-ray diffraction (XRD) and Branauer-Emmett-Teller (BET) isotherm studies. The material exhibited a maximum adsorption capacity of 22.2 mg g^{-1} in accordance with the Langmuir isotherm model. The mesoporous nature of the material was ascertained from the nitrogen adsorption isotherm study and the adsorption process was in accordance with second order kinetics. The spontaneity of the adsorption process could be confirmed from the study of the adsorption thermodynamics. The composite material could be regenerated using sodium hydroxide as the eluent. The adsorbent could be reused with quantitative recovery for 10 adsorption–desorption cycles. An aqueous phase feed volume of 400 mL could be quantitatively treated by column method at 100 mg L^{-1} concentration of Cr(VI) with a preconcentration factor of 50. The applicability of the method was demonstrated in the quantitative removal of total chromium from a chrome tannery effluent sample.

Alejandra Pérez-Fonseca et al (2011) [94] showed Chitosan Supported onto gave Fiber—Postconsumer HDPE Composites for Cr(VI) Adsorption. Composites of high-density polyethylene and agave fibers coated with chitosan were used as adsorbent for Cr(VI). The adsorptions were made in batch and continuous systems. Different kinetic models were used to characterize the batch adsorption and to determine the adsorption capacity of the compound. To test the composite regeneration/reuse capability, the chromium content in the composite material was desorbed using different acids. The coated composites were characterized by scanning electron microscopy (SEM), attenuated total reflectance infrared spectroscopy (ATR-IR), and X-ray photoelectric spectroscopy (XPS). From the results it was found that the composite has a maximum

adsorption capacity of 200 mg Cr(VI)/g of chitosan at pH 4. Sulfuric acid proved to be a good desorbent of Cr(VI), allowing the material to be reused while keeping its adsorption properties. Finally, the results showed that the continuous system has higher sorption capacity than the batch system; it was determined that the system needs a minimum retention time of 20 min in order to use the material in the treatment of contaminated effluents.

1.20 Objectives with specific aims and possible outcome

Chromium is a common contaminant present in wastewaters. Industrial sources of Cr(VI) include leather tanning, textile dying cooling tower blow down, plating, electroplating, anodizing baths, rinse waters, etc. As a result, their effluents contain significant amounts of this metal. Chromium exhibits two oxidation states: Chromium (VI) and Chromium (III). At high levels, Chromium (VI) is more toxic than chromium (III) and is considered to be a group "A" human carcinogen because of its mutagenic and carcinogenic properties[95]. Different techniques have been employed for Chromium(VI) removal from wastewaters. Physicochemical treatments are commonly used because these techniques are more economical than the electrochemical ones . Sorption process is one of the most effective physical processes that may be used to remove Cr (VI) from wastewaters. The use of different type of composite materials for removal of Cr(VI) from industrial effluents has been reported earlier [81-94] .

In view of the importance of removing chromium species from waste water the present study envisages the following:

(1) Preparation of (i) silicon (IV) oxide by hydrolyzing tetraethylorthosilicate (TEOS) in ethanol-water solvent in acid medium ; (ii) iron oxide from iron hydroxide formed by

electrochemical method and (iii) iron oxide – silica composites containing different percentages of iron oxide by impregnating the synthesized silicon (IV) oxide and iron oxide following Sol-Gel method.

(2) To study the interaction of Cr(VI) in aqueous medium with the synthesized iron-oxide-silicon dioxide composite and hence to evaluate Cr(VI) removal efficiency of the iron oxide-silicon dioxide composite from aqueous medium.

The synthesized silicon (IV) oxide, iron oxide and iron oxide-silicon (IV) oxide composite will be characterized by FT-IR, TGA/DTA,XRD ,SEM and EDS.

(3) Sorption efficiency of the synthesized iron oxide-silicon (IV) oxide composites toward Cr(VI) was studied by investigating the effects of different (i) dosages of adsorbent, (ii) initial concentrations of Cr(VI) solution with contact time and (iii) pH of Cr(VI) solution with contact time. Cr(VI) adsorbed on iron oxide-silicon (IV) oxide composite was analysed by FT-IR technique to better understand the interaction of Cr(VI) with iron oxide-silicon (IV) oxide composite.

2. Experimental

2. Experimental

2.1.0 Materials and Chemicals used

2.1.1. Materials used

Adsorbate : Hexavalent chromium . Analytical grade potassium dichromate (VI) (BDH) were used as a precursor to Cr (VI).

Adsorbent : Iron oxide- SiO_2 composites of varied compositions were prepared in this research work according to the procedures described in section **2.2.3-2.2.5**

Solvent used: Double Distilled Water (DDW), pure ethanol (BDH) and analytical grade acetone (BDH) .

2.1.2 Chemical reagents used

All the chemical reagents used were of analytical grades. The following chemical reagents were used in this research :

(i) Tetraethylorthosilicate (TEOS) (Aldrich, Germany)

(ii) 1,5-Diphenylcarbazide (Farco, China)

(iii) Hydrochloric acid, HCl (Merck, Germany)

(iv) Sulphuric acid, H_2SO_4 (Merck, Germany)

(v) Phosphoric acid, H_3PO_4 (Merck, Germany)

(vi) Acetone (Merck, Germany)

(vii) Ethanol (Merck, Germany)

(viii) Ammonium Hydroxide (Merck, India)

(ix) Potassium dichromate (BDH, England)

(x) Sodium Chloride (Merck, India)

(xi) Sodium Hydroxide (Merck, India)

2.1.3 Instruments used

A number of instruments were used to analyze and characterize silicon (IV) oxide, iron oxide and iron oxide- SiO_2 composites prepared in this research. These includes :

(i) Scanning Electron Microscope (SEM)*(Model:JEOL JSM-6490LA, Made in Japan)

(ii) UV-Visible Recording Spectrophotometer (Model: UV-1601 Shimadzu Corporation, Made in Japan)

(iii) Simultaneous Thermal Analyzer (TGA/DTA)** (Model: SII EXSTAR6000 TG-DTA6300 Seiko Instrument Inc., Made in Japan)

(iv) X-Ray Diffractiometer (XRD)** (Model:X'Pert, Philips, Made in Netherland)

(v) FT-IR instrument(Model : FTIR -8400/8900,Shimadzu, Made in Japan)

(vi) Digital Balance (Model: FR-200 , Made in Japan)

(vii) pH Meter (Model: Ultra basic-10, Denver Instrument, Made in Germany)

(viii) Centrifuge Machine (Model: Hettich Universal 16A, Made in Germany)

(ix) Oven (Model: LDO-030E, Daihan Labtech Co. Ltd, Made in Korea)

(x) Hot plate (Model : MS 300 MTUPS)

(xi) Pyrex glassware

(xii) Ultrasonic Steri-cleaner (Model: LU-2, Labnics Equipment, Made in U.S.A.)

(xiii) Shaker (Heidolph Unimex 1010, Made in Germany)

(xiv) Atomic Absorption Spectrophotometer (AAS) (Model : PerkinElmer AAnalyst 800 , Made in U.S.A.)

(xv) Electro coagulator

[* Courtesy of Centre for Advanced Research in Sciences, University of Dhaka.
** Courtesy of BCSIR, Dhaka.]

2.2.0 Preparation of silicon (IV) oxide, iron oxide and Fe_2O_3 -SiO_2 composites

Silicon (IV) oxide, iron oxide and Fe_2O_3 -SiO_2 composites were prepared according to the following processes.

2.2.1 Preparation of silicon (IV) oxide

Silicon (IV) oxide was prepared by hydrolysis of tetraethylorthosilicate (TEOS) in ethanol. The ionic equation for the reaction between tetraethylorthosilicate (TEOS) and water in ethanol is:

$$Si(OR)_4 + H_2O \rightarrow HO\text{-}Si(OR)_3 + R\text{-}OH \ ; [\ R = C_2H_5\ ]$$

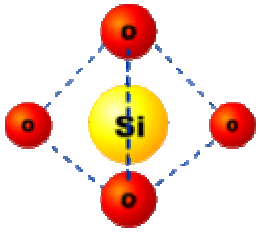

Figure 2.1(a) : Structure of silicon (IV) oxide

A simple one step protocol was used for the preparation of silica, which involves with the hydrolysis and condensation of tetraethylorthosilicate (TEOS) in ethanol : water mixture under acidic condition at room temperature. For the preparation of silicon (IV) oxide from TEOS ; TEOS, water and ethanol were mixed at 1.00 : 10.20 : 3.85 molar ratio[96]. At first 10.60 mL ethanol was taken in a 100 cm^3 beaker, and then 10.70 mL of TEOS was added followed by 9.00 mL water containing 0.20 mL molar HCl. It was then stirred constantly using a thermostated magnetic stirrer at ambient temperature for about one hour. The stirred mixture was then allowed to stand for two days for ageing so that gel formation was completed.

Figure 2.1 (b) : Photo of the prepared silicon (IV) oxide

The gel of silicon (IV) oxide was collected as a residue by filtration. Distilled water was poured on the silicon (IV) oxide gel several times to ensure removal of chloride or any other undesirable ions from silicon (IV) oxide because the presence of impurity will cover up the surface and hence the actual surface area will decrease. The gel was dried in an oven at 110^0C for 4 hours. Silicon (IV) oxide thus prepared was preserved in a desiccator for characterization. Schematic representation of the process is shown below :

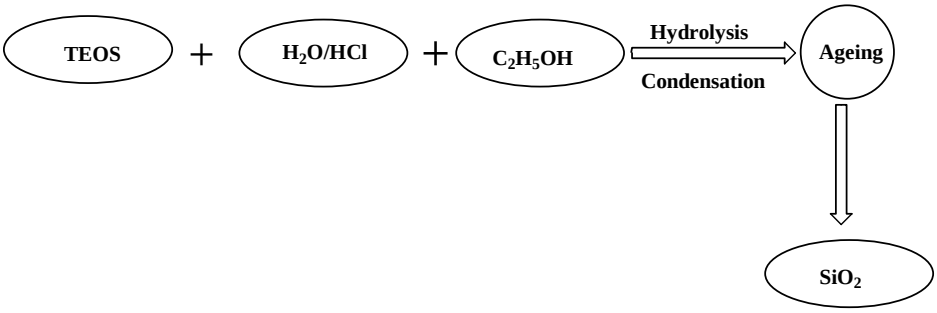

2.2.2 Electrochemical preparation of iron oxide

The electrochemical experiment was carried out in a two-electrode electrochemical cell containing iron as sacrificial electrodes. The experimental set up included the electrode assembly, a DC power supply unit, a voltage stabilizer, a resistance box to regulate the current and a multimeter to read the current values. The electrode assembly consisted of

pairs of iron plates (7.0 cm × 7.0 cm × 0.15 cm) placed in parallel arrangement. A photograph of the experimental set up is shown in **Figure 2.2 (a)** which is based on the diagram reported by Mollah et al[97]:

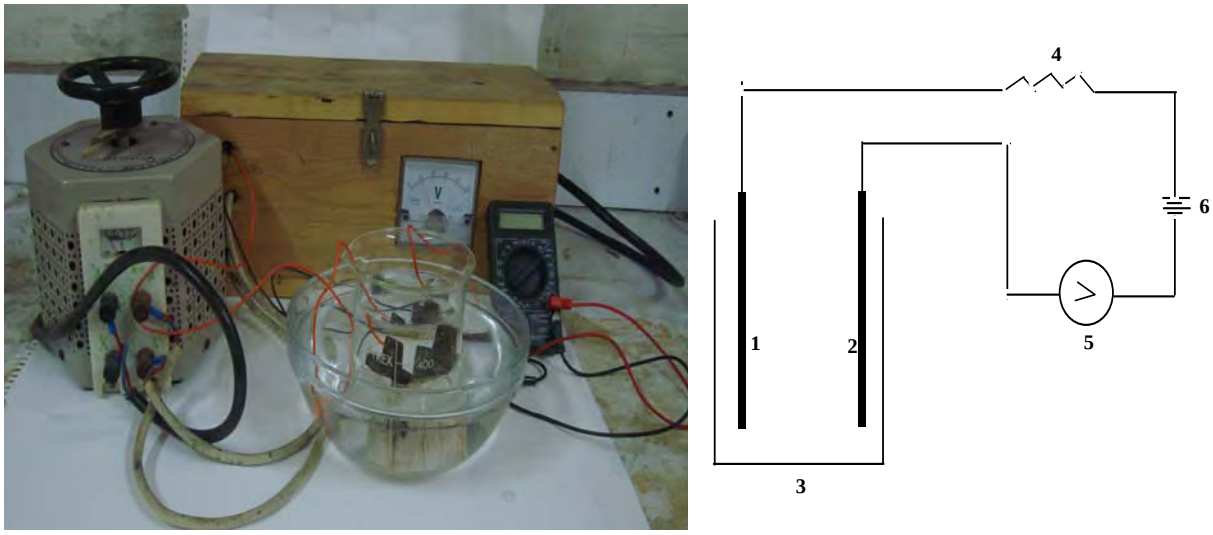

Figure 2.2: (a) Electro-coagulator (b) Schematic diagram of the cell. 1. Anode, 2.Cathode , 3. Pyrex beaker, 4. Variable resistance, 5. Ammeter , 6. D.C. source

500.0 mL of 0.025M aqueous NaCl (99.5%) solution was taken in a 1L beaker and the electrodes were immersed into it. An electrode holder made of ebonite kept the anode and cathode separated by definite distance (2.2 cm). Anode and cathode were fully immersed in the electrolytic solution. Electrolysis was then carried out for about one hour when suspension of oxyhydroxides was generated into the electrolytic solution. Usually a current of 1A was used for electrolysis. At the end of each run, the suspension was kept in open air for 24 hours to settle completely and then filtered through a 2.5 μm pore size membrane filter and the recovered solid was washed with double distilled water until free from chloride. The solid mass was dried in an oven at a temperature of 120^0C for 24 hours.

$$2\ FeO(OH) \rightarrow Fe_2O_3 + H_2O$$

Figure 2.2 (c) : Photo of the prepared iron oxide

2.2.3 Preparation of Fe_2O_3 - SiO_2 composite (1:1) by Sol-Gel method

(i) Reddish brown precipitate of iron (III) hydroxide was prepared according to the procedure described in **Section 2.2.2.**

(ii) In a 100 mL beaker TEOS and ethanol were mixed at the molar ratio 1.00 : 3.85 for which 10.70 mL TEOS and 10.60 mL ethanol were used. In a different beaker, 8.80 mL water (1.00:10.20 ratio with TEOS) was taken and reddish brown precipitate of iron (III) oxide prepared according to the process described in **Section 2.2.2** was instantly added into it and was sonicated for about 30 minutes. After that the ethanol solution containing TEOS was added to the beaker containing iron (III) hydroxide. Dilute HCl solution was added to maintain the pH value of 5.0 and the mixture was sonicated for about 30 minutes. After sonication, the mixture was left for 24 hours at ambient temperature to form SiO_2-$Fe(OH)_3$ composite. The composite settled at the bottom of the beaker. The clear solution was discarded carefully using a pipette. Double distilled water was added to the composite and stirred for half an hour and then again left for 2 hours to settle the composite. The clear solution was again discarded carefully using a pipette. This process was repeated several times to ensure complete removal of chloride and other undesirable ions from the composite. Water from the $Fe(OH)_3$-SiO_2 composite was evaporated by gently heating with a low flame

and then the composite was heated in the woven at 300^0C for 6 hours to convert it into Fe_2O_3-SiO_2 composite.

$$SiO_2\text{-}Fe(OH)_3 \rightarrow Fe_2O_3\text{-}SiO_2 + H_2O$$

The steps are schematically shown in **Figure 2.3 .**

The Fe_2O_3-SiO_2 composite (1:1) thus prepared was preserved for characterization and subsequent uses.

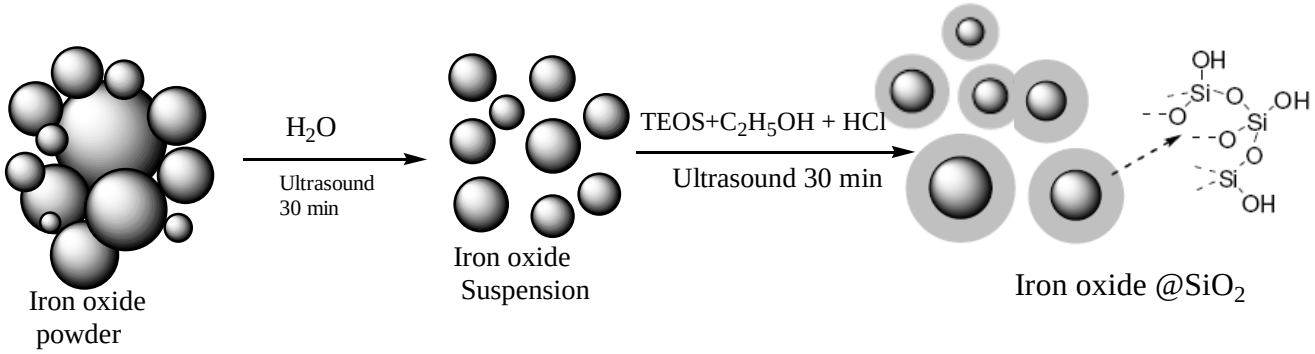

Figure 2.3: Illustration of the silica-coated iron oxide composite stepwise protocol

2.2.4 Preparation of Fe_2O_3 -SiO_2 composite (3:7) by Sol-Gel method

Fe_2O_3 - SiO_2 composite (3:7) was prepared according to the procedure described in **Section 2.2.3**. In this case 1.93 g iron oxide powder, 6.30 mL TEOS, 6.20 mL ethanol and 5.20 mL water were used.

2.2.5 Preparation of Fe_2O_3 - SiO_2 composite (7:3) by Sol-Gel method

Fe_2O_3 - SiO_2 composite (7:3) was prepared according to the process described in **Section 2.2.3**. In this case 5.0 gm iron oxide powder, 3.0 mL TEOS, 2.90 mL ethanol and 2.50 mL ethanol were used.

2.3.0 Characterization of silicon (IV) oxide, iron oxide and Fe_2O_3 - SiO_2 composites

Silicon (IV) oxide, iron oxide and Fe_2O_3 - SiO_2 composites prepared in this research were characterized by FT-IR, XRD, TGA-DTA and SEM –EDS techniques.

2.3.1 FT-IR spectroscopic investigation of Silicon (IV) oxide, iron oxide, Fe_2O_3 - SiO_2 composite (1:1),(3:7), (7:3) and Fe_2O_3 - SiO_2 composite (1:1) after adsorption of Cr(VI)

The prepared silicon (IV) oxide, iron oxide, Fe_2O_3 - SiO_2 composites and Cr(VI) treated (1:1) Fe_2O_3 - SiO_2 composite were investigated by FT-IR Spectroscopy.

The molecular characterization were carried out by FT-IR spectrophotometer (Model: FT IR -8400/8900) using potassium bromide pellet. The pellets were prepared by mixing 1.00 mg of finely ground dry sample of each compound under investigation and 100.0 mg of spectroscopic grade dry potassium bromide. The mixture was ground thoroughly in an agate mortar and pressed between a pair of dies under a pressure of 8-9 tons using hydraulic press for 5 minutes. The spectra was recorded between 4000-400 cm^{-1} with 2 cm^{-1} resolutions. Usually 32 scans were averaged to record a spectrum. The FT-IR spectra and corresponding absorption bands for silicon (IV) oxide, iron oxide and Fe_2O_3 - SiO_2 composites are presented in **Figures 3.1, 3.2, 3.3, 3.4, 3.5** and **Table 3.1, 3.2, 3.3** respectively in **Section 3.1.1.** The FT-IR spectra for Cr(VI) treated Fe_2O_3- SiO_2 composite (1:1) is presented in **Figure 3.6 and Table 3.4.**

2.3.2 X-Ray Diffraction (XRD) analysis of silicon (IV) oxide, iron oxide and Fe_2O_3 - SiO_2 composites

The phase composition of prepared silicon (IV) oxide, iron oxide and Fe_2O_3 - SiO_2 composites were analysed by an X-ray Diffractiometer .

The XRD analysis of the samples were carried out by an X-ray Diffractiometer (XRD) (Model : Philips X'pert) with CuK_α radiation (λ = 1.54178 A^0) source with a nickel filter. The samples were grounded to a fine powder and loaded into an aluminum sample holder with dimension (15 ×10 × 2) mm^3 over base line adhesive . Powder specimens were filtered with 400 mesh sieves preceding the x-ray diffraction analysis.

The samples were scanned from 10^0 to 90^0 at diffraction angle 2θ in steps of 0.02^0 and time for each step data collection was 1 second. The XRD machine was fully computer controlled and the data were stored in hard disk memory of the computer for further analysis. All the data of the samples were analysed using computer to d-values of the fundamental peaks and their intensity. The spacing between the crystal phases d was calculated using Bragg's equation:

$$\lambda = 2d \sin\theta$$

Where λ is the wavelength of the incident radiation and Cu (K_α).The raw materials and hydrated pastes were characterized using the d values of their main fundamental peaks (at least four for each) by comparing the d values and their intensity ratios with the data book of " Selected Power Diffraction Data for Minerals". Phases were identified from their strongest peak of 100% I, where I is the intensity of the peak.

The X-ray Diffraction patterns of silicon (IV) oxide, iron oxide and Fe_2O_3 - SiO_2 composite (1:1) are given in **Section 3.1.2**

2.3.3 Thermo gravimetric Analysis (TGA) and Differential Thermal Analysis (DTA)

Thermo gravimetric Analysis (TGA) and Differential Thermal Analysis (DTA) of the samples were carried out using simultaneous Thermal Analyzer (DTA/ TGA) (Model-SII EXSTAR6000 TG-DTA6300 Seiko Instrument Inc., Japan). Liquid nitrogen gas was used as a stripping gas.

Thermo gravimetric Analysis (TGA): The samples were heated at the rate of 0.5^0C min^{-1} from ambient to ≈ 1000^0C and its weight loss were measured using a balance equipped with the analyzer.

Differential Thermal Analysis (DTA): The samples were continuously heated at a constant rate 10^0C min^{-1} and the temperature difference between inert compound and the sample was recorded. Differences in temperature occur if reactions, which either release (exothermic effect) or consume (endothermic effect) energy take place. These effects were recorded as peaks on the plot of temperature difference against temperature.

The thermograms of Thermo gravimetric Analysis (TGA) / Differential Thermal Analysis (DTA) of silicon (IV) oxide, iron oxide and Fe_2O_3 - SiO_2 composite (1:1) are shown in **Figures 3.10, 3.11, 3.12** respectively in **Section 3.1.3.**

2.3.4 Scanning Electron Microscope (SEM) and Energy Dispersive X-ray Spectroscopy (EDS) analysis of silicon (IV) oxide, iron oxide and Fe_2O_3 - SiO_2 composites

The samples of silicon (IV) oxide, iron oxide and Fe_2O_3 - SiO_2 composites were analysed by Scanning Electron Microscope (SEM) and Energy Dispersive X-ray Spectroscopy (EDS). SEM is a type of electron microscope that creates various images by focusing a high energy beam of electrons onto the surface of the sample and detecting signals from the interaction of the incident electron with the sample's surface. SEM images have greater depth of field (curved surfaces are resolved properly) yielding a characteristic 3D appearance useful for understanding surface structure of a sample. Magnification is of order 10000 X and resolution 10 nm. Analyses were carried out on a JOEL JSM6490LA, (Japan) equipped with germanium detector and diamond window. The samples were mounted using double-sided tape and electrically conducted by coating with metal in AGAR AUTO SOPTTER COATER of the SEM in order to have clear images.

The SEM images of the prepared silicon (IV) oxide, iron oxide and Fe_2O_3 - SiO_2 composites are presented in the **Figures 3.13, 3.15, 3.17, 3.19 and 3.21** respectively in **Section 3.1.4**. The EDS spectra of silicon (IV) oxide, iron oxide and Fe_2O_3 - SiO_2 composites are presented in the **Figures 3.14, 3.16, 3.18, 3.20 and 3.22** respectively in **Section 3.1.4**.

2.3.5 UV-Visible Spectrophotometer

For absorption spectroscopic measurements a double UV-Visible spectrophotometer, Model UV-160A (Shimadzu, Japan) was used. The instrument was equipped with a temperature controlled ($\pm 0.1^0$) cell component and spectral data processing facility. The sensitivity of the equipment was 0.002 absorbance unit at a signal to noise ratio of 1.0. A quartz cell of path length 1.0 cm was used in this research work.

2.4.0 Interactions of Cr(VI) in aqueous solution with the prepared Fe_2O_3 - SiO_2 composites

The interactions of Cr(VI) with composites Fe_2O_3 - SiO_2 have been studied by investigating:

(i) The effects of different (a) dosages of composites as a sorbent (b) initial concentrations and shaking time (c) pH of Cr(VI) solution and shaking time on adsorption of Cr(VI) on composites

(ii) The adsorption isotherm and the sorption kinetics of Cr(VI) on Fe_2O_3 - SiO_2 composites as adsorbents.

Experimental procedure for the determination of Cr(VI) by absorption spectroscopy is outlined below.

2.4.1 Preparation of 1,5-Diphenyl Carbazide (DPC) solution

25 cm^3 0.5% solution of 1,5-Diphenyl Carbazide (DPC) was prepared by dissolving 0.125 gm 1,5-Diphenyl Carbazide (DPC) in 100% acetone. Freshly prepared DPC solution was used in each experiment.

2.4.2 Determination of concentration of Cr(VI) from aqueous system

The Concentration of Cr(VI) species in aqueous solution was determined spectrophotometrically according to the method reported earlier [98].

2.4.3 Preparation of aqueous solution of Cr (VI)

Potassium dichromate (VI) was used as a precursor to (Cr^{6+}). To prepare aqueous solution of Cr(VI), finely powdered $K_2Cr_2O_7$ was heated at 110^0C in an oven for 30-45 minutes and allowed to cool in a desiccator. Then 500 cm^3 of 100mgL^{-1} Cr(VI) solution was prepared by dissolving 0.1416 g of $K_2Cr_2O_7$ in double distilled water. Dilute solutions were prepared from this stock solution as per requirements.

2.4.4 Determination of maximum absorption of Cr(VI) -1,5-Diphenyl Carbazide (DPC) complex

100 cm^3 of 1.5 mgL^{-1} Cr(VI) solution was neutralized by 1% NH_4OH solution. In order to keep pH value 2.0 requisite volume of 1:1 H_2SO_4 and 85% H_3PO_4 was added to the solution. 2 mL of 0.5% DPC was added to this solution and the solutions was allowed to stand for about 5-10 minutes for complete complex formation. DPC, which is a highly selective agent for complex formation with Cr (VI), reacts with Cr(VI) to form a red-violet complex. Absorption spectrum (**Figure 2.4**) at maximum absorbance (λ_{max}) was measured using a quartz cell of path length 1.0 cm by a UV-Visible Spectrophotometer.

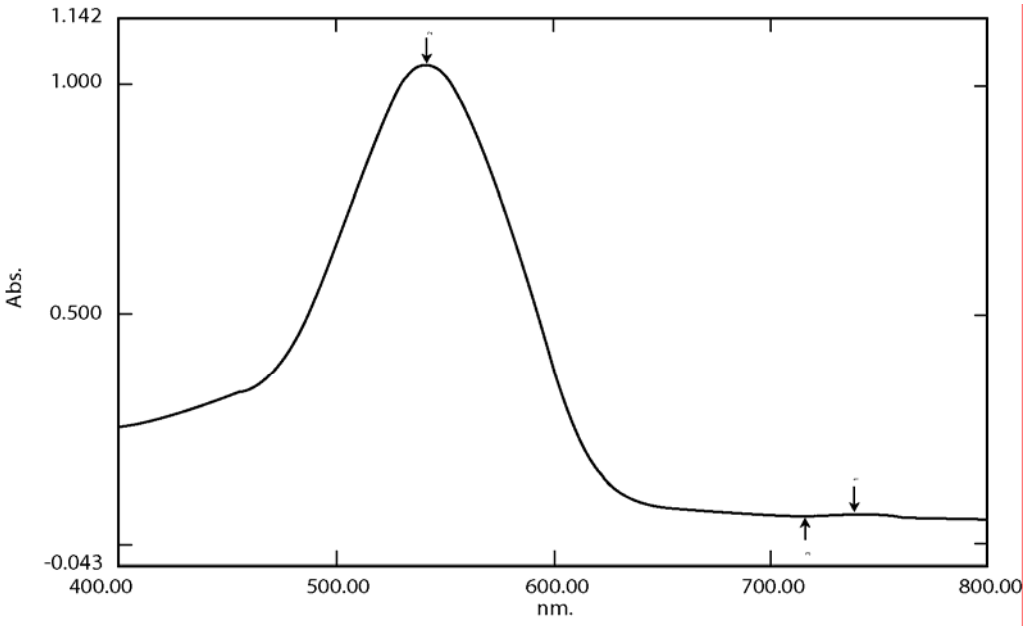

No.	P/V	Wavelength	Abs.
1	↑	738.00	0.067
2	↑	541.50	1.044
3	↓	716.50	0.063

Figure 2.4 : Absorption spectrum of Cr(VI)-DPC complex

The spectrum of the complex showed absorption maximum (λ_{max}) at 541.50 nm. All experiments in this study for quantitative determination of Cr(VI) was carried out at 541.50 nm.

2.4.5 Construction of calibration curve and determination of molar Absorption Coefficient (ε) for Cr(VI) -1,5-Diphenyl Carbazide (DPC) complex

In order to quantitatively determine the concentration of Cr(VI) in aqueous solution, a calibration curve was first constructed. A standard solution of 5.0 mgL^{-1} of Cr(VI) solution was prepared from 100 mgL^{-1} stock solution. A number of standard solutions of concentrations ranging from 0.1 to 1.5 mgL^{-1} were prepared by appropriate dilution of 5.0 mgL^{-1} of Cr(VI) solution with double distilled water. Complex formation of each of these standard solutions with the DPC was carried out according to the same procedure as described earlier in **Section 2.4.4** . Absorbance of all the solutions were

measured at (λ_{max}) 541.50 nm using a quartz cell of path length 1.0 cm. The calibration curve was constructed by plotting the absorbance of the Cr(VI) –DPC complex against the corresponding concentrations of Cr(VI). The experimental data and the corresponding plot are shown in the **Table.2.1** is shown in **Figure 2.5.**

Table 2.1 : Calibration curve for Cr(VI) in aqueous solution

Experimental conditions: pH of Cr(VI) solution = 2.0 ± 0.2 ; (λ_{max}) of the complex = 541.50 nm, Reference: Double distilled water

Concentration of Cr(VI) solution (mgL^{-1})	Absorbance
0.1	0.0921
0.3	0.2628
0.5	0.4639
0.8	0.7493
1.0	0.8755
1.3	1.1505
1.5	1.28

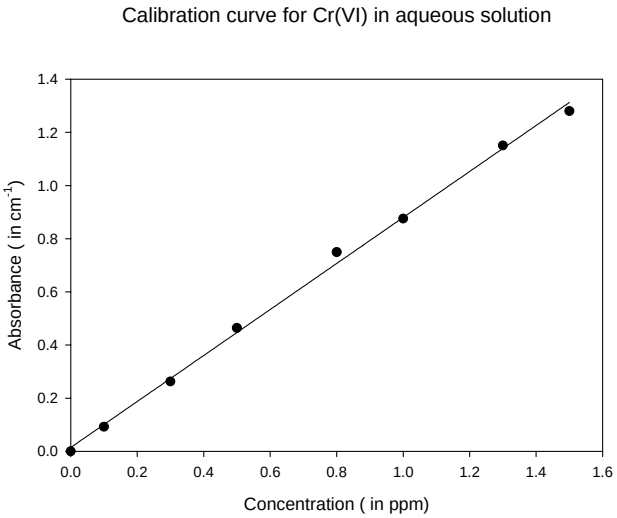

Figure 2.5 Calibration curve for Cr(VI) –DPC complex

The plot is a straight line and it passes through the origin. This nature of the plot suggests the validity of the Beer-Lambert law. The molar absorption coefficient (ε) for Cr(VI) – DPC complex at 541.5 nm was determined from the slope of the linear plot (**Figure 2.5)** and it was found to be 0.89 $Lmg^{-1}cm^{-1}$.

2.4.6.0 Adsorption studies

Interactions of Cr(VI) with the composites have been studied by investigating the effects of different parameters such as adsorbent dosage, Cr(VI) concentration, shaking time and pH of the Cr (VI) solution .

2.4.6.1 Investigation of the adsorption efficiency of Cr(VI) in aqueous solution for Fe_2O_3, SiO_2 and Fe_2O_3 - SiO_2 composite (1:1)

Details of experimental procedures have been described in the **Section 2.4.6.1.** To investigate the effect of adsorption of Cr(VI) from aqueous solution by the iron oxide , silicon (IV) oxide and Fe_2O_3 - SiO_2 composite (1:1), 0.20 g of sorbent of each type were taken . 100 cm^3 of 10 mgL^{-1} of Cr(VI) solution was freshly prepared from 500cm^3 50 mgL^{-1} of Cr(VI) solution by appropriate dilution with DDW. pH of 100 cm^3 10 mgL^{-1} of Cr(VI) solution was carefully adjusted at pH 4.8. 20cm^3 of this 10 mgL^{-1} of Cr(VI) solution was added to different type of the sorbent in a series of reagent bottles. Then the bottles were shaken for 20 minutes by a thermostated mechanical shaker at 250 rpm shaking speed and at temperature (30±0.2) ^{0}C. After the stipulated 20 minutes time, the bottles were withdrawn altogether from the shaker and then the supernatant was removed from the sorbent as soon as possible and centrifuged repeatedly until a clear solution was obtained. After that the clear solution was diluted to 10 times of its initial concentration and then the absorbance of the clear solution was measured spectrophotometrically according to the reported procedure[98].

The experimental data is shown in **Table 3.5 Section 3.2.1.**

2.4.6.2 Investigation of the effect of variation of adsorbent dosage on adsorption of Cr(VI) in aqueous solution for Fe_2O_3 - SiO_2 composite (1:1)

Details of experimental procedures have been described in the **Section 2.4.6.2.** To investigate the effect of sorbent (Fe_2O_3 - SiO_2 composite) on Cr(VI) adsorption on Fe_2O_3 - SiO_2 composite (1:1), different dosages ranging from 0.05 g to 0.30 g of Fe_2O_3 - SiO_2 composite (1:1) were considered as sorbent . 250 cm^3 of 50 mgL^{-1} of Cr(VI) solution was freshly prepared from 500cm^3 100 mgL^{-1} of Cr(VI) solution by appropriate dilution with DDW. pH of 250 cm^3 50 mgL^{-1} of Cr(VI) solution was carefully adjusted at pH 4.8. 25cm^3 of this 50mgL^{-1} of Cr(VI) solution was added to different amounts of the sorbent in a series of reagent bottles. Then the bottles were shaken for 20 minutes by a thermostated mechanical shaker at 250 rpm shaking speed and at temperature (30 ± 0.2^0) ^{0}C. After the stipulated 20 minutes time, the bottles were withdrawn altogether from the shaker and then the supernatant was removed from the sorbent as soon as possible and centrifuged repeatedly until a clear solution was obtained. The absorbance of the clear solution was measured by using AAS to determine the actual concentration of the Cr(VI) solution after its adsorption on the composite .

The experimental data and the corresponding plot are shown in **Table 3.6** and **Figure 3.23** respectively in **Section 3.2.2.**

2.4.6.3 Determination of the effect of different initial concentrations of Cr(VI) solution and shaking time on adsorption of Cr(VI) onto Fe_2O_3 -SiO_2 composite (1:1)

To investigate the effect of different initial concentrations of Cr(VI) solutions toward adsorption on Fe_2O_3 - SiO_2 composite (1:1), Cr(VI) solution of varied concentration were prepared. 250 cm^3 of 40 mgL^{-1} and 50 mgL^{-1} of Cr(VI) solution was freshly prepared from 100 mgL^{-1} of Cr(VI) solution by appropriate dilution with DDW. pH of 250 cm^3 40 mgL^{-1} and 50 mgL^{-1} of Cr(VI) solution were carefully adjusted at pH 4.8. 25cm^3 of Cr(VI) solution were then added to 0.20 g of the sorbent in a series of reagent bottles. Then the bottles were shaken by a thermostated mechanical shaker at 250 rpm shaking speed and at temperature $(30\pm0.2^0)\ ^0C$. After definite interval of time each of the bottles were withdrawn from the shaker. Then the supernatant was removed from the sorbent as soon as possible and centrifuged repeatedly until a clear solution was obtained. The absorbance of the clear solution was measured by using atomic absorption spectrophotometer to determine the actual concentration of the Cr(VI) solution after its adsorption on the composite .

The experimental data and the corresponding plot are shown in **Table 3.7** and **Figure 3.24** respectively in **Section 3.2.3**

2.4.6.4 Determination of the effects of pH of Cr(VI) solution and shaking time on adsorption of Cr(VI) onto Fe_2O_3 / SiO_2 composite (1:1)

The experiments were carried out at pH 4.80, 3.00 and 8.00 to understand the effect of pH on the adsorption of Cr(VI) on Fe_2O_3 - SiO_2 composite (1:1). The pH 4.8, 3.0 and 8.0 of 50 mgL^{-1} of Cr(VI) solution were carefully adjusted by adding freshly

prepared 0.1M HCl or 0.1M NaOH solution as required with pH meter. 25cm^3 of 50 mgL^{-1} Cr(VI) solution having pH 4.8 was added to 0.20 g of the sorbent in a series of reagent bottles. Then the bottles were shaken by a thermostated mechanical shaker at 250 rpm shaking speed and at temperature (30±0.2) ^{0}C. After definite interval of time each of the bottles were withdrawn from the shaker. Then the supernatant was removed from the sorbent as soon as possible and centrifuged repeatedly until a clear solution was obtained. The absorbance of the clear solution was measured by using AAS to determine the actual concentration of the Cr(VI) solution after its adsorption on the composite .

The experiments were repeated at pH 3.0 and 8.0. The experimental data and the corresponding plots are shown in **Table 3.10** and **Figure 3.27, 3.28** respectively in **Section 3.2.4.**

2.4.6.5 Adsorption isotherm of Cr(VI)onto Fe_2O_3 - SiO_2 composite (1:1)

Batch adsorption studies were conducted to determine adsorption isotherm of Cr(VI) adsorption on Fe_2O_3 - SiO_2 composite (1:1) . 0.20 g of the Fe_2O_3 - SiO_2 composite (1:1) was taken in a series of reagent bottles . 250 cm^3 of 100 mgL^{-1} of Cr(VI) solutions was freshly prepared in a volumetric flask . Cr(VI) solutions of varying initial concentrations ranging from 10 to 60 mgL^{-1} were freshly prepared by diluting 250 cm^3 of 100 mgL^{-1} of Cr(VI) solution with DDW. The pH of the each dilute Cr(VI) solutions were maintained constant at 4.8 . 25cm^3 of Cr(VI) solutions of these varying concentrations was added to 0.20 g of the sorbent in a series of reagent bottles. It was previously determined that 20 to 30 minutes time was sufficient to attain equilibrium adsorption . The bottles were, therefore, shaken in a thermostated

mechanical shaker for 20-30 minutes. Thereafter, all the bottles were removed from the shaker and then the supernatant was removed from the sorbent as soon as possible and centrifuged repeatedly until a clear solution was obtained. The absorbance of the clear solution was measured by using AAS to determine the actual concentration of the Cr(VI) solution after its adsorption on the composite .

The amounts of Cr(VI) adsorbed per gram of the composite were calculated from the difference between initial concentration and final concentration of Cr(VI) solution before adsorption and after adsorption. The experimental data and the corresponding plots are shown in **Table 3.11** and **Figure 3.29** respectively in **Section 3.3.1.**

2.4.6.6 Determination of the effect of shaking time on adsorption of Cr(VI) on Fe_2O_3 - SiO_2 composite (3:7)

To investigate the effect of shaking time on Cr(VI) adsorption on Fe_2O_3 - SiO_2 composite (3:7), Cr(VI) solution of 50 mgL^{-1} was used at pH 4.8 . Adsorption experiments were carried out according to the same process as described earlier in **Section 2.4.6.3** . The experimental data and the corresponding plot are shown in **Table 3.8** and **Figure 3.25** respectively in **Section 3.2.3.**

2.4.6.7 Determination of the effect of shaking time on adsorption of Cr(VI) on Fe_2O_3 - SiO_2 composite (7:3)

To investigate the effect of shaking time on Cr(VI) adsorption on Fe_2O_3 - SiO_2 composite (7:3), Cr(VI) solution of 50 mgL^{-1} was used at pH 4.8 . Adsorption experiments were carried out according to the same process as described earlier in **Section 2.4.6.3** . The experimental data and the corresponding plot are shown in **Table 3.9** and **Figure 3.26** respectively in **Section 3.2.3.**

2.4.6.8 Sorption Dynamics

The kinetic study of sorption of Cr(VI) on Fe_2O_3 - SiO_2 composite (1:1) was carried out by investigating the effect of shaking time on % sorption of Cr (VI) on the Fe_2O_3 - SiO_2 composite (1:1). In order to study the sorption dynamics, freshly prepared 25cm^3 of 50 mgL^{-1} Cr(VI) solution was added to 0.20 g of the sorbent in a series of reagent bottles. Then the bottles were shaken by a thermostated mechanical shaker at 250 rpm and at temperature (30±0.2) ^{0}C for definite interval of shaking time ranging from 5 minutes to 120 minutes. After definite interval of time each of the bottles were withdrawn from the shaker. Then the supernatant was removed from the sorbent as soon as possible and centrifuged repeatedly until a clear solution was obtained. The absorbance of the clear solution was measured by using AAS to determine the actual concentration of the Cr(VI) solution after its adsorption on the composite . The amounts of Cr(VI) adsorbed per gram of the composite at different shaking time were calculated. The experimental data, Lagergren plot for Cr(VI) adsorption and plot for validation of Morris-Weber equation for Cr(VI) adsorption on the composite are shown in **Table 3.13** and **Figure 3.31 and Figure 3.32** respectively in **Section 3.4.0.**

3. Results and Discussion

3.0 Results and Discussion

The results and discussion are presented in two parts. Characterization of silicon (IV) oxide, iron oxide and iron oxide - SiO_2 composites are presented in **Section 3.1.0**. Interaction of Cr(VI) with the composites are presented in **Section 3.2.0**.

3.1.0 Characterization of silicon (IV) oxide, iron oxide and iron oxide-SiO_2 composites

Silicon (IV) oxide, iron oxide and iron oxide- SiO_2 composites were found to be white, brown and light brown respectively.

Silicon (IV) oxide, iron oxide and iron oxide- SiO_2 composites have been characterized by FT-IR spectroscopy, X-ray Diffraction (XRD), Thermogravimetric Analysis(TGA), Differential Thermal Analysis (DTA) , Energy dispersive X-ray spectroscopy (EDS) and Scanning Electron Microscopy (SEM) techniques .

3.1.1 FT-IR spectroscopic investigation

The silicon (IV) oxide, iron oxide and iron oxide - SiO_2 composites were investigated by FT-IR spectroscopy for molecular characterization. A sample of Cr (VI) treated composite (1:1) was also analysed to elucidate the mechanism of interaction of Cr(VI) with the composite. The methods of preparation and treatments of samples have been described in **Section 2.3.1.**

FT-IR spectra of silicon (IV) oxide, iron oxide, iron oxide- SiO_2 composites are shown in **Figures 3.1, 3.2, 3.3, 3.4, 3.5** respectively and FT-IR spectra of iron oxide-SiO_2 composite (1:1) after adsorption of Cr (VI) are shown in **Figure 3.6.**

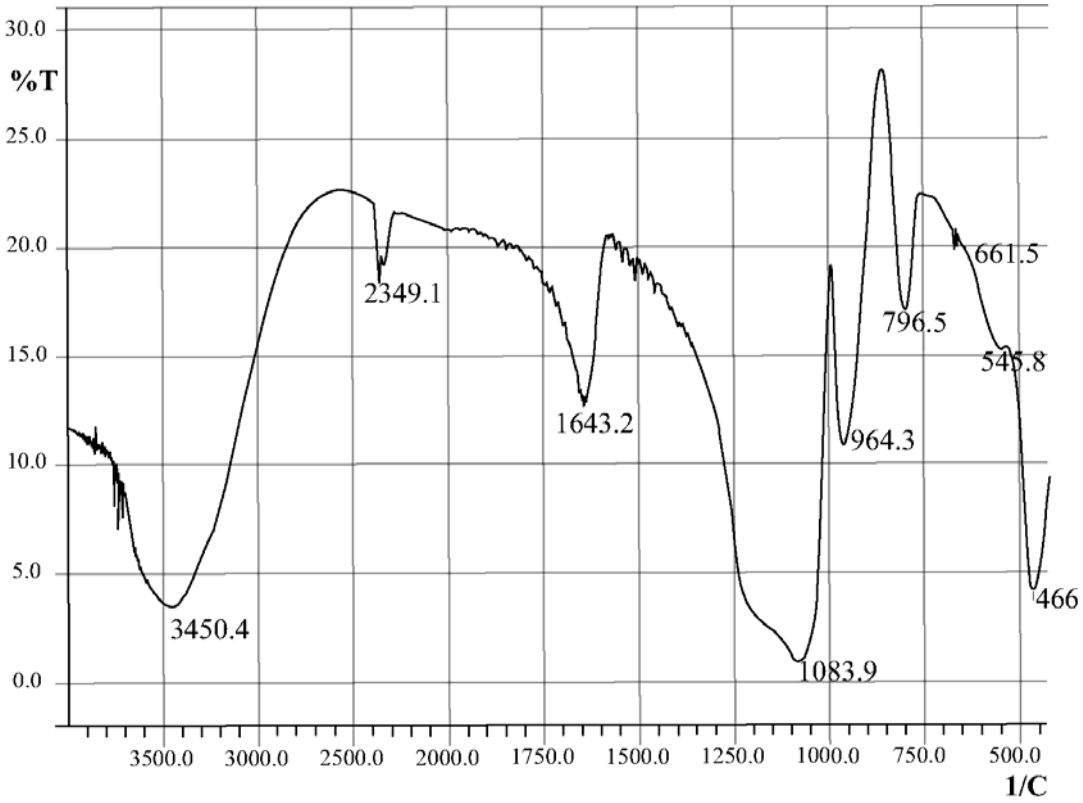

Figure 3.1 : FT-IR spectrum of silicon (IV) oxide

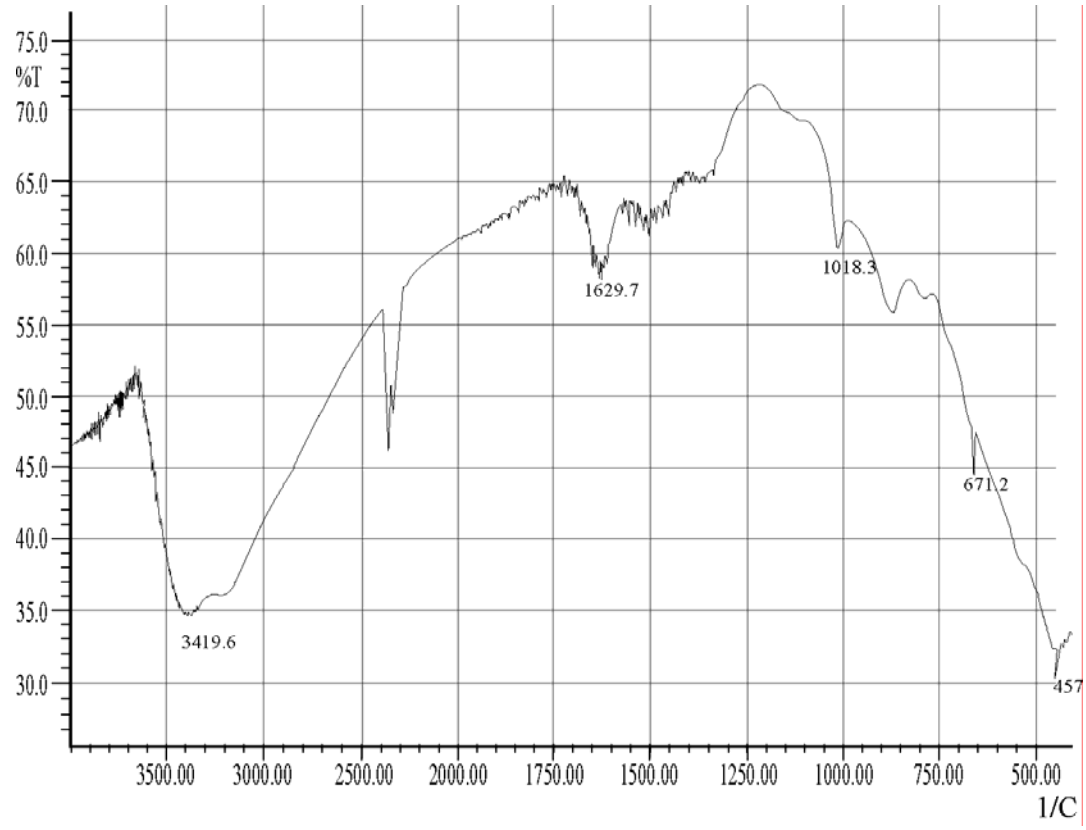

Figure 3.2 : FT-IR spectrum of iron (III) oxide

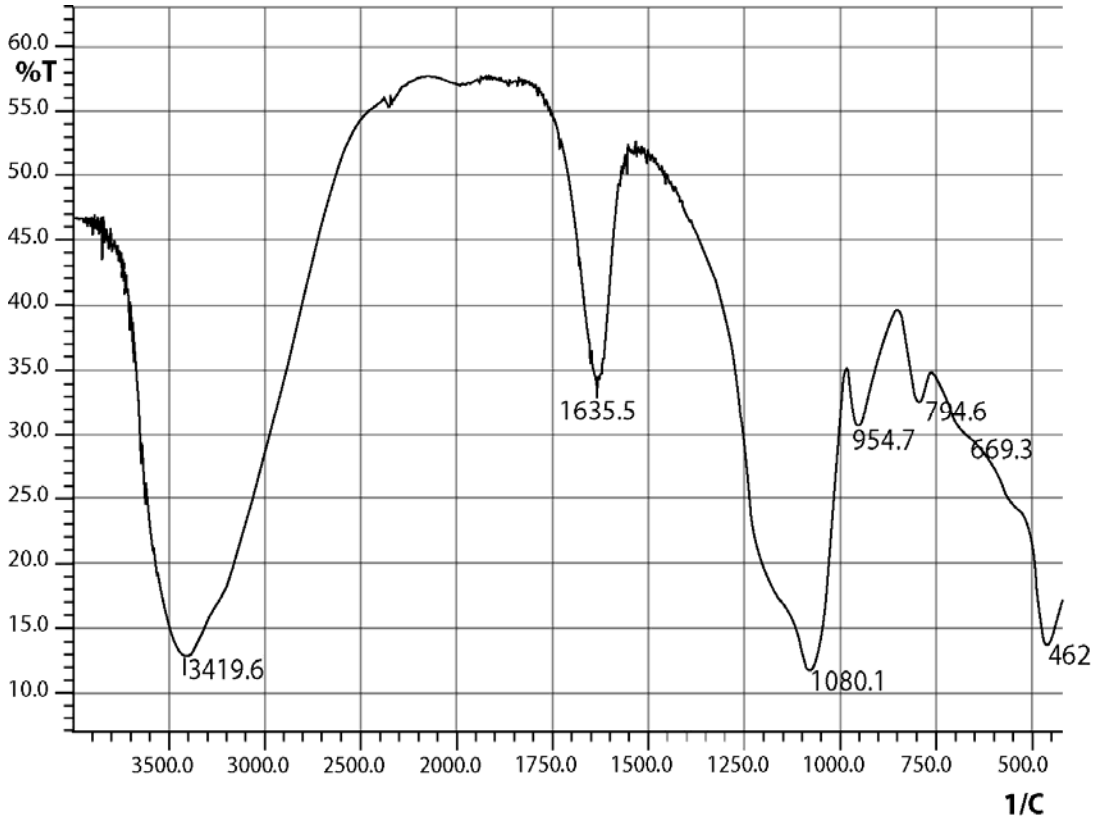

Figure 3.3 : FT-IR spectrum of iron oxide- SiO_2 composite (1:1)

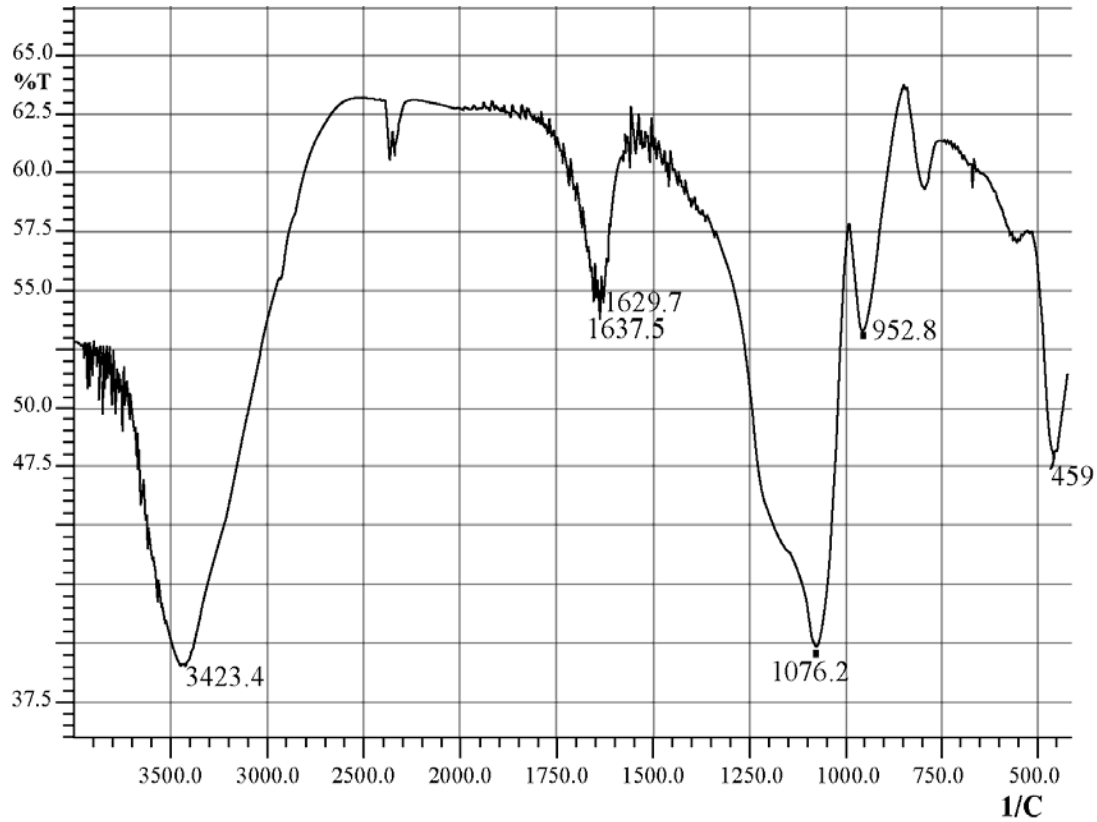

Figure 3.4 : FT-IR spectrum of iron oxide- SiO_2 composite (3:7)

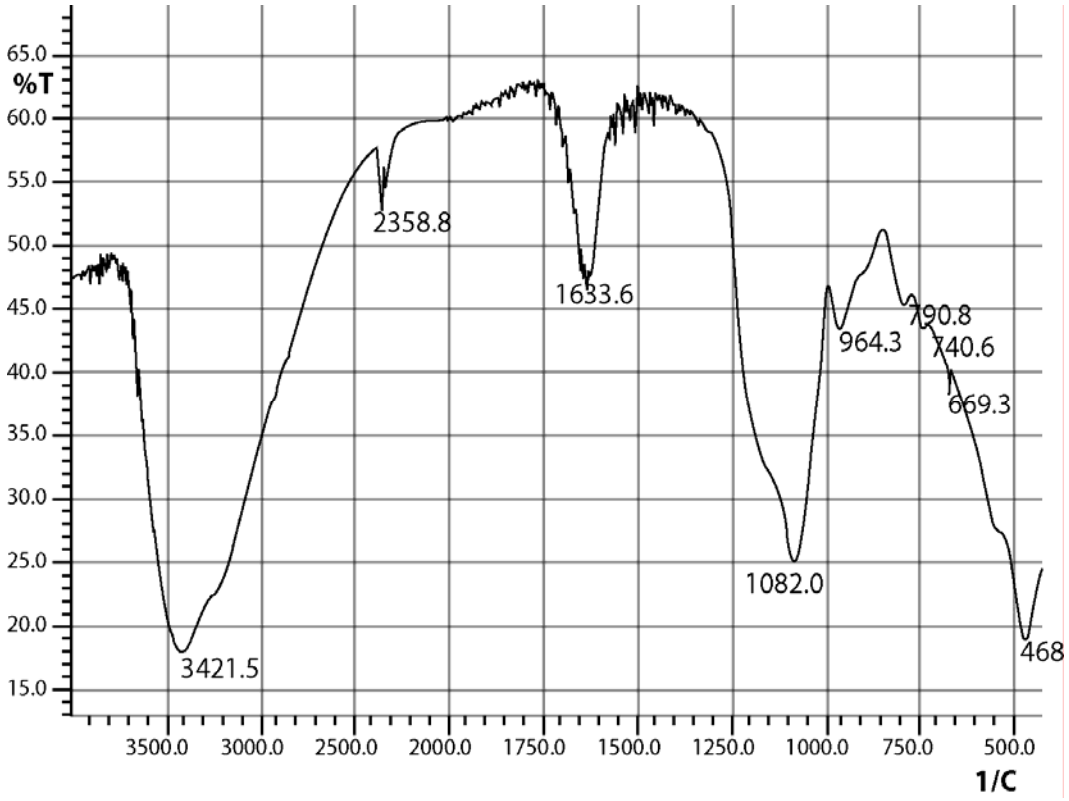

Figure 3.5 : FT-IR spectrum of iron oxide- SiO_2 composite (7:3)

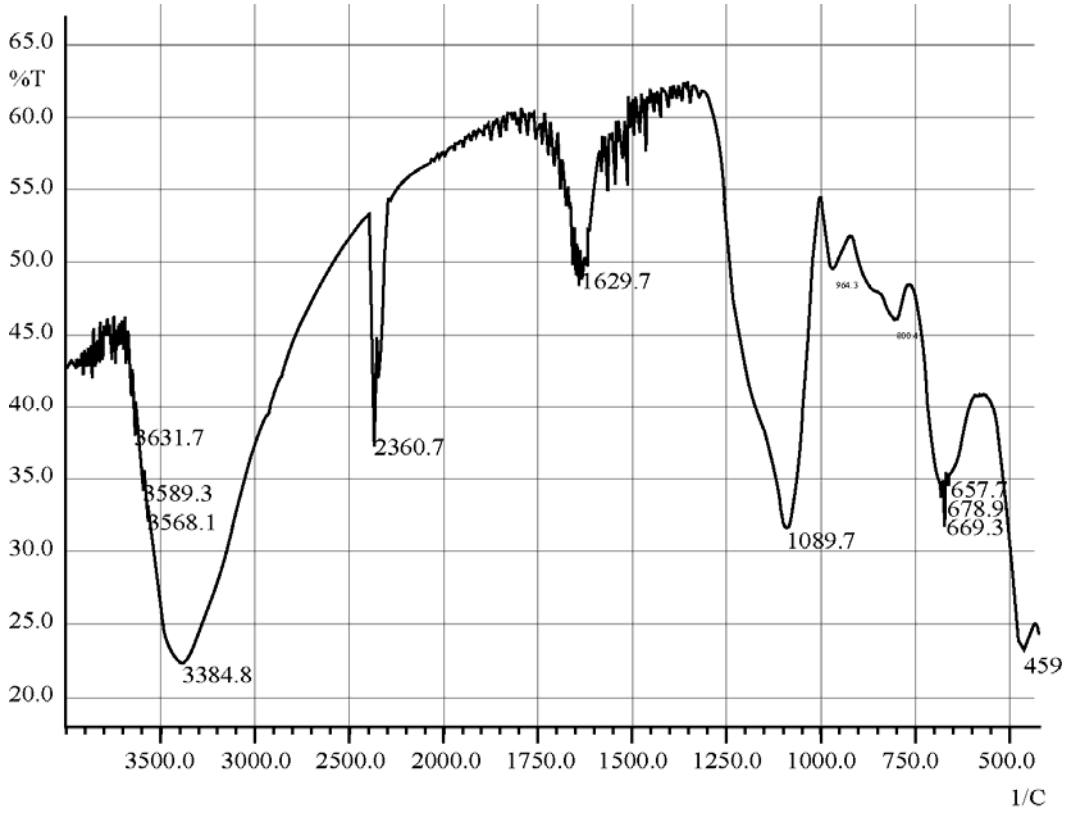

Figure 3.6: FT-IR spectrum of iron oxide-SiO_2composite (1:1) after adsorption of Cr(VI)

Characteristics absorption bands of FT-IR analyses of the silicon (IV) oxide and iron oxide are presented in **Table 3.1** and **3.2** along with reported absorption bands of pristine silicon (IV) oxide and iron (III) oxide.

Table 3.1: FT-IR absorption bands of silicon (IV) oxide with band assignments and reported bands of its pristine sample

Probable band assignment	Absorption bands (cm^{-1}) [**99**]	Experimentally obtained absorption band (cm^{-1})
Si-O-Si bond vibration	450-460	466
Symmetric stretching vibrations of Si-O-Si belonging to ring structures	800-820	797
Asymmetric stretching vibration of Si-O-Si	1000-1260	1081
Combination of vibrations of the SiO_2 network	1640,1870,1960	1643
Due to stretching and bending vibrations of Si-O-H and O-H bonds in surface water molecules	3000-4000	3450

Close examination of **Table 3.1** shows that major absorption bands of the silicon (IV) oxide are in good agreement with the reported values of its authentic sample. Therefore, the FT-IR analysis supports that the sample prepared was silicon (IV) oxide.

Table 3.2: FT-IR absorption bands of iron (III) oxide with band assignments

Name of the iron oxide	Characteristics IR bands (cm^{-1})	References
Hematite	345,470,540	**100**
Maghemite	400,450,570,590,630	**100**
Magnetite	400,580	**101**
Goethite	890,797	**100**
Lepidocrocite	1026,1161,753	**100**
Akaganeite	840,640	**100**
Feroxyhite	1110,920,790,670	**100**
Magnetite Type of iron oxide	3420,1630, 580, 671 and 457	Present experiment

The bands at 457 cm^{-1} and 580 cm^{-1} were assigned to the stretching and torsional vibration modes of the hematite Fe-O bonds in the tetrahedral and octahedral sites respectively , which are in good agreement with the results reported by Mollah M.Y.A[102]. The absorption bands at 3420 and 1630 cm^{-1} are due to stretching and bending vibrations of O-H bonds in surface water molecules. Thus the synthesized iron oxide shows the absorption bands which are in good agreement with the reported absorption bands of magnetite (Fe_2O_3) type of iron oxide. Therefore, the FT-IR analysis provides the evidence that magnetite (Fe_2O_3) type of iron oxide was electrochemically generated in this research.

Table 3.3: FT-IR absorption bands of silicon(IV) oxide, iron oxide, Fe_2O_3-SiO_2 composites

Absorption band of silicon (IV) oxide (cm^{-1})	Absorption band of iron (III) oxide (cm^{-1})	Absorption band of Fe_2O_3-SiO_2 composite (1:1) (cm^{-1})	Absorption band of Fe_2O_3-SiO_2 composite (3:7) (cm^{-1})	Absorption band of Fe_2O_3-SiO_2 composite (7:3) (cm^{-1})
466	457	462	459	468
797	795	795	796	791
964	955	955	953	964
1084	1018	1080	1076	1082
1643	1630	1636	1638	1634
2349	2360	2360	2360	2359
3450	3420	3420	3423	3422

Close examination of **Table 3.3** shows that major absorption bands at 462, 795, 955, 1080, 1636, 2360 and 3420 cm^{-1} shown by Fe_2O_3-SiO_2 composite (1:1) were in good agreement with those shown by its constituents silicon (IV) oxide and iron (III) oxide. These FT-IR results indicate the presence of both silicon (IV) oxide and iron (III) oxide in Fe_2O_3-SiO_2 composite (1:1).

Further examination of **Table 3.3** , reveals that major absorption bands at 459, 796, 953, 1076, 1638, 2360 and 3423 cm^{-1} shown by Fe_2O_3-SiO_2 composite (3:7) are in good agreement with those shown by its constituents silicon (IV) oxide and iron (III) oxide. The FT-IR results thus indicate that the composite is made up of silicon (IV) oxide and iron (III) oxide. It is also noteworthy that most of the absorption bands appeared in case of Fe_2O_3-SiO_2 composite (3:7) are in good agreement with that shown by silicon (IV) oxide. These results supports that Fe_2O_3-SiO_2 composite (3:7) contains maximum percentage of silicon (IV) oxide, which is in good conformity with the theoretical consideration.

Further examination of **Table 3.3** , shows that major absorption bands at 468, 791, 1082, 1634, 2359 and 3422 cm^{-1} shown by Fe_2O_3-SiO_2 composite (7:3) are in good agreement with those shown by its constituents silicon (IV) oxide and iron (III) oxide. These FT-IR results indicate that the composite was made up of silicon (IV) oxide and iron (III) oxide. It is also noteworthy that most of the absorption bands appeared in case of Fe_2O_3-SiO_2 composite (7:3) are in good agreement with that shown by iron (III) oxide. These results supports that Fe_2O_3-SiO_2 composite (7:3) contains maximum percentage of iron (III) oxide, which is in good conformity with the theoretical consideration.

In case of all of the composites, formation of new bands and absence of several bands of their respective constituents clearly indicate that interaction between constituents silicon (IV) oxide and iron (III) oxide has occurred during formation of the composites. Therefore, the FT-IR analysis suggests that Fe_2O_3-SiO_2 composites have been formed.

Table 3.4: FT-IR absorption bands of Fe_2O_3-SiO_2 composite (1:1) and Cr (VI) treated Fe_2O_3-SiO_2 composite (1:1)

Absorption band of Fe_2O_3-SiO_2 composite (1:1) (cm^{-1})	Absorption band of Cr (VI) treated Fe_2O_3-SiO_2 composite (1:1) (cm^{-1})
462	459
795	800
955	964
1080	1090
1636	1630
2360	2361
3420	3385

Examination of **Table 3.4** reveals that new bands appear at 679, 1450, 1550 and 2361 cm^{-1} in Cr(VI) treated Fe_2O_3-SiO_2 composite (1:1). Formation of these new bands is probably due to the presence of adsorbed Cr (VI) in the composite. The bands that

appeared at 462, 795, 955, 1636 and 3420 cm^{-1} in untreated Fe_2O_3-SiO_2 composite (1:1) have been shifted to 459, 800, 964, 1630 and 3385 respectively after treating the same composite with Cr(VI). The shifting of bands may be due to substrate-sorbent interaction. The vibrational changes along with shifting of vibrational bands clearly suggest chemical interaction of Cr(VI) with Fe_2O_3-SiO_2 composite (1:1). These results support that Cr(VI)interacts with and Fe_2O_3-SiO_2 composite (1:1) upon adsorption.

3.1.2 X-Ray Diffraction Analysis

The phase compositions of the samples were analysed by XRD technique. X-ray powder diffraction patterns of these were recorded at ambient temperature. The XRD patterns of these samples are presented in **Figures 3.7, 3.8 and 3.9** respectively.

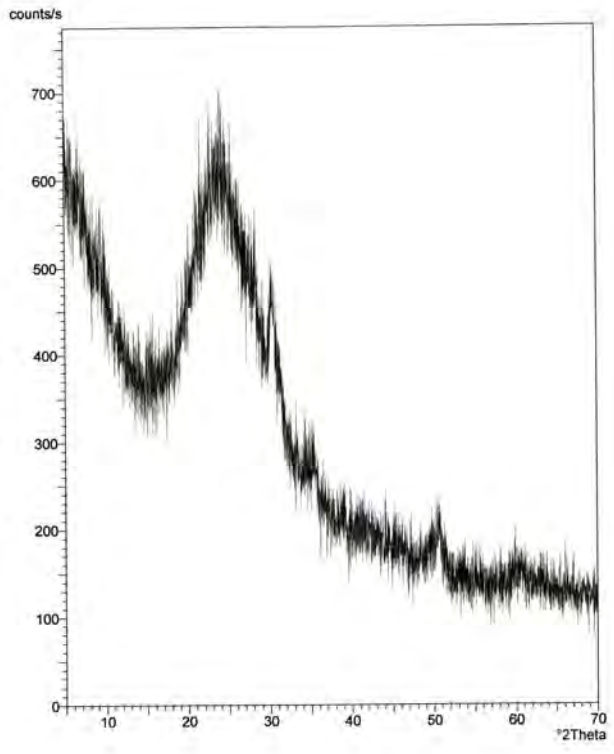

Figure 3.7 : XRD pattern of SiO_2

X-ray diffraction using CuKα radiation (Philips X'pert) was used to determine the phase composition of silica particles. The characteristics diffuse peak of the silica XRD was observed at about 20º which indicates that the silica particles are amorphous . This demonstrates that a high percentage of these particles are amorphous, but a few of them are crystalline. The result is in good agreement with the result reported by Meera basa[103] and Tabatabaei[104].

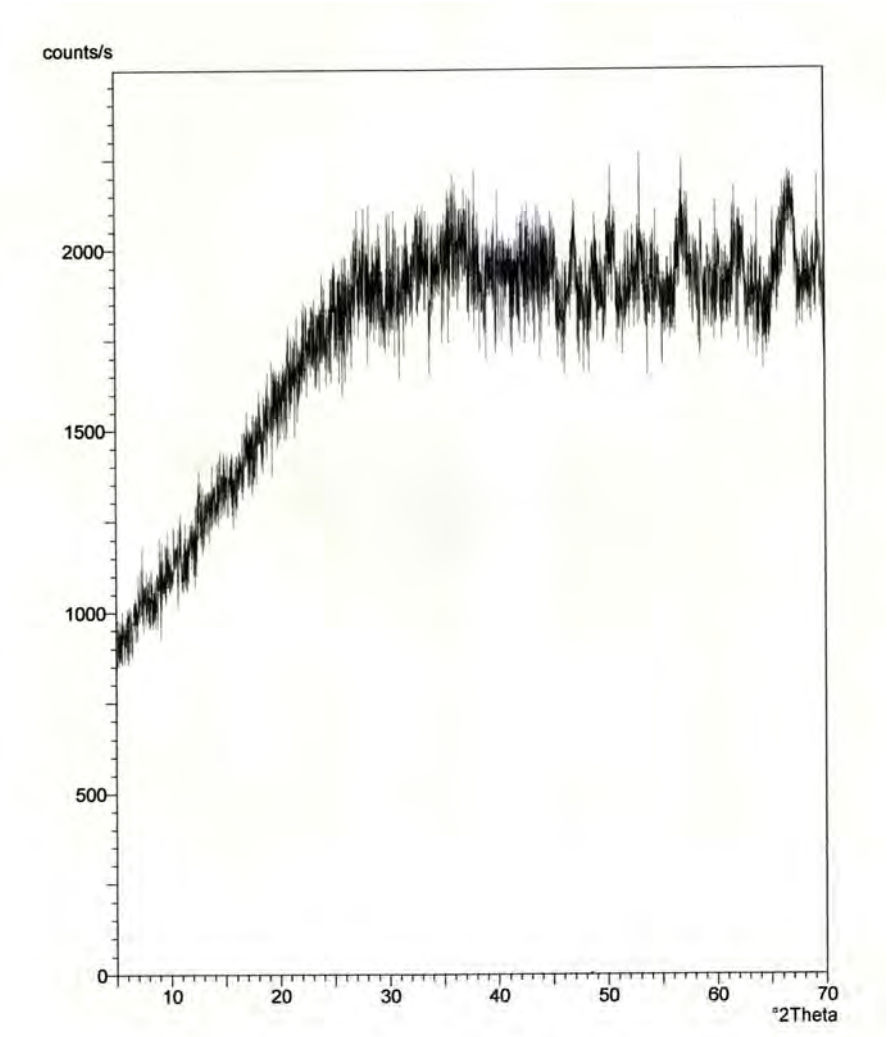

Figure 3.8 : XRD pattern of iron oxide

Iron-oxide prepared by electrochemical method were characterized by XRD technique. **Figure 3.8** represents the X-ray diffraction spectra of iron oxides. The 2θ value of iron oxide sample is found to match with JCPDS-33-0664, confirming the formation of Fe_2O_3.

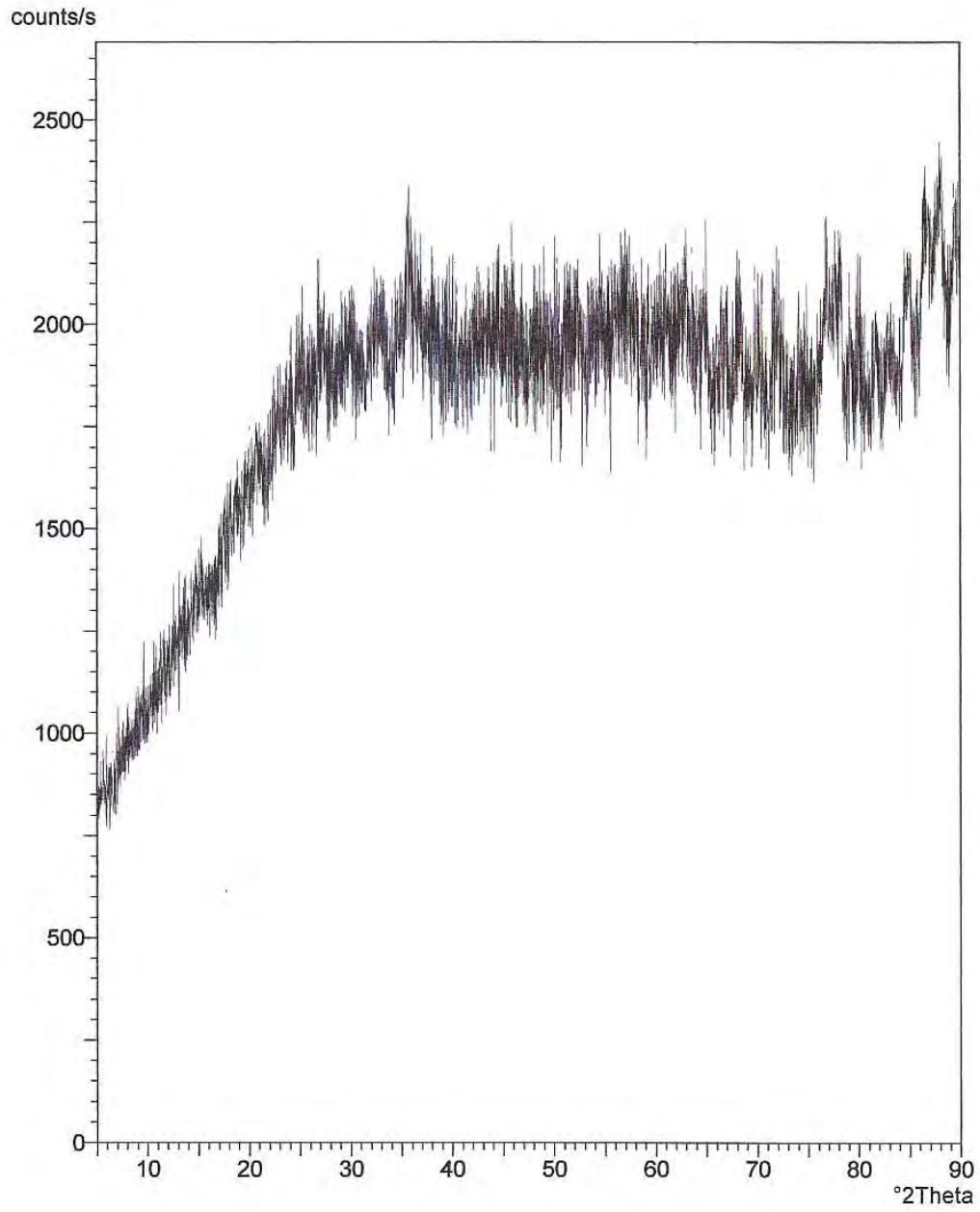

Figure 3.9: XRD pattern of Fe_2O_3-SiO_2 composite (1:1)

Figure 3.9 shows the XRD patterns of the thermally treated iron oxide-silica composite (1:1). In the sample, besides the broad band characteristic for the presence of the amorphous silica gel , the amorphous Fe_2O_3 was evidenced. This could be assigned to the bonding of the iron into Si-O-Fe-O-Si polymeric bonds, that do not break at low temperatures of the thermal treatment. The results are in good agreement with the result reported by Raileanu et al[105].

3.1.3 Thermo gravimetric Analysis (TGA) and Differential Thermal Analysis (DTA)

The experimental procedures were described in **Section 2.3.3.** The thermograms of silicon (IV) oxide, iron (III) oxide and Fe_2O_3-SiO_2 composite (1:1) are presented in **Figures 3.10 to 3.12 respectively.**

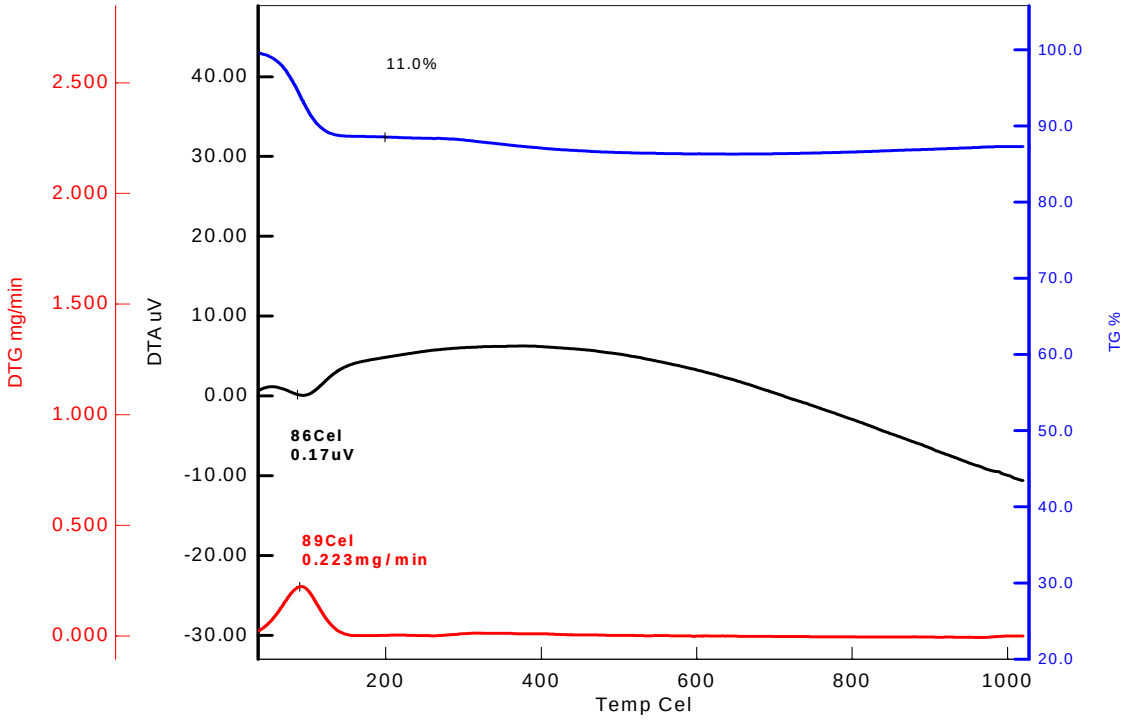

Figure : 3.10 TGA /DTA pattern of silicon (IV) oxide

Thermograph of silica (IV) oxide (**Figure 3.10**) shows gradual weight loss from 40^0 to 160^0C (11.0%), almost a steady state from 160^0C onward. Weight loss may be due to removal of free water (absorbed from atmosphere) and presence of any structural water.

Thermogram of Differential Thermal Analysis (DTA) (**Figure 3.10**) shows an endothermic effect between 86-150^0 C temperature ranges. The endothermic effect may be due to removal of structural water. The result is in good agreement with the result reported by Qingyin Wu[106].

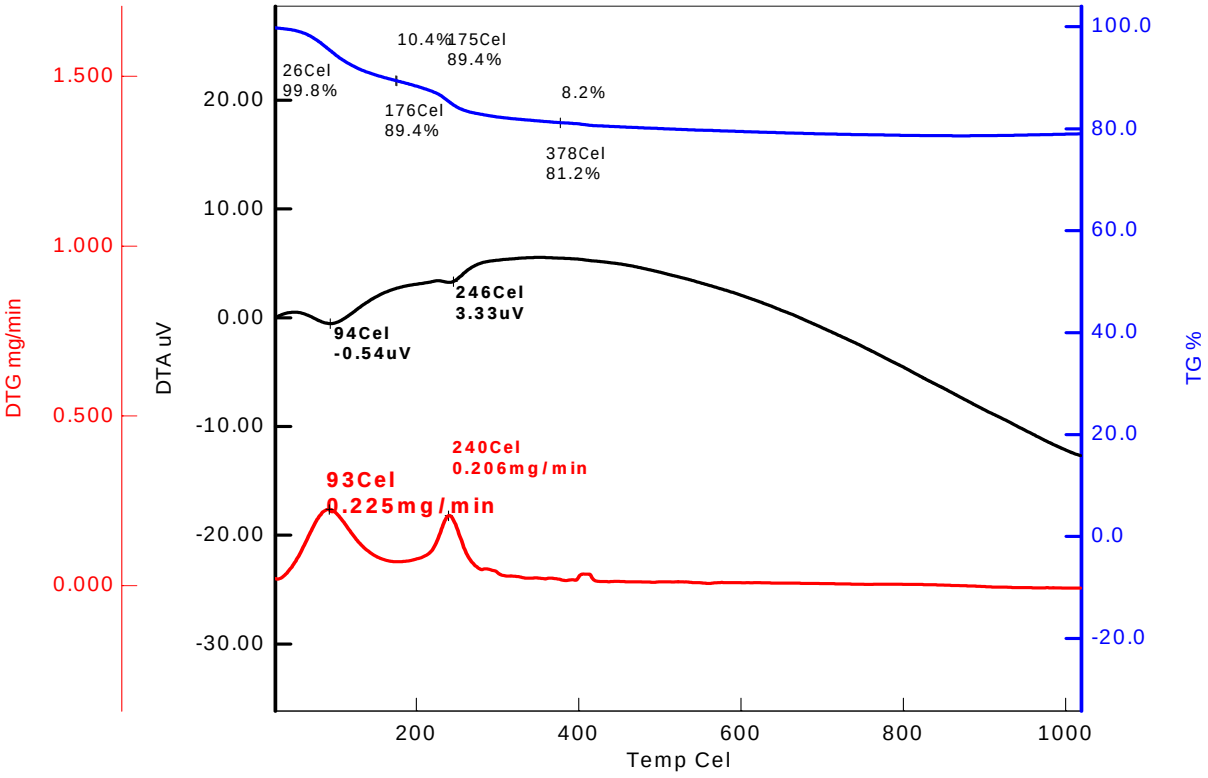

Figure : 3.11 TGA /DTA pattern of iron (III) oxide

Thermograph of iron (III) oxide (**Figure 3.11**) shows gradual weight loss from 26^0 to 176^0C (10.4%) and 176^0 to 378^0C (8.2 %) , almost a steady state from 378^0C onward. Weight loss may be due to removal of free water absorbed from atmosphere and

presence of any structural water. Gradual weight loss from 250^0 to 400^0C (8.2%) was due to dehydroxylation for structural OH.

Differential Thermal Analysis (DTA) (**Figure 3.11**) shows two endothermic peak at 94^0 C and 246^0 C temperature . The endothermic effect at 94^0 C may be due to removal of physically bound water and the endothermic effect at 246^0 C is due to removal of structurally bound water. Exotherm between 250^0 to 300^0C is due to recrystallization process involving transformation of smaller crystals into larger one. The DTA/TG result shown above for iron oxide is in good agreement with the data reported by Balek et al[107].

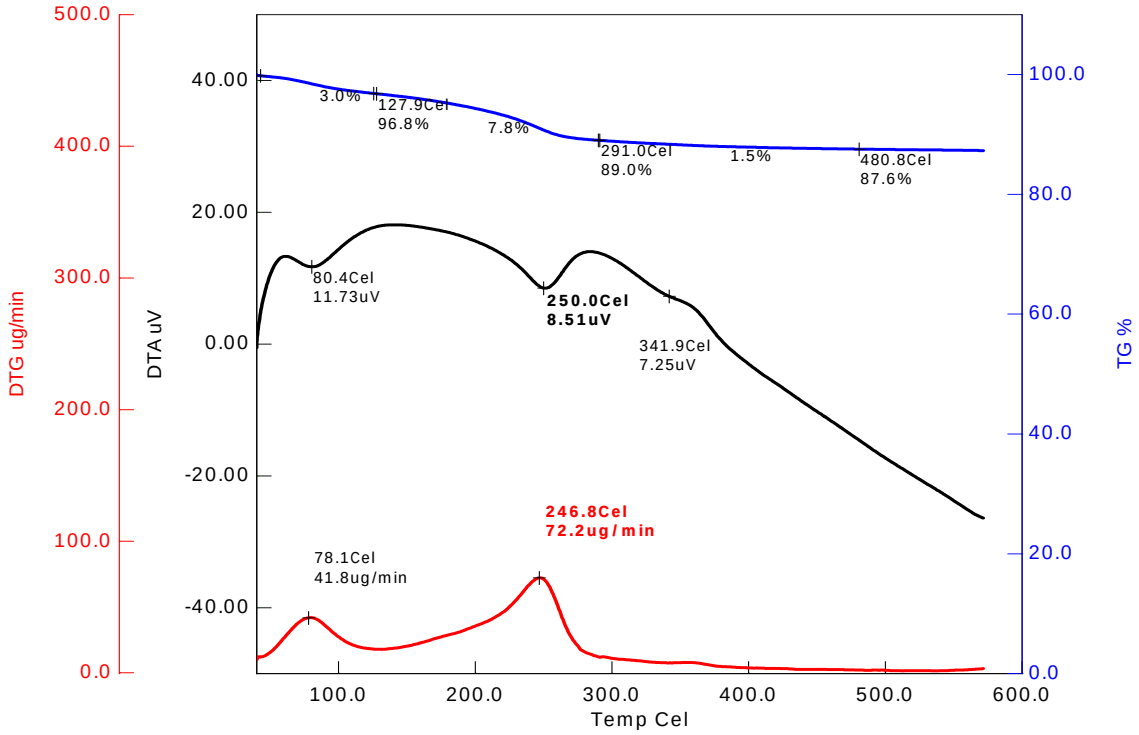

Figure : 3.12 TGA /DTA pattern of iron oxide-silica composite (1:1)

Thermograph of Fe_2O_3-SiO_2 composite (1:1) (**Figure 3.12**) shows gradual weight loss from 26^0C to 290^0C (11.0%), almost a steady state from 290^0C onward. Weight loss may

be due to removal of free water absorbed from atmosphere and presence of any structural water.

Differential Thermal Analysis (DTA) (**Figure 3.12**) shows two endothermic peak at 80.4^0C and 250^0C and three exothermic peak at 160^0C , 300^0C and 360^0C. The endothermic effect at 80.4^0C and 250^0C may be due to removal of structural water. Endothermic peak at 341.9^0C corresponds to decomposition of goethite phase . Exothermic peak at 300^0C can be considered to be due to the growth of goethite (α-FeOOH) , an intermediate step of hematite. Other exothermic peaks are due to recrystallization process involving transformation of smaller crystals into larger one. The DTA/TGA result shown above are in good agreement with the result shown by Ennas et al[108]and Palomares[109].

3.1.4 Energy Dispersive X-ray Spectroscopy (EDS) and Scanning Electron Microscopic (SEM) Analysis

The chemical composition of the samples were determined by energy dispersive X-ray spectroscopy (EDS). The topographical and morphological examination of silicon (IV) oxide, iron oxide and the composites were carried out by SEM examination. SEM images of the prepared samples are presented in the **Figures 3.13, 3.15, 3.17, 3.19 and 3.21** respectively. EDS of the prepared samples are presented in the **Figures 3.14, 3.16, 3.18, 3.20 and 3.22** respectively.

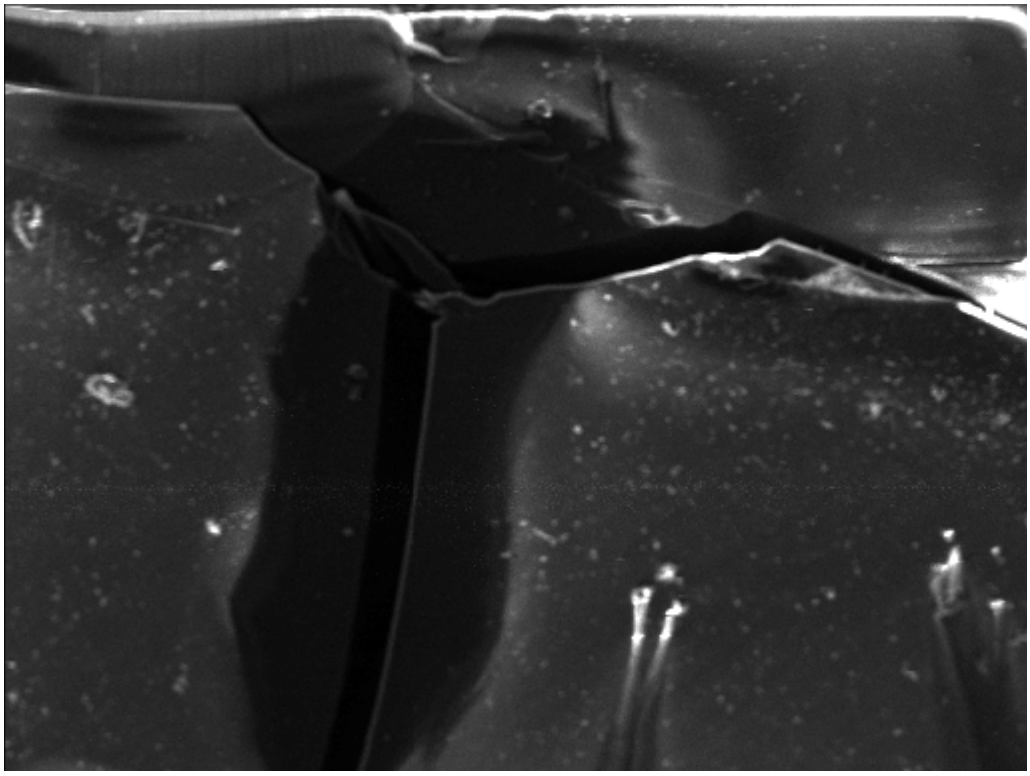

Figure 3.13 SEM image of prepared silicon (IV) oxide

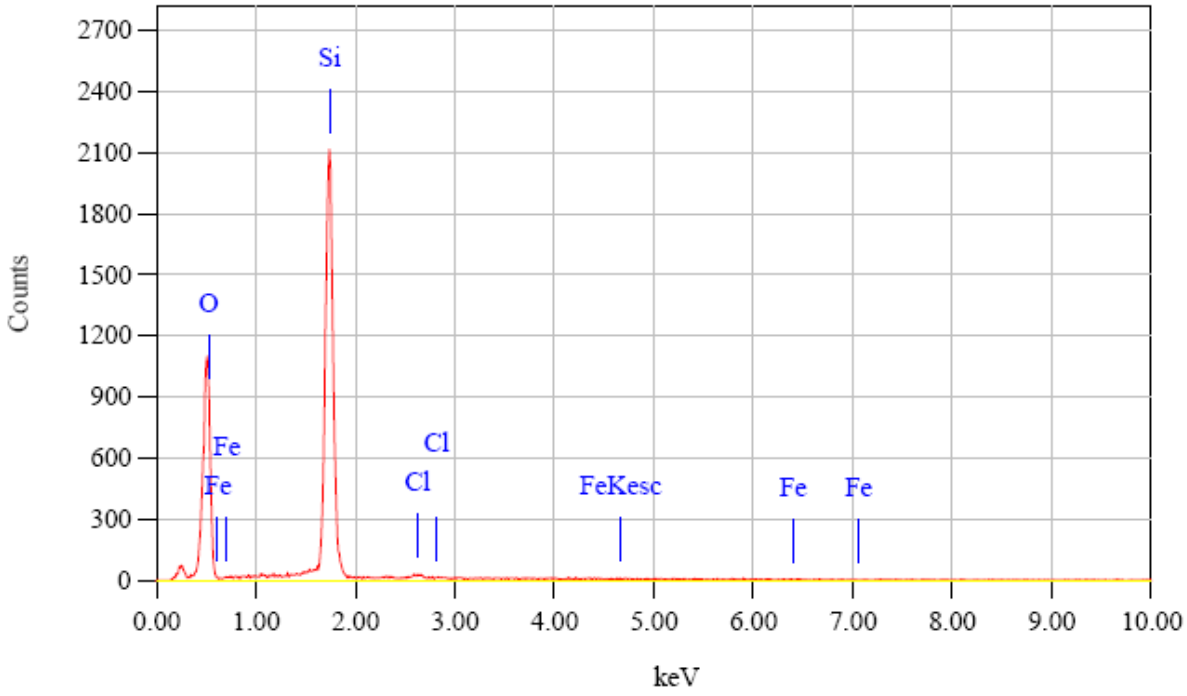

Figure 3.14 : EDS of prepared silicon (IV) oxide

ZAF Method Standardless Quantitative Analysis
Fitting Coefficient : 0.2927

Element	(keV)	Mass%	Error%	Atom%
O K	0.525	57.86	0.37	70.74
Si K	1.739	41.60	0.23	28.97
Cl K	2.621	0.45	0.27	0.25
Fe K	6.398	0.09	0.81	0.03
Total		100.00		100.00

The SEM and EDS results of silicon(IV) oxide are shown in the **Figure 3.13 and 3.14**.The particles are in aggregated form. EDS result suggests the presence of Si and oxygen elements, confirming the formation of SiO_2 particles. Theoretically Si-O ratio is 0.875 and experimentally the value is 0.72 , which is very close to the expected value. EDS result indicate the presence of trace amount of Cl as impurities.

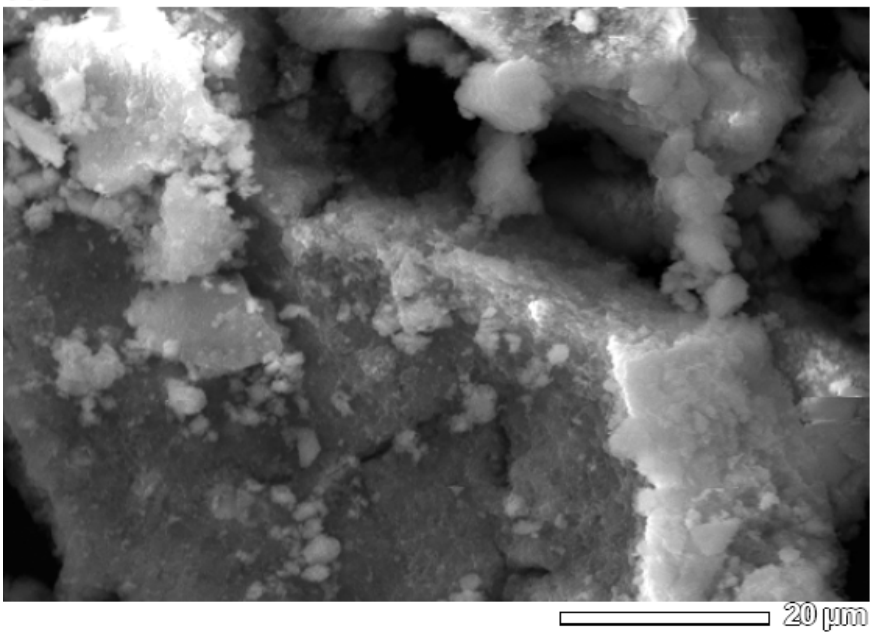

Figure 3.15 : SEM image of prepared iron (III) oxide

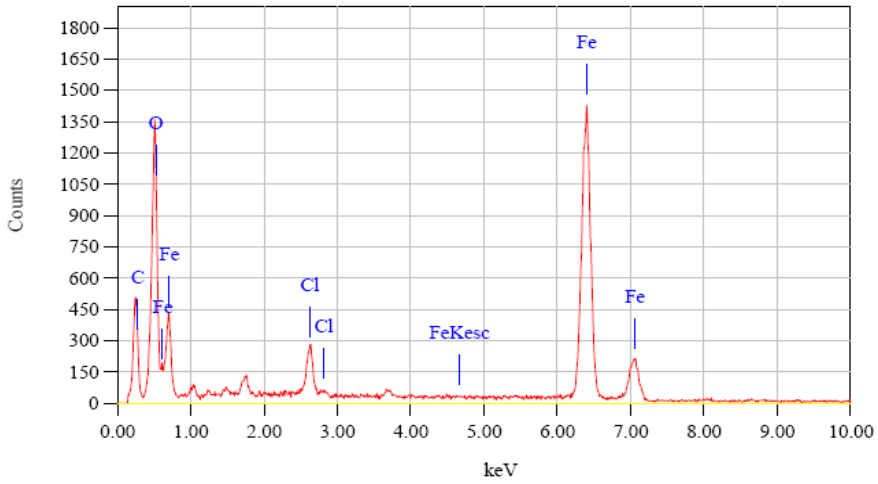

ZAF Method Standardless Quantitative Analysis
Fitting Coefficient : 0.3435

Element	(keV)	Mass%	Error%	Atom%	Compound	Mass%	Cation	K
C K	0.277	12.63	0.18	27.08				3.0628
O K	0.525	27.80	0.22	44.72				32.2215
Cl K	2.621	2.81	0.14	2.04				3.1877
Fe K	6.398	56.76	0.46	26.16				61.5279
Total		100.00		100.00				

Figure 3.16 : EDS of prepared iron (III) oxide

Figure 3.15 and 3.16 represents the SEM and EDS images of iron(III) oxide. These figures suggests the aggregation of the particles and small grains were present at the surface. However the elemental analysis suggests the presence of Fe and O atomic percentage, indicates the formation of the iron oxide. Theoretically Fe-O ratio is 2.33 and experimentally the value is 2.04 , which is very close to the expected value. EDS result indicate the presence of small amount of Cl as impurities.

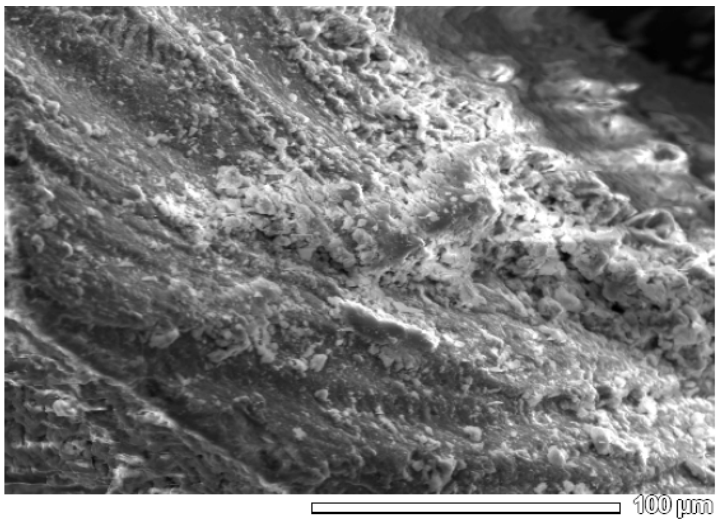

Figure3.17 : SEM image of prepared Fe_2O_3-SiO_2 composite (1:1)

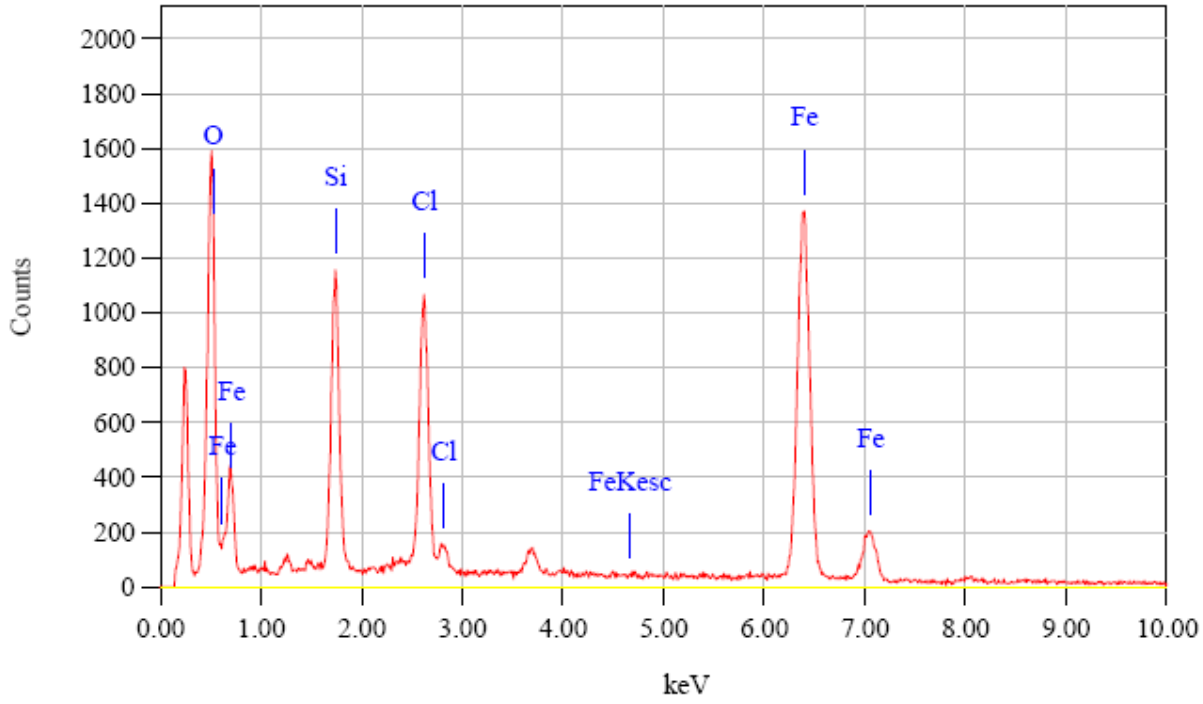

ZAF Method Standardless Quantitative Analysis
Fitting Coefficient : 0.3552

Element	(keV)	Mass%	Error%	Atom%	Compound	Mass%	Cation	K
O K	0.525	30.07	0.29	54.95				32.6701
Si K	1.739	10.47	0.25	10.90				7.3565
Cl K	2.621	10.07	0.20	8.30				10.2908
Fe K	6.398	49.39	0.63	25.85				49.6827
Total		100.00		100.00				

Figure 3.18 : EDS of prepared Fe_2O_3-SiO_2 composite (1:1)

The SEM and EDS results of the prepared composite, shown in the **Figures 3.17 and 3.18** , indicate the formation of the composite. The EDS result indicates the formation of the composite of composition (1:1). Theoretically Fe-Si to O ratio is 1.75 and experimentally it is found as 1.99, which is close to the expected value, confirming the formation of Fe_2O_3-SiO_2 composite (1:1) . The EDS result also indicate the presence of small amount of Cl as impurities.

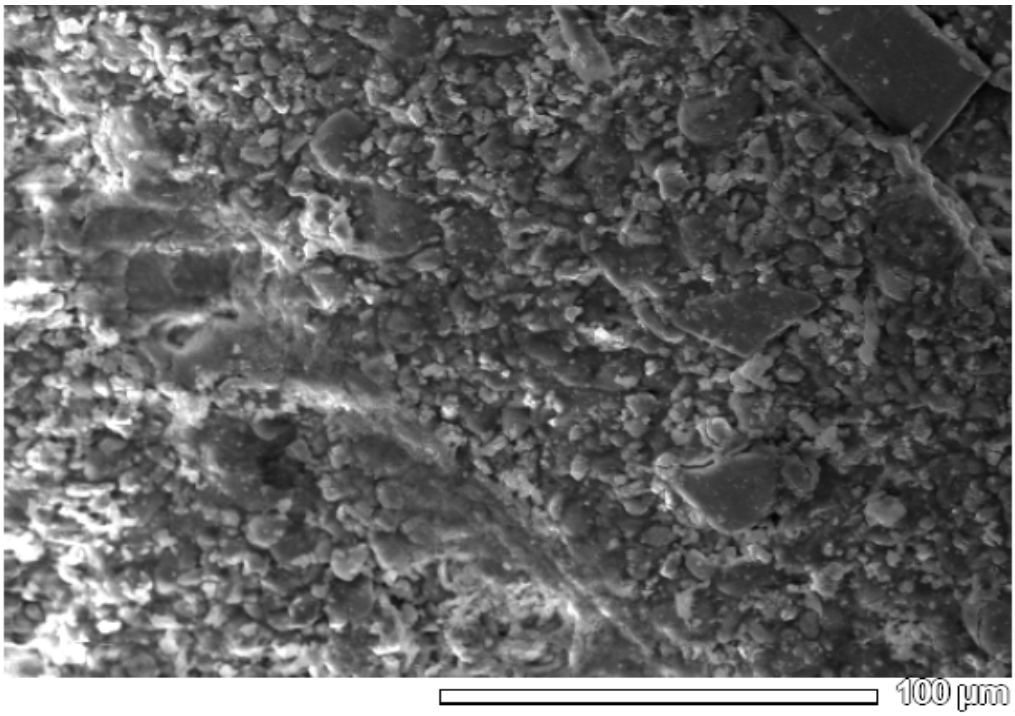

Figure 3.19 : SEM image of prepared Fe_2O_3-SiO_2 composite (3:7)

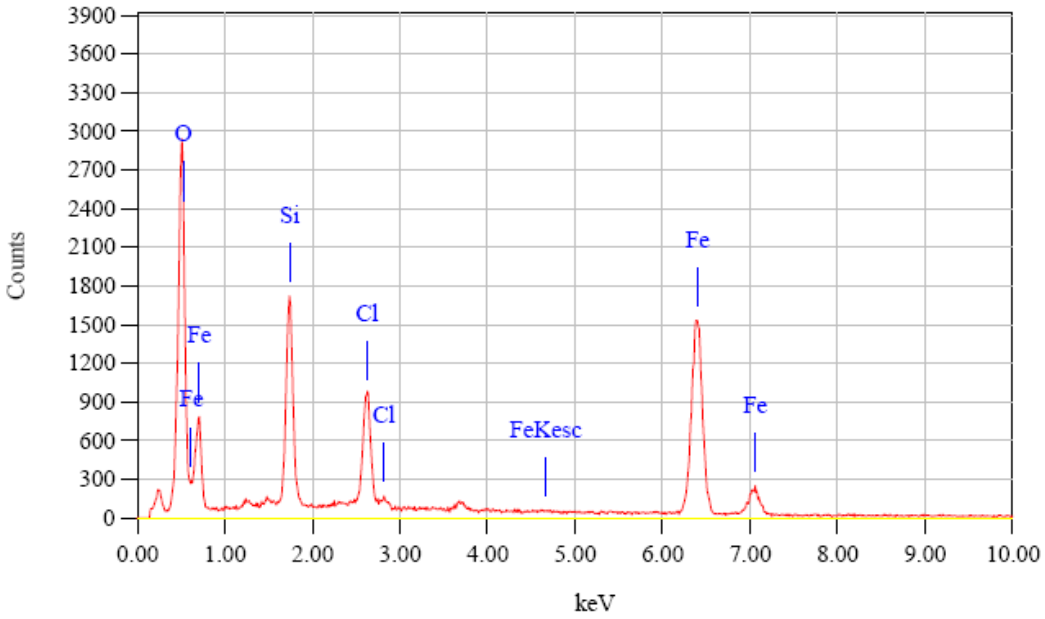

ZAF Method Standardless Quantitative Analysis
Fitting Coefficient : 0.2543

Element	(keV)	Mass%	Error%	Atom%	Compound	Mass%	Cation	K
O K	0.525	38.22	0.20	63.15				43.3570
Si K	1.739	12.13	0.18	11.42				8.4174
Cl K	2.621	7.07	0.15	5.27				6.9636
Fe K	6.398	42.58	0.46	20.16				41.2621
Total		100.00		100.00				

Figure3.20 EDS of prepared Fe_2O_3-SiO_2 composite (3:7)

The SEM and EDS results of the prepared composite, shown in the **Figures 3.19 and 3.20** , indicate the formation of the composite. The EDS result indicates the formation of the composite of composition (3:7). Theoretically Fe-Si to O ratio is 1.44 and experimentally it is found as 1.43, which is close to the expected value, confirming the formation of Fe_2O_3-SiO_2 composite (3:7) . The EDS result also indicate the presence of small amount of Cl as impurities.

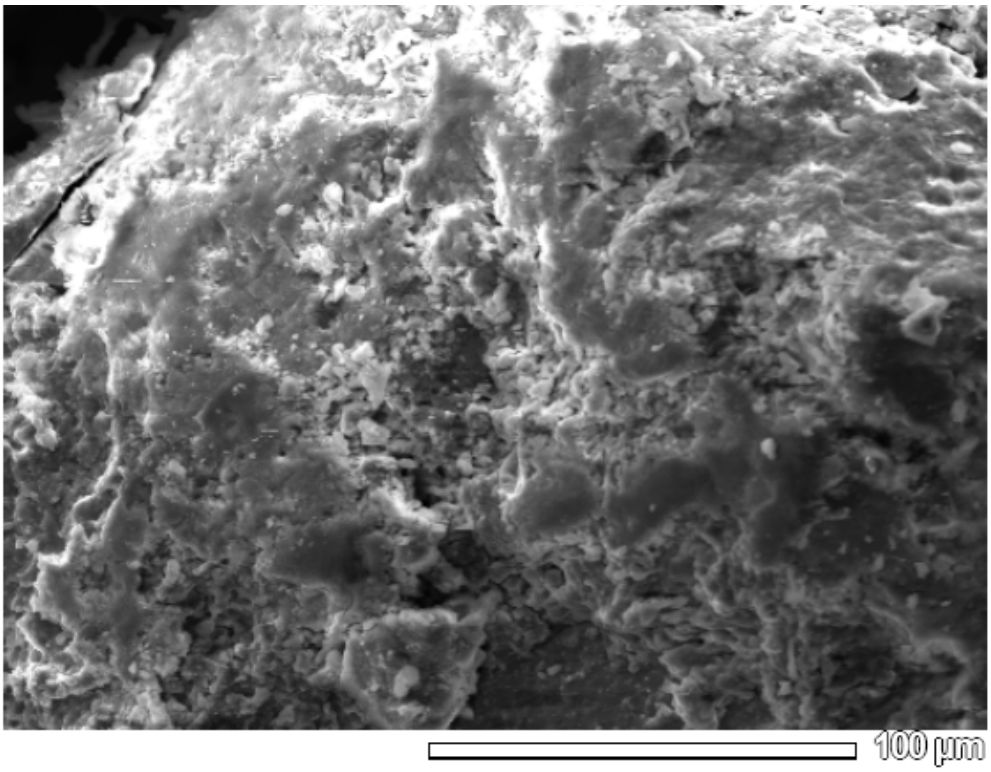

Figure 3.21 : SEM image of Fe_2O_3-SiO_2 composite (7:3)

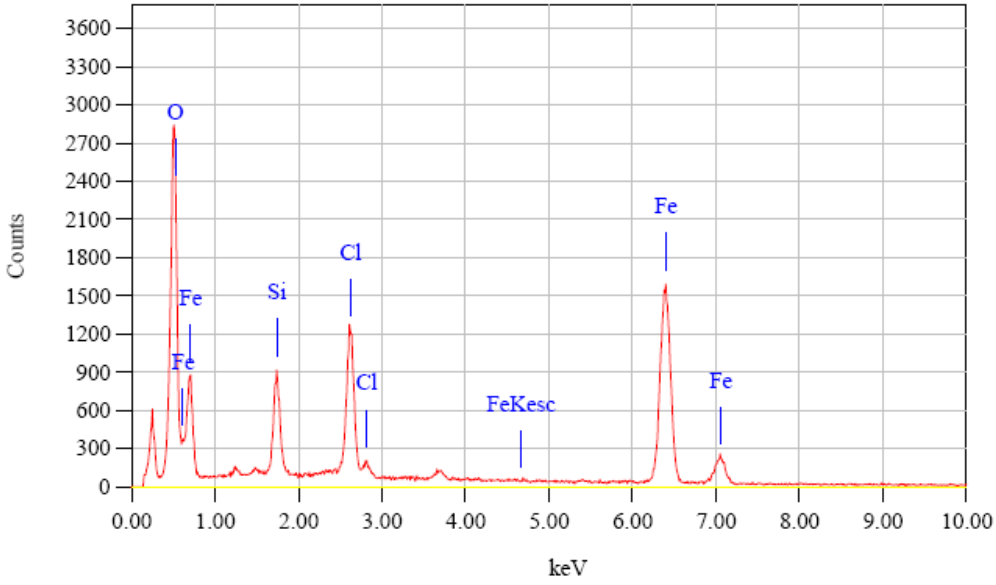

ZAF Method Standardless Quantitative Analysis
Fitting Coefficient : 0.2889

Element	(keV)	Mass%	Error%	Atom%	Compound	Mass%	Cation	K
O K	0.525	39.15	0.21	65.44				43.8954
Si K	1.739	6.05	0.20	5.76				3.9816
Cl K	2.621	9.28	0.16	7.00				9.1437
Fe K	6.398	45.51	0.50	21.79				42.9793
Total		100.00		100.00				

Figure 3.22: EDS of prepared Fe_2O_3-SiO_2 composite (7:3)

The SEM and EDS results of the prepared composite, shown in the **Figures 3.21 and 3.22** , indicate the formation of the composite. The EDS result indicates the formation of the composite of composition (7:3). Theoretically Fe-Si to O ratio is 2.00 and experimentally it is found as 1.33, which is close to the expected value, confirming the formation of Fe_2O_3-SiO_2 composite (7:3) . The EDS result also indicate the presence of small amount of Cl as impurities.

The SEM and EDS results of all the prepared composite of varied compositions , shown above , are in good agreement with the result reported by Meera Basa[103].

3.2.0 Interactions of Cr(VI) in aqueous solution with the Fe_2O_3-SiO_2 composites

The interactions of Cr(VI) with the Fe_2O_3-SiO_2 composites were studied by investigating the

(i) effects of different (a) dosages of composites as a sorbent , (b) initial concentrations and shaking time , (c) pH of Cr(VI) solution and (d) shaking time on adsorption of Cr(VI) on the composites .

(ii) adsorption isotherm and sorption kinetics of Cr(VI) on the composites as adsorbents.

Experimental results and discussion are presented in following Sections:

3.2.1 Investigation of the adsorption efficiency of Cr(VI) in aqueous solution for Fe_2O_3, SiO_2 and Fe_2O_3 - SiO_2 composite (1:1)

Details of the experimental procedures have been described in **Section 2.4.6.1**. The experimental data are presented in **Table 3. 5** .

Table 3.5 : The adsorption efficiency of Cr(VI) in aqueous solution for Fe_2O_3, SiO_2 and Fe_2O_3 - SiO_2 composite (1:1)

Experimental conditions: Volume of Cr(VI) solution = 20.0 cm^3, pH of Cr(VI) solution = 4.8 ± 0.2, Temperature = (30.0 ± 0.2) ^{0}C, Shaking speed = 250 rpm, Shaking Time = 20 minutes

Assumed Conc. (mgL^{-1}) /Initial absorbance	Actual Conc. (mgL^{-1})	Adsorbnt	Absorbance	Conc. at time t (Ct)	Amount adsorbed, x (mg)	Percentage of Cr (VI) adsorbed
10.00 / 1.062 (× 10)	11.93	Fe_2O_3	0.296 (× 10)	3.33	0.172	72.10
		SiO_2	0.799 (×10)	8.98	0.059	24.73
		Fe_2O_3 - SiO_2 composite	0.065 (×10)	0.73	0.224	93.88

The experimental data shown above, indicate that maximum amount of Cr(VI) removal is achieved by using Fe_2O_3-SiO_2 composite (1:1) and thus in this study the removal efficiency of Cr(VI) is studied by using the Fe_2O_3-SiO_2 composite of varied composition.

3.2.2 Investigation of the effect of variation of adsorbent dosage on adsorption of Cr(VI) in aqueous solution for Fe_2O_3-SiO_2 composite (1:1)

Details of the experimental procedures have been described in **section 2.4.6.2 .** The experimental data and corresponding plots are presented in **Table 3. 6** and **Figure 3.23** respectively.

Table 3.6 : The effect of variation of adsorbent dosage on adsorption of Cr(VI) in aqueous solution for Fe_2O_3-SiO_2 composite (1:1)

Experimental conditions: Volume of Cr(VI) solution = 25.0 cm^3, pH of Cr(VI) solution = 4.8 ± 0.2, Temperature = (30.0 ± 0.2) ^{0}C, Shaking speed = 250 rpm, Shaking Time = 20 minutes

Assumed Conc. (mg/L)	Actual Conc. (mg/L)	Dosage (g)	Conc.(Ct) at time t	Amount adsorbed, x (mg)	Amount adsorbed, x/m (mg/g)	Percentage of Cr (VI) removed
50.00	48.88	0.051	23.37	0.638	12.510	52.21
		0.102	9.06	0.996	9.765	81.51
		0.151	2.90	1.15	7.616	94.11
		0.201	2.27	1.17	5.821	95.90
		0.252	1.24	1.19	4.722	97.54
		0.302	1.97	1.17	3.874	95.90

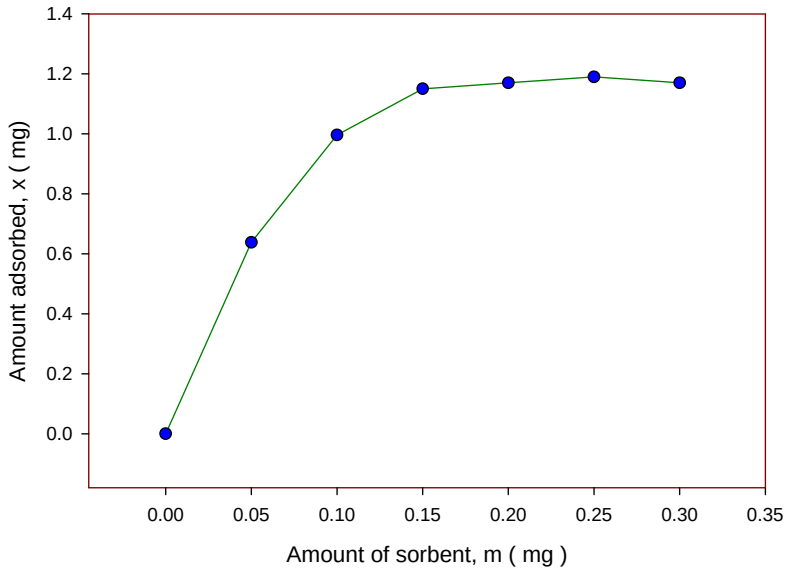

Figure 3.23: Effect of adsorbent [Fe_2O_3-SiO_2 composite (1:1)] dosage on Cr(VI) adsorption

The **Figure 3.23** shows that adsorption increases from 0.05g to 0.15g and stays almost constant up to 0.30 g of the sorbent dosage. This analysis provides a good guideline in choosing 0.20 g of as a perfect dosage which was sufficient to investigate sorption effect of Cr(VI) on the composite for a definite amount of Cr(VI) solution.

3.2.3. Determination of the effects of initial concentrations of Cr(VI) solution and shaking time on adsorption of Cr (VI) on Fe_2O_3-SiO_2 composites

In order to investigate the effect of different initial concentrations, viz, 40 and 50 mgL^{-1} of Cr(VI) solution at constant pH 4.8 and shaking time on Cr(VI) adsorption on the Fe_2O_3-SiO_2 composites, amount of Cr(VI) adsorbed per gram of the composite (x/m) were determined. Details of the experimental procedures for these measurements have been described in **Sections 2.4.6.3, 2.4.6.6 and 2.4.6.7** respectively. The adsorption data for Fe_2O_3-SiO_2 composite (1:1) are presented in **Table 3.7** and the corresponding plots of x/m against shaking time, t are shown in the **Figure 3.24.** The adsorption data for Fe_2O_3-

SiO_2 composite (3:7) are presented in **Table 3.8** and the corresponding plots of x/m against shaking time, t are shown in **Figure 3.25.** The adsorption data for Fe_2O_3-SiO_2 composite (7:3) are presented in **Table 3.9** and the corresponding plots of x/m against shaking time, t are shown in **Figure 3.26.**

Table 3.7: Determination of the effects of initial concentrations of Cr(VI) solution and shaking time on adsorption of Cr (VI) on Fe_2O_3-SiO_2 composite (1:1)

Experimental conditions: Volume of Cr(VI) solution = 25.0 cm^3, pH of Cr(VI) solution = 4.8 ± 0.2, Temperature = (30.0 ± 0.2) ^{0}C, Shaking speed = 250 rpm, Mass of adsorbent taken ≈ / = 0.20 gm

Assumed Conc. (mg/L)	Actual Conc. (mg/L)	Shaking time (minutes)	Conc. (Ct) at time t	Amount adsorbed, x (mg)	Mass of adsorbent, m (g)	Amount adsorbed, x/m (mg/g)	Percentage of Cr(VI) removed
40.00	41.51	0	0.000	0.000	0.000	0.000	0.00
		10	3.548	0.949	0.202	4.70	91.43
		20	2.241	0.982	0.201	4.89	94.61
		40	1.709	0.995	0.203	4.90	95.86
		60	1.577	0.999	0.201	4.97	96.24
		90	1.543	0.999	0.202	4.95	96.24
		120	1.388	1.003	0.203	4.94	96.63
50.00	48.88	0	0.000	0.000	0.000	0.000	0.00
		10	4.795	1.10	0.202	5.45	90.16
		20	4.154	1.12	0.201	5.57	91.80
		40	2.595	1.16	0.203	5.71	95.08
		60	1.871	1.18	0.201	5.87	96.72
		90	2.288	1.17	0.202	5.79	95.90
		120	2.148	1.17	0.201	5.82	95.90

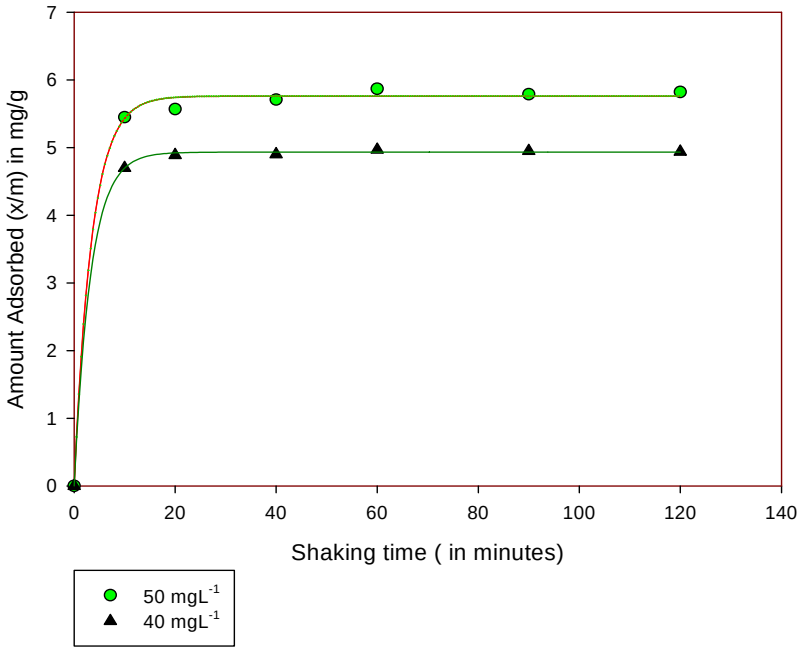

Figure 3.24: Effects of initial concentrations of Cr(VI) solution and shaking time on adsorption of Cr(VI) on Fe_2O_3-SiO_2 composite (1:1)

Table 3.8: Determination of the effects of shaking time on adsorption of Cr (VI) on Fe_2O_3-SiO_2 composite (3:7)

Experimental conditions: Volume of Cr(VI) solution = 25.0 cm^3, pH of Cr(VI) solution = 4.8 ± 0.2, Temperature = (30.0 ± 0.2) ^{0}C, Shaking speed = 250 rpm, Mass of adsorbent taken ≈ / = 0.20 gm

Assumed Conc. (mg/L)	Actual Conc. (mg/L)	Shaking time (minutes)	Conc.(Ct) at time t	Amount adsorbed, x (mg)	Mass of adsorbent, m (g)	Amount adsorbed, x/m (mg/g)	Percentage of Cr(VI) removed
50.00	48.88	0	0.000	0.000	0.000	0.000	0.00
		10	3.894	1.13	0.203	5.57	92.62
		20	3.115	1.14	0.201	5.67	93.44
		40	2.027	1.17	0.203	5.76	95.90
		60	1.532	1.18	0.202	5.84	96.72
		90	1.355	1.19	0.202	5.89	97.54
		120	1.401	1.19	0.201	5.92	97.54

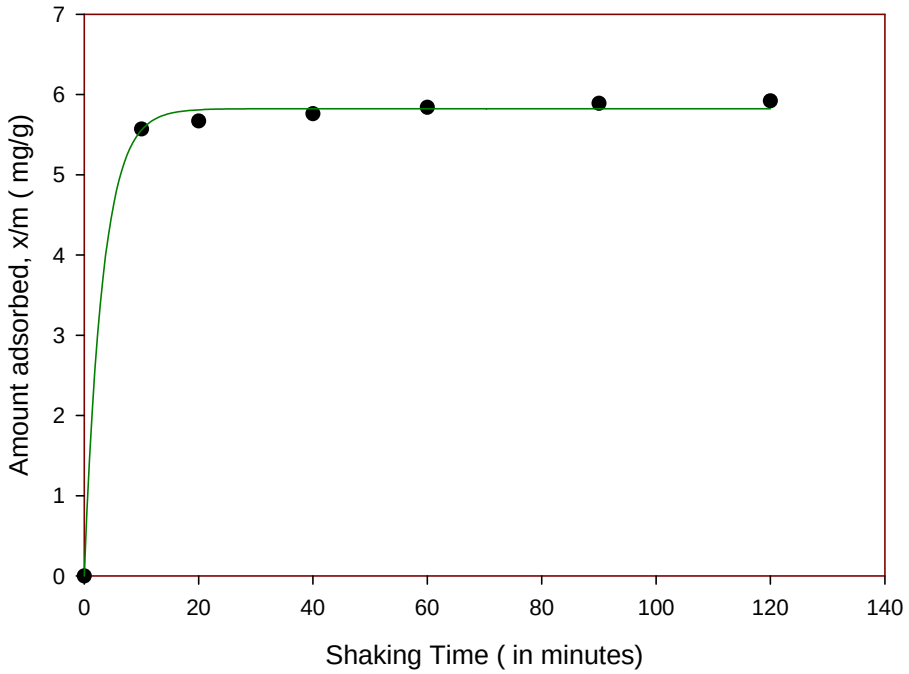

Figure 3.25: Effects of shaking time on adsorption of Cr(VI) on Fe_2O_3-SiO_2 composite (3:7)

Table 3.9: Determination of the effects of shaking time on adsorption of Cr (VI) on Fe_2O_3-SiO_2 composite (7:3)

Experimental conditions: Volume of Cr(VI) solution = 25.0 cm^3, pH of Cr(VI) solution = 4.8 ± 0.2, Temperature = (30.0 ± 0.2) ^{0}C, Shaking speed = 250 rpm, Mass of adsorbent taken ≈ / = 0.20 gm

Assumed Conc. (mg/L)	Actual Conc. (mg/L)	Shaking time (minutes)	Conc.(Ct) at time t	Amount adsorbed, x (mg)	Mass of adsorbent, m (g)	Amount adsorbed, x/m (mg/g)	Percentage of Cr (VI) removed
50.00	48.88	0	0.000	0.000	0.000	0.000	0.00
		10	10.11	0.969	0.201	4.82	79.30
		20	5.79	1.077	0.201	5.36	88.13
		40	5.78	1.078	0.203	5.31	88.22
		60	5.35	1.088	0.201	5.41	89.03
		90	5.13	1.094	0.202	5.42	89.53
		120	3.76	1.13	0.203	5.57	92.47

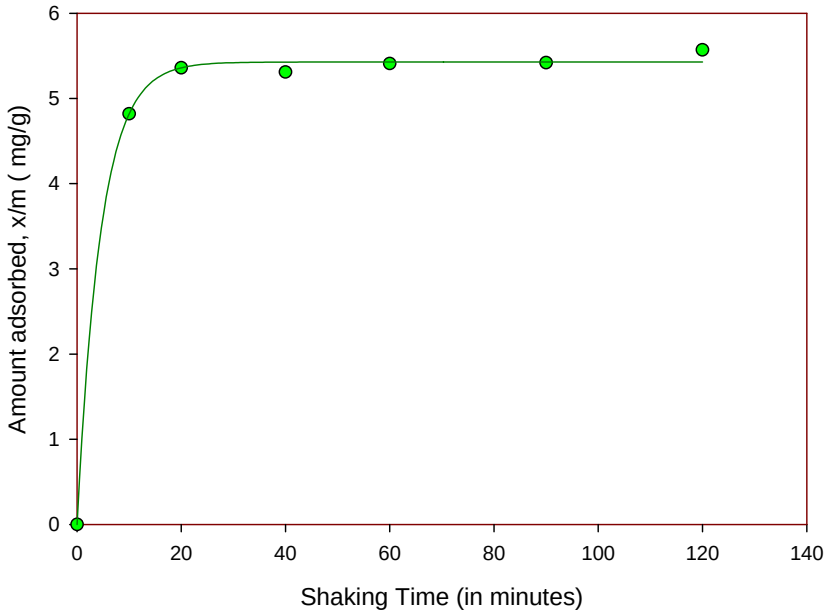

Figure 3.26: Effects of shaking time on adsorption of Cr(VI) on Fe_2O_3-SiO_2 composite (7:3)

The progresses of Cr(VI) adsorption at different initial concentrations 40 and 50 mgL^{-1} of Cr(VI) solution on iron oxide-silica composites with shaking time are shown graphically in **Figure 3.24, Figure 3.25 and Figure 3.26** respectively. The result show that the rate of adsorption in all the cases are significantly rapid initially within first 15 minutes (about 78-94%) at all concentrations of Cr (VI) solution which gradually falls off until equilibrium was attained. However, equilibrium was practically attained in about 20 minutes.

The experimental data indicate that the amount (mgg^{-1}) of Cr(VI) adsorbed by the Fe_2O_3-SiO_2 composites at equilibrium increased with increase in initial concentration of Cr(VI) in aqueous solution. However, the percentage removal efficiency for Cr(VI) from aqueous system by the Fe_2O_3-SiO_2 composites appears to increase with increase in the initial concentration of Cr(VI) in aqueous solution.

3.2.4. Determination of the effects of variation in pH of Cr(VI) solution and shaking time on adsorption of Cr (VI) on Fe_2O_3-SiO_2 composite (1:1)

Investigation for these studies was conducted according to the procedure described in **Section 2.4.6.4.**

Preliminary experiments showed that the composite remain stable over a pH range of 2-9. Presence of iron in the supernatant liquid could not be detected by chemical tests.

Adsorption of Cr(VI) on Fe_2O_3-SiO_2 composite (1:1) at ambient temperature was investigated at different pH, viz. 3.0, 4.8 and 8.0. The kinetics of adsorption was measured by measuring the amount of Cr(VI) adsorbed as function of shaking time. The data are presented in **Table 3.10.** The corresponding plots of the amount of Cr(VI) adsorbed per gram of adsorbent (x/m) against shaking time, t are shown in **Figure 3.27.** The rate of adsorption of Cr(VI) seems to be very little influenced by pH ; the time required to reach equilibrium is about 20 minutes over the whole range of pH investigated.

However, the amount of Cr(VI) adsorbed on the composites was profoundly influenced by pH. **Figure 3.28** shows the variation of the amount of Cr(VI) adsorbed per gram of the adsorbents with pH. At pH 3.0 maximum amount of Cr(VI) was adsorbed (about 98%) , at pH 4.8 the amount of Cr(VI) adsorbed was 96.5% and about 77% at pH 8.0 . So it can be said that the Cr(VI) removal efficiency decreases with increases in pH.

Table 3.10: Determination of the effects of variation in pH of Cr(VI) solution and shaking time on adsorption of Cr (VI) on Fe_2O_3-SiO_2 composite (1:1)

Experimental conditions: Volume of Cr(VI) solution = 25.0 cm^3, Temperature = (30.0 ± 0.2) ^{0}C, Shaking speed = 250 rpm, Mass of adsorbent taken ≈ / = 0.20 gm (for pH 3.0 and 4.8) and 0.25 gm for pH 8.0

pH	Assumed Conc. (mg/L)	Actual Conc. (mg/L)	Shaking time (minutes)	Conc. (Ct) at time t	Amount adsorbed, x (mg)	Mass of adsorbent, m (g)	Amount adsorbed, x/m (mg/g)	Percentage Cr (VI) removed
3.0	50.00	48.88	0	0.000	0.000	0.000	0.000	0.00
			10	1.956	1.173	0.201	5.84	95.99
			20	1.468	1.185	0.201	5.90	96.97
			40	1.147	1.193	0.202	5.91	97.63
			60	1.001	1.197	0.201	5.96	97.95
			90	0.840	1.201	0.200	6.00	98.28
4.8	50.00	48.88	0	0.000	0.000	0.000	0.000	0.00
			10	4.795	1.10	0.202	5.45	90.16
			20	4.154	1.12	0.202	5.57	91.80
			40	2.595	1.16	0.201	5.71	95.08
			60	1.871	1.18	0.201	5.87	96.72
			90	2.288	1.17	0.203	5.79	95.90
8.0	50.00	48.88	0	0.000	0.000	0.000	0.000	0.00
			10	3.243	1.14	0.251	4.54	74.45
			20	2.522	1.16	0.251	4.62	75.53
			40	2.221	1.17	0.250	4.68	76.27
			60	1.866	1.18	0.252	4.68	77.25
			90	1.673	1.18	0.250	4.72	77.25

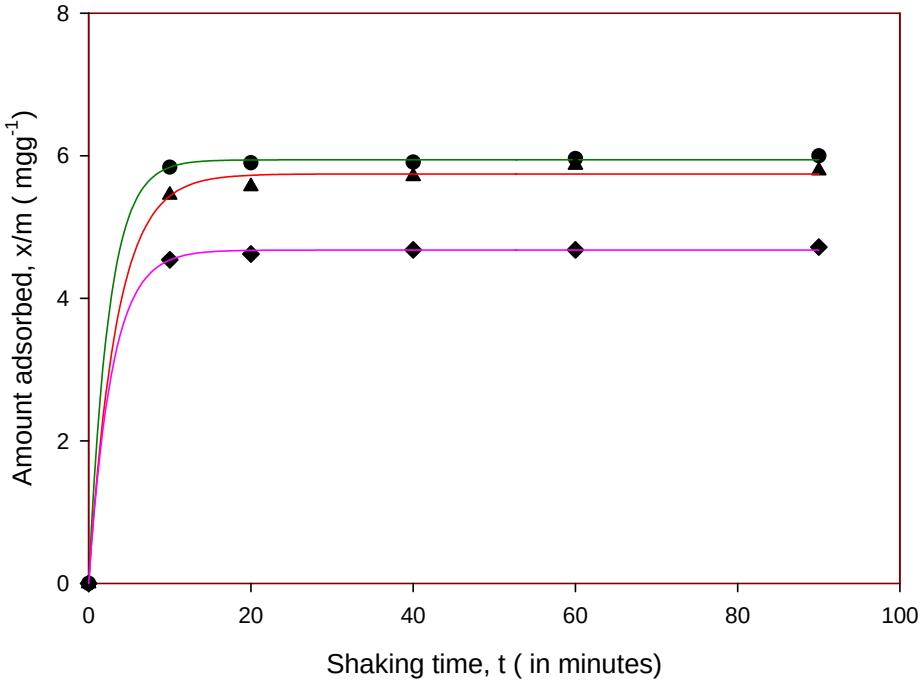

Figure 3.27: Effects of effects of variation in pH of Cr(VI) solution and shaking time on adsorption of Cr (VI) on Fe_2O_3-SiO_2 composite (1:1)

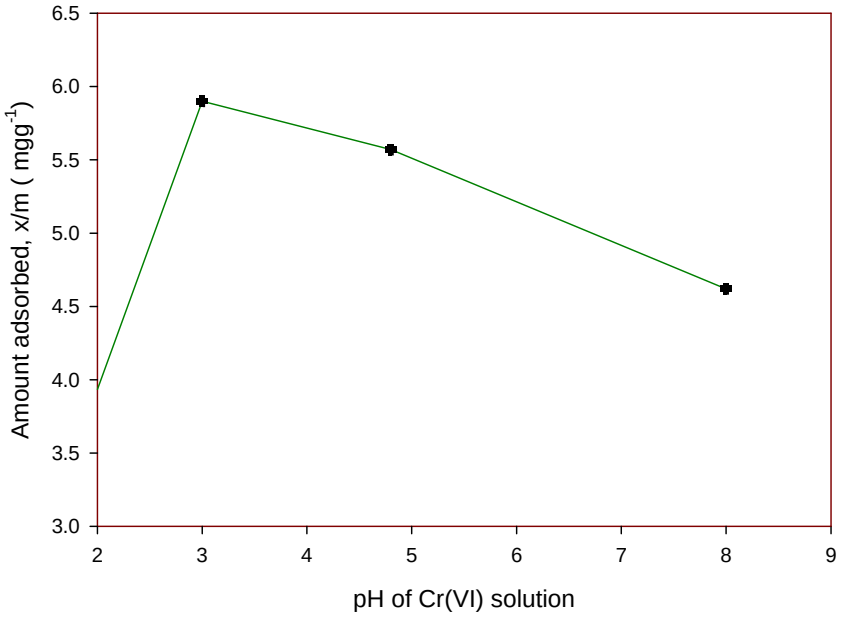

Figure 3.28: Variation of Cr(VI) solution adsorption with shaking time on Fe_2O_3-SiO_2 composite (1:1) at pH 3.0, 4.8 and 8.0 of Cr(VI) solution

Surfaces of Fe_2O_3-SiO_2 composite (1:1) were likely to be covered with hydroxyl groups in aqueous medium that vary in forms at different pH. The surface charge was neutral at pH_{zpc} below the $pH_{zpc,}$ the adsorbent surfaces were positively charged that favours anions adsorption. On the other hand, at pH greater than pH_{zpc} ($pH > pH_{zpc}$) the surfaces of the adsorbent were negatively charged which disfavours anion adsorption. The electrostatic repulsion between Cr(VI) and the negatively charged adsorbent will result a decrease in percentage removal of Cr(VI) from the adsorption medium. Also, at higher pH, the concentration of OH^- anions increases in the aqueous medium, which competes with Cr(VI) species in solution. Besides this, chances of hydrogen bonding by the hydroxyl protons with the oxygen present on the silica surface cannot be ignored.

3.3.0 Adsorption isotherm

Isotherm for adsorption of Cr(VI) from aqueous solution on the Fe_2O_3-SiO_2 composite (1:1) has been investigated to study interaction of Cr(VI) with the composites.

3.3.1. Adsorption isotherm of Cr(VI) on Fe_2O_3-SiO_2 composite (1:1)

Experimental procedure has been described in **Section 2.4.6.5.**

The experimental data and corresponding plots for adsorption isotherm of Cr(VI) are shown in **Table 3.11** and **Figure 3.29** respectively.

Table 3.11: Adsorption isotherm of Cr(VI) on Fe_2O_3-SiO_2 composite (1:1)

Experimental conditions: Volume of Cr(VI) solution = 25.0 cm^3, Temperature = (30.0 ± 0.2) ^{0}C, Shaking speed = 250 rpm, Mass of adsorbent taken ≈ / = 0.20 gm, pH = 4.8

Assumed Conc. (mg/L)	Actual Conc. C_0 (mg/L)	Equilibrium Conc. C_e (mg/L)	Amount adsorbed, x (mg)	Mass of adsorbent, m (g)	Amount adsorbed, x/m (mg/g)	Percentage adsorbed
0.00	0.00	0.00	0.00	0.00	0.00	0.00
10	10.06	0.16	0.2475	0.208	1.19	98.41
20	20.49	0.605	0.4973	0.202	2.46	97.05
40	41.51	2.24	0.982	0.201	4.89	94.61
50	48.88	4.15	1.118	0.201	5.56	91.80
60	58.05	8.65	1.235	0.210	5.85	85.11

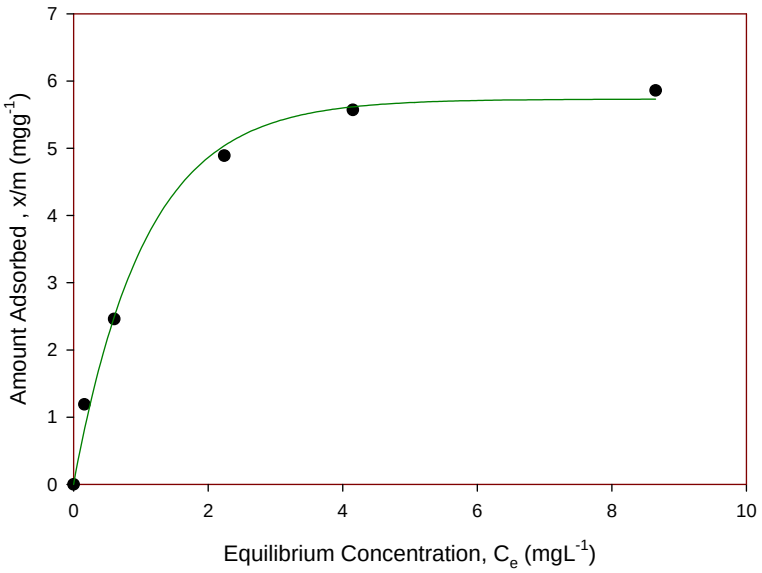

Figure 3.29: Adsorption isotherm of Cr (VI) on Fe_2O_3-SiO_2 composite (1:1)

The experimental result of adsorption isotherm for adsorption of Cr(VI) on Fe_2O_3-SiO_2 composite (1:1) shows that 5.57 mg (91.80%) of Cr(VI) was removed from its aqueous solution per gram of Fe_2O_3-SiO_2 composite (1:1) when 48.88 mgL^{-1} of Cr(VI) solution at pH 4.8 at 30.0 ^{0}C was put in contact with Fe_2O_3-SiO_2 composite (1:1) for 20 minutes.

3.3.1.1 Nature of the experimental adsorption isotherm for adsorption of Cr(VI) on Fe_2O_3-SiO_2 composite (1:1)

The experimental isotherm appeared to be a Langmuir isotherm. Therfore, a through test was performed by fitting the experimental data to the Langmuir equation. According to the Langmuir equation

$$\frac{C_e}{Q} = \frac{1}{K_a Q_m} + \frac{C_e}{Q_m}$$

A plot of C_e / (x/m) against C_e should be a straight line, where x/m=Q is the amount adsorbed per gram of adsorbent at an equilibrium concentration of C_e and Q_m is corresponding amount for the formation of a monolayer. The calculated data for the Langmuir plot are shown in **Table 3.12** and the Langmuir plot is shown in the **Figure 3.30.**

Table 3.12: Langmuir adsorption isotherm of Cr(VI) on Fe_2O_3-SiO_2 composite (1:1)

Experimental conditions: Volume of Cr(VI) solution = 25.0 cm^3, Temperature = (30.0 ± 0.2) ^{0}C, Shaking speed = 250 rpm, Mass of adsorbent taken ≈ / = 0.20 gm, pH = 4.8

Assumed Conc. (mg/L)	Actual Conc. C_0 (mg/L)	Equilibrium Conc. C_e (mg/L)	Amount adsorbed, x (mg)	Q (x/m) mg/g	C_e / Q mg/L
0.00	0.00	0.00	0.00	0.00	0.00
10	10.06	0.16	0.2475	1.19	0.13
20	20.49	0.605	0.4973	2.46	0.25
40	41.51	2.24	0.982	4.89	0.46
50	48.88	4.15	1.118	5.56	0.75
60	58.05	8.65	1.235	5.85	1.48

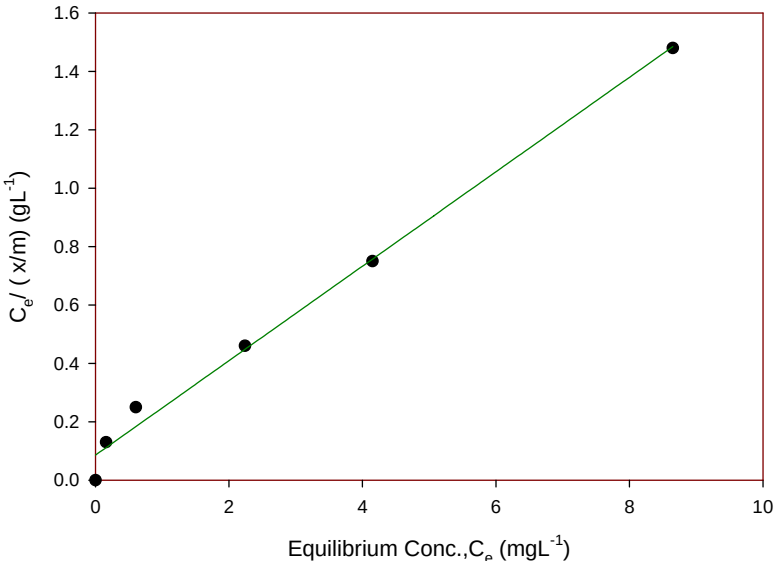

Figure 3.30: Langmuir plot for the adsorption of Cr (VI) on Fe_2O_3-SiO_2 composite (1:1)

The figure shows a linear plot of C_e / (x/m) against C_e. The fitting of the experimental data to a straight line is excellent, indicating the validity of the Langmuir model of adsorption. The values of the Langmuir constants, Q_m and K_a were determined from the plot and found to be 6.17 mgg^{-1} and 1.80 Lmg^{-1} respectively. The essential characteristics of Langmuir isotherm is expressed in terms of a dimensionless constant separation factor or equilibrium parameter, R_L which is defined by the relation :

$$R_L = [1 / (1+ K_aC_o)]$$

Where K_a is the Langmuir constant and C_o is the initial concentration of Cr(VI).

The equilibrium parameter, R_L can easily be calculated using the values C_o and K_a as found earlier. Data for calculating the values of R_L are shown in **Table 3.12.**

Table 3.13: Determination of equilibrium parameters from Langmuir adsorption isotherm of Cr(VI) on Fe_2O_3-SiO_2 composite (1:1)

Initial Concentration C_o mg/L	K_a L/mg	1+ K_a C_o	R_L
10.06	1.80	19.108	0.052
20.49		37.882	0.026
41.51		75.718	0.013
48.88		88.984	0.011
58.05		105.49	0.009

It is found from the **Table 3.12** that $0< R_L <1$. This indicates favourable adsorption of Cr(VI) on Fe_2O_3-SiO_2 composite (1:1) at all concentrations and the pH of Cr(VI) studied.

3.4.0 sorption dynamics

Experimental procedure has been described in **Section 2.4.6.8.**

The rate constant for the sorption of Cr(VI) on Fe_2O_3-SiO_2 composite (1:1) has been determined from the first order rate expression given by Lagergren[110].

$$\ln(Q_e - Q) = \ln Q_e - k_{ad}\, t$$

Where k_{ad} is the rate constant for adsorption, Q (mg/g) is the amount of Cr(VI) adsorbed per gram of adsorbent at time t and Q_e (mg/g) is the amount of Cr(VI) adsorbed per gram of adsorbent at equilibrium time.

The data and plot of $\ln(Q_e - Q)$ vs shaking time are presented in the **Table 3.13** and **Figure 3.31** respectively.

Table 3.14: Data for sorption kinetics

Experimental conditions: Volume of Cr(VI) solution = 25.0 cm^3, Temperature = (30.0 ± 0.2) ^{0}C, Shaking speed = 250 rpm, Mass of adsorbent taken ≈ / = 0.20 gm, pH = 4.8

Assumed Conc. (mg/L)	Actual Conc. (mg/L)	Shaking time (minutes)	Conc.(Ct) at time t	Amount adsorbed, x (mg)	Q (x/m) (mg/g)	Q_e-Q (mg/L)	ln (Q_e-Q)	$t^{1/2}$ ($min^{1/2}$)
50.00	48.88	0	0.000	0.000	0.000	0.00	0.00	0.00
		5	6.850	1.05	5.21	0.36	-1.02	2.24
		10	4.795	1.10	5.45	0.12	-2.12	3.16
		15	4.550	1.11	5.52	0.05	-3.00	3.87
		20	4.154	1.12	5.57	-	-	-
		40	2.595	1.16	5.71	-	-	-
		60	1.871	1.18	5.87	-	-	-
		90	2.288	1.17	5.79	-	-	-
		120	2.148	1.17	5.82	-	-	-

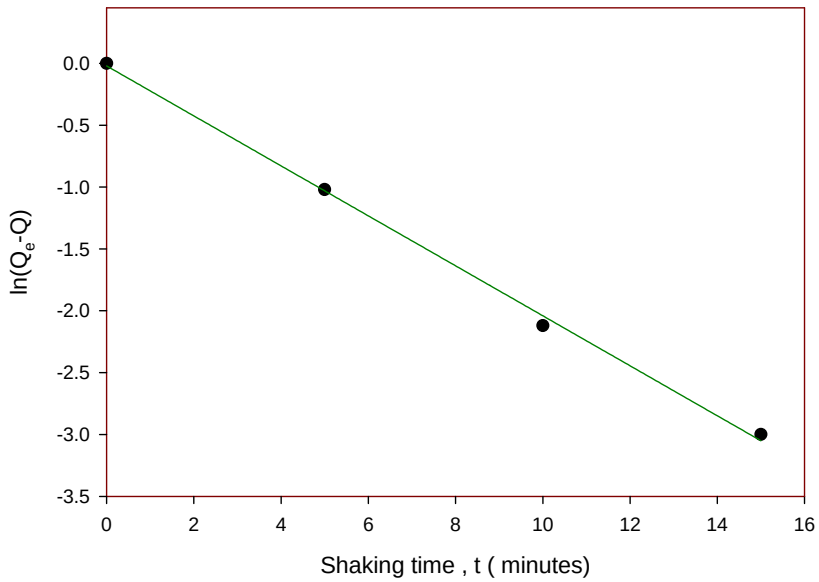

Figure 3.31: Lagergren plot for the adsorption of Cr (VI) on Fe_2O_3-SiO_2 composite (1:1)

Linear plot of ln(Q_e - Q) vs shaking time indicates the applicability of Lagergren equation and the first order nature of the adsorption process. The value of the rate constant k_{ad} for adsorption was computed from the slope of the straight line in **Figure 3.31** and was found to be 0.2 min^{-1} at 30.0 ^{0}C.

The rate constant of intra-particle transport, k_d, was calculated using the equation of Weber and Morris[111].

$$Q = k_d\, t^{1/2}$$

Where Q is the amount of Cr(VI) adsorbed (mg/g) per gram of the adsorbent at time t. A plot of Q vs $t^{1/2}$ is shown in **Figure 3.32.**

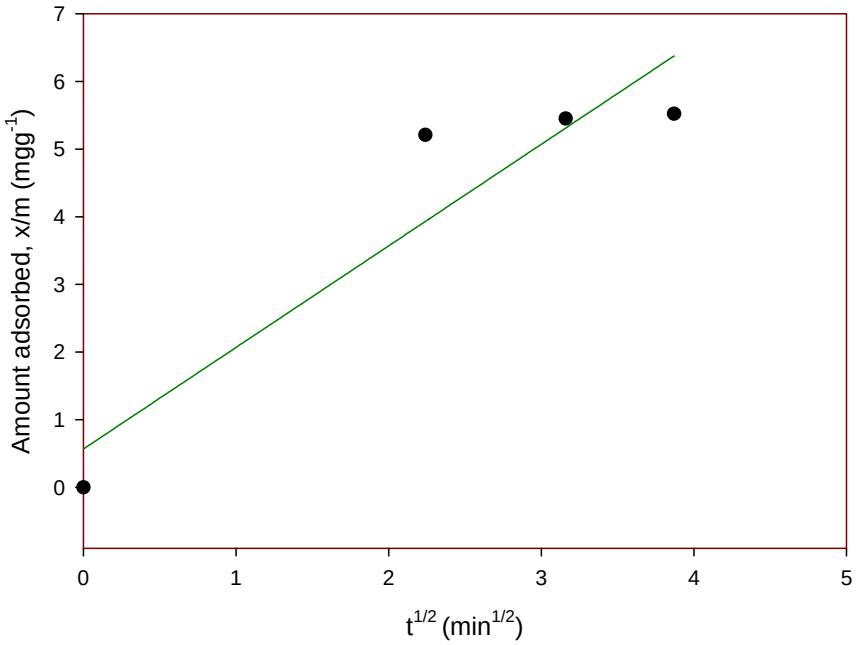

Figure 3.32: Validation of Morris-Weber equation for sorption of Cr (VI) on Fe_2O_3-SiO_2 composite (1:1)

It is clear that the linear plot of Q vs $t^{1/2}$ does not pass through the origin. It thus indicates that the pore diffusion is not the only rate-controlling step in the removal of Cr(VI) in aqueous system, especially for the first minutes of shaking time[112]. The rate constant k_d of intra-particle transport was computed from the slope of the **Figure 3.32** and was found to be 1.51 mg g^{-1} $min^{-1/2}$ at 30.0 ^{0}C.

4. Conclusion

4. Conclusion

Iron oxide- SiO_2 composite was prepared by Sol-Gel method . This composite was used to remove Cr(VI) from aqueous solution. Cr(VI) is a potential toxic substance, which is widely used in leather and textile industries. Since tetraethylorthosilicate and metallic iron are comparatively low cost reagents, these were used as precursors to silicon (IV) oxide and iron (III) oxide in this research. Silicon (IV) oxide and iron oxide , as constituents of the iron oxide - SiO_2 composites, were prepared earlier and characterized by FT-IR , XRD, TGA/DTA ,SEM and EDS techniques. XRD and FT-IR results confirm that *Magnetite* (Fe_2O_3) type of iron (III) oxide and *Tridymite (*SiO_2) type of silicon (IV) oxide were prepared in this research.

Iron oxide-SiO_2 composites prepared by different method has been characterized by FT-IR, XRD, TGA/DTA , SEM and EDS techniques. Analytical results obtained by the above techniques lead us to conclude that iron oxide- SiO_2 composites were formed due to interaction between silicon (IV) oxide and iron (III) oxide.

Removing efficiency of Cr(VI) by the iron oxide- SiO_2 composites were determined by studying adsorption of Cr(VI) in aqueous solution on the composites under different experimental conditions , such as sorbent dosages, initial concentration and pH of Cr(VI) solution and shaking time. Adsorption was found to be dependent on pH and initial concentration of Cr(VI) solution. Results of adsorption studies suggest that iron oxide removes 72.1% , silicon (IV) oxide removes 24.73% and iron oxide – silicon (IV) oxide composite removes 93.88% Cr(IV) from aqueous solution. Therefore, it can be said that iron oxide – silicon (IV) oxide composites plays effective role in adsorption of Cr(VI)

from aqueous solution. Studies of the sorption kinetics show that equilibrium adsorption was attained in 20 minutes depending on other experimental conditions. The kinetic data justified Lagergren first-order kinetic equation. Adsorption isotherm study showed that the results fulfilled the Langmuir Model of adsorption isotherm.

However, effects of the following parameters on Cr(VI) adsorption on SiO_2-iron oxide are recommended for further studies:

(i) Cr(VI) adsorption on iron oxide- SiO_2 composites may be studied at different temperatures in order to observe effect of temperature on Cr(VI) adsorption on the composites. This will enable to calculate the enthalpy of adsorption.

(ii) Surface charge and zpc should be determined to better understand the surface properties of the adsorbent.

(iii) Adsorption of other heavy metals present in waste water on the prepared composites may be studied.

5. References

REFERENCES

1. Corcoran,E., Nellemann,C., Baker,E., Bos,R., Osborn,D., Savelli,H., "Sick water? The central role of wastewater management in sustainable development" A rapid response assessment, United Nations Environment Programme (UNEP) (2010) ISBN: 978-82-7701-075-5

2. www. en. wikipedia .com

3. (a) www. Banglapedia . com ; (b) Anis Ahmed, " It was once the lifetime of the Bangladeshi capital", Reuters, May 18,2009 ; (c) www. BangladeshNews.com.bd ; (d) Islam Faisal, Rumi Shammin, Juhaina Junaid, " Industrial Pollution in Bangladesh", The World Bank, WED 2004, SDNM ; (e) Samir Barua , " karnaphuli pollution proves fatal for marine fisheries in Bay " , 28th May, 2005, BDNews

4. Chowdhury, N. S. and Clemett, A. E. V. (2006) Industrial pollution and its threat to Mokesh Beel wetland in Kaliakoir. MACH technical report, Dhaka.

5. Aquatic Ecology and dangerous substances : Bangladesh perspective; Diffuse Pollution Conference Dublin 2003 8C Ecology:

6. Arias-Barreiro,C.R., Nishizaki,H., Okubo,K., Aoyama,I., Mori, I.C., " Ecotoxicological characterization of tannery wastewater in Dhaka,Bangladesh", Journal of Environmental Biology , July 2010, 31 , 471-475 (2010)

7. Imamul Huq,S.M., " Critical Environmental Issues Relating to Tanning Industries in in Bangladesh",

8. "Pollution gets to groundwater" , The Daily Star, 26 April,2009

9. UNIDO: Regional programme for pollution control in the tanning industry in south - east Asia : Chrome balance in leather processing (2000).

10. (a) Gain, P.: Bangladesh Environment: Facing the 21st century. Society for Environment and Human Development (SEHD), Dhaka, Bangladesh (2002).

(b) Nath, K., D. ; Singh, S. ; Shyam and Sharma, Y.K.: "Phytotoxic effects of chromium and tannery effluent on growth and metabolism of Phaseolus mungo Roxb." J. Environ. Biol., 30, 227-234 (2009).

11. (a) Kashem, M.A. and B.R. Singh: "Heavy metal contamination of Soil and Vegetation in the vicinity of industries in Bangladesh." Water Air Soil Pollut., 115, 347-361 (1999).

(b) Shams, K.M., Tichy G., Fischer A., Filip K., Sager M.,Bashar A.,Peer T. and Jozic M., "Chromium contamination from tannery wastes in the soils of Hazaribagh area in Dhaka City, Bangladesh and aspects of its phytoremediation", Geophys Res. Abstr., 10 (2008).

(c) Zahid, A., K.D. Balke, M.Q. Hassan and M. Flegr: "Evaluation of aquifer environment under Hazaribagh leather processing zone of Dhaka city", Environ. Geol., 50, 495-504 (2006).

12. Arias-Barreiro C.R., Nishizaki H., Okubo K., Aoyama I. and Mori I.C. "Ecotoxicological characterization of tannery wastewater in Dhaka, Bangladesh " Journal of Environmental Biology, 31, 471-475 (2010)

13. (a) Pellerin, C. and Booker S. M., " Reflections on hexavalent chromium. Health hazards of an industrial heavyweight.", Environ. Hlth. Persp., 108, 402-407 (2000).

(b) Shanker, A.K., Cervantes C., Loza-Tavera H. and Avudainayagam S.: "Chromium toxicity in plants" Environ. Int., 31, 739-753 (2005).

(c) Kuykendall, J.R., Miller K.L., Mellinger K.N. and Cain A.V., " Waterborne and dietary hexavalent chromium exposure causes DNA-protein crosslink (DPX) formation in erythrocytes of largemouth bass (Micropterus salmoides)", Aquat. Toxicol., 78, 27-31 (2006).

14. Ahmed, A.U. and Reazuddin, M. " Industrial Pollution of Water Systems in Bangladesh", University Press Limited, Dhaka, Bangladesh pp 175-178.(2000)

15. Abdul Hannan , Md. " Studies on the interactions of Chromium (VI) with SiO_2-Iron oxide composite obtained by Sol-Gel method", M.Phil thesis,2007

16. Steven, J.D.,Davies L.J., Stanley E.K., Abbott R.A., Ihnat M., Bidstrup L., and Jaworski J.F., " Effects of chromium in the Canadian environment" Nat. Res. Coun. Canada, NRCC No. 15017. 168 pp. Avail from publications, NRCC / CNRC, Ottawa, Canada, K1A OR6.(1976)

17. Langard, S., and Norseth, T. "Chromium" Pages 383-397 in Friberg, L., Nordberg, G. F., and Vouk, V. B.,(eds). Handbook on the toxicology of metals. Elsevier/North Holland Biomedical press

18. Towill,L.E., Shriner C.R., Drury J.S, Hammons A.S., and Holleman J.W. " Review of the environmental effects of pollutants: Chromium (III)"U.S. Environment Protection Agency Rep.600/1-78-023.287pp (1979)

19. Ecological Analysts,Inc. "The source, chemistry, fate and effects of chromium in aquatic environments". Avail from American Petroleum Institute,2101 L St. N.W.,Washington, DC 20037. 207pp (1981)

20. PDF File, Biological Report 85(1.6) Contaminant Hazard Reviews January 1986 Report No.6 "Chromium Hazards to fish, wildlife and invertebrates :A synoptic review" by Ronald Eisler Patuxent wildlife research center U.S. fish and wildlife service Laurel, MD 20708

21. Taylor F.G., Jr., and Parr P.D., "Distribution of chromium in vegetation and small mammals adjacent to cooling towers". J. Tenn. Acad Sci. 53: 87-91.(1979)

22. NAS. "Medical and Biological effects of environmental pollutants. Chromium". Nat. Acad. Sci.,Div.Med.Sci.,Nat.Res.Coun.,Washington,DC.155 pp (1974)

23. Snyder,J.D., Davies L.J., Stanley E.K., Abbott R.A., Ihnat M., Bidstrup L., and Jaworski J.F. "Effects of chromium in the Canadian environment". Nat. Res.

Coun. Canada, NRCC No.15017.168 pp. Avail. From Publications, NRCC/CNRC, Ottawa,Canada,K1A OR6 (1976)

24. Post, M.A.., and Campbell P.G. " Lead chromate pigments-a literature survey on environmental and toxic effects". U.S. Dep. Comm. Nat. Bur. Stand. Rep. NBSIR 80-1974.38pp.(1980.)

25. Hatherill,J.R. "A review of the mutagenicity of chromium." Drug Chem. Toxicol. 4:185-195 (1981.)

26. Gang. D. , Banerji, S. K. , and Clevenger, T. E.. " Chromium (VI) removal by modified PVP coated silica gel". Department of Civil and Environment Engineering, University of Missouri-Columbia, Columbia, MO 65211.

27. Smith,R.G. and Lee. D.H.K.. "Chromium in Metallic Contaminants and Human Health". Academic Press New York (1972)

28. Dupont,L., Guillon,E.,. "Removal of hexavalent chromium with a lignocellusic substrate extracted from wheat bran". Environ.Sci.Technol.37,4235-4241(2003)

29. Ouki,S.K.,Neufeld,R.D.," Use of activated carbon for recovery of chromium from industrial wastewaters" J.Chem.Technol-Biotechnol.70,3-8 (1997)

30. Ayuso,E.A.,Sanchez,A.G.,Querol,X., "Purification of metal electroplating wastewaters using zeolites." Water Res. 37,4855-4862 (2003)

31. Jashim Uddin M., Miron M. S. and Mollah M. Y. A., " Removal of chromium (VI) from wastewater by electro reduction and coagulation" J. Sandi Chem Sol. 11 (3), 457 -464 (2007).

32. Agency for Toxic Substances and Disease Registry (ATSDR) . "Toxicological profile for chromium". U.S. Department of Health and Human Services. Public Health Service (1993)

33. Agency for Toxic Substances and Disease Registry (ATSDR) . "Toxicological profile for chromium". (Update) U.S. Department of Health and Human Services. Public Health Service (1998)

34. Zhang and Li, Zhang, J, Li,X "Chromium pollution of soil and water in Jinzhou". Journal of Chinese Preventive Medicine 21, 262-264 (1987)

35. The California safe Drinking Water and Toxic Enforcement Act of 1986.

36. IARC (1990). IARC. "Monographs on the Evaluation of the Carcinogenic Risk of Chemicals to Humans: Chromium, Nickel and welding", Vol.49,International Agency for Research on Cancer, World Health Organization, Lyon, France. Jackson to Steven A. Book. June11,1991

37. U.S. EPA . "Chromium (VI) Integrated Risk Information System (IRIS)" (http//www.epa.gov/iris)(1998b)

38. Langard S. and Norseth T., Br. J. Ind. Med. 32, 62-65,(1975)

39. ACGIH, "Documentation of Threshold Limit Values", 4th edn. American Conference on Governmental Industrial Hygienists Ink. Cincinnati, OH,1980.

40. Cohen et al ; Cohen, MD., Kargacin, B., Klein, CB., Costa,M., "Mechanisms of Chromium carcinogenicity and toxicity" Critical Reviews in Toxicology 23,255-281(1993)

41. Costa, M "Toxicity and anticarcinogenicity of Cr(VI) in animal models and humans". Critical Reviews in Toxicology 27,431-442 (1997)

42. www.me.vccs.edu

43. Mojdeh Owlad & Mohamed Kheireddine Aroua & Wan Ashri Wan Daud & Saeid Baroutian "Removal of Hexavalent Chromium-Contaminated Water and Wastewater: A Review" Water Air and Soil Pollution, Vol. 200, No. 1-4, P 59-77 (2008)

44. Gode F. and Pehlivan E., "Removal of chromium from aqueous solutions using Lewatit S 100: The effect of pH, time, metal concentration and temperature", Journal of Hazardous Materials, vol. 2, no.136, pp.330-337, (2006)

45. Hintermeyer B.H., Lacour N.A., Perezpadilla A., and Tavani E.L., "Separation of the chromium(III) present in a tanning waste water by means of precipitation,

reverse osmosis and adsorption" Latin American Applied Research, vol.38, pp.63- 71, (2008)

46. Bernnardo G.R.R, Jose Rene R.M and Catalina A.D.T, "Chromium (III) uptake by agro- waste Biosorbents : Chemical characterisation, sorption-desorption studies and mechanism", Journal of Hazardous Materials, vol. 170, no.2-3, pp.:845-854, (2009)

47. Cassano A., Drioli1v E., Molinaril R., and Bertolutti C., "Quality improvement of recycled chromium in the tanning operation by membrane processes", Desalination, vol.108, pp.193-203, (1996.)

48. Radwan A. Al-Rasheed, "Water treatment by heterogeneous photo-catalysis as overview", Presented at 4th SWCC Acquired Experience Symposium held in Jeddah, 2005.

49. Babel, S., & Kurniawan, T. A. "Low-cost adsorbents for heavy metals uptake from contaminated water: a review". Journal of Hazardous Materials, 97(1–3), 219–243. (2003)

50. Aggarwal, D., Goyal, M., & Bansal, R. C. "Adsorption of chromium by activated carbon from aqueous solution." Carbon, 37(12), 1989–1997.

51. Ahalya, N., Ramachandra, T. V., & Kanamadi, R. D. "Biosorption of heavy metals". Research Journal of Chemistry and Environment, 7(4), 71–79. (2003).

52. Chaudry, M. A., Ahmad, S., & Malik, M. T. "Supported liquid membrane (SLM) technique applicability for the speciation of chromium from tannery wastes". Waste Management (New York, N.Y.), 17(4), 211–218. (1997).

53. (a) High strength composite , Pichai Rusmee ; (b) www. Substech.com ;

(c) www. Virginia . edu ; (d) www. Efunda.com ; (e) Prof. P.C. Pandey ,

Composite material, web based course

54. Yu, M., Tarnopolskii, T. Kincis, Handbook of Composites, vol.3, Institute of Polymer Mechanics, Vatvian S.S.R., p. 266.

55. Pedro Henrique Cury Camargo; Kestur Gundappa Satyanarayana; Fernando Wypych "Nanocomposites: synthesis, structure, properties and new application opportunities", Mat. Res. vol.12 no.1 São Carlos Jan./Mar. 2009

56. Roy R, Roy RA, Roy DM. "Alternative perspectives on "quasi-crystallinity": non-uniformity and nanocomposites". *Materials Letters*. 4(8-9):323-328.(1986)

57. Schmidt D, Shah D, Giannelis EP. "New advances in polymer/layered silicate nanocomposites". Current Opinion in Solid State & Materials Science. 6(3):205-212 (2002).

58. Gleiter H. " Materials with ultrafine microstructures: retrospectives and perspectives". Nanostructured Materials. 1(1):1-19.(1992)

59. Michail O. Danilov and Gennady Ya. Kolbasov "Electrochemical method for the preparation of nanocomposites based on carbon nanotubes and chromium oxides for oxygen electrodes " Journal of Solid State Electrochemistry ; Volume 14, Number 12, 2169-2172,

60. Yan X.B., Tay B.K., Chen G. , Yang S.R. "Synthesis of silicon carbide nitride nanocomposite films by a simple electrochemical method" Electrochemistry Communications 8 737–740 (2006)

61. Maria Zaharescu, Maria Crisan, Jitianu A. And Crisan D. " Sio_2 – Iron oxide Composites obtained by Sol-gel method "Institute of Physical Chemistry, Romanian Academy, Splaiul Independentei 202, Bucharest, Romania.

62. Bradly J.Clapsaddle, Alexander E.Gash, Joe H.Sacher, Jr. and Randall L Simpson. "Silicon oxide in an iron (III) oxide matrix : the sol-gel synthesis and characterization of Fe-Si mixed oxide nanocomposites that contain iron oxide as the major phase" Lawrence Livermore National Laboratory, Chemistry and Material science, Directorate and Energetic Materials Centre, P.O. Box 808, L-092, Livermore, CA 94550, USA

63. Predoia, R. Cléracb, A. Jitianuc, M. Zaharescuc, M. Crisanc, M. Raileanue " Study of $FeO\text{-}SiO_2$ nanoparticles by sol-gel synthesis" Digest Journal of Nanomaterials and Biostructures Vol. 1, No. 3, p. 93 – 97 (2006)

64. www.gelest.com

65. Brinker, C.J.; G.W. Scherer (1990). Sol-Gel Science: The Physics and Chemistry of Sol-Gel Processing. Academic Press. ISBN 0121349705.

66. Hench, L.L.; J.K. West (1990). "The Sol-Gel Process". Chemical Reviews 90: 33.

67. Klein, L. (1994). Sol-Gel Optics: Processing and Applications. Springer Verlag. ISBN 0792394240.

68. Wright, J.D. and Sommerdijk, N.A.J.M., Sol-Gel Materials: Chemistry and Applications

69. (a) www.allprojectreports.com ; (b) www.xamlified.com ; (c) www.old.iupac.org ; (d) Lecture in the course “Surface Physics and nano physics”, By Bo Hellsing , Department of Physics, Göteborg University 2008 ; (e) www.NJIT.edu / PIERO. M. ARMENANTE ; (f) www . Sussex.ac.uk / Dr. Mark Osborne

70. Surfaces and Interfaces of Solid Materials by H. Lüth, Springer-Verlag page 489-498 (1995)

71. Oura K. et al., Surface Science, An Introduction. Berlin: Springer, ISBN 978-3-540-00545-2. (2003)

72. Oura, K.; Lifshits V. G.; Saranin A. A.; Zotov A. V.; Katayama M. Surface Science, An Introduction. Berlin: Springer. ISBN 3540005455.(2003)

73. Principles of Adsorption and Reaction on Solid Surfaces. Wiley Inter science. pp. 240. ISBN 0-471-30392-5.(1996)

74. Brunauer, Emmett and Teller , J. Am. Chem. Soc 60,309

75. www.chem.qmul.ac.uk

76. (a) www. Gasmet.fi ; (b) www. Chem..orst.edu ; (c) www. Wcaslab.com

77. www. Xraydiffraction.com

78. (a) www. Portal.tugraz.at (b) www. Serc.carleton.edu (c) www. Unl.edu (d) www.mos.org (e) www. Academic.udayton.edu

79. (a) www. Anasys.co.uk (b) E. Post , NETZSCH (c) www . siint . com

80. Albino Kumar P., Manabendra Ray and Saswati Chakraborty "Hexavalent chromium removal from wastewater using aniline formaldehyde condensate coated silica gel" , Journal of Hazardous Materials, Vol. 143, issues 1-2, page 24-32 ,8 May 2007

81. Sangkorn Kongjao, Somsak Damronglerd and Mali Hunsom "Simultaneous removal of chromium and organic pollutants in tannery wastewater by electroprecipitation technique", Journal Korean Journal of Chemical Engineering Issue Volume 24, Number 5 / September, 2007

82. Bailey R.P., Bennet T. and Benjamin M.M., Wat. Sci.Tech.Vol.26,No.5-6,pp.1239-1244,(1992)

83. Borai E. H., El-Dessouky S. I. and Hassan H. S. "Mixed silica and alumina hosted carboxylate oxide for removal of chromium species from wastewater ", Adsorption Vol. 13, Number 1, 61-71, (2007)

84. Mansoor Anbia and Nourali Mohammadi "A fast and efficient method for the removal of hexavalent chromium from aqueous solutions " Journal of Porous Materials Volume 18, Number 1,13-21,(2011)

85. Samani MR, Borghei SM, Olad A, Chaichi MJ "Removal of chromium from aqueous solution using polyaniline--poly ethylene glycol composite ", J Hazard Mater. Vol. 15; p 248-254 (2010).

86. Gupta V.K. , Shilpi Agarwal, Tawfik A. Saleh " Chromium removal by combining the magnetic properties of iron oxide with adsorption properties of carbon nanotubes" Water research,Vol.1,1-6 (2011)

87. Veera M. Boddu, Krishnaiah Abburi,Jonathan L. Talbott,and Edgar D. Smith " Removal of Hexavalent Chromium from Wastewater Using a New Composite Chitosan Biosorbent" *Environ. Sci. Technol.*,37 (19), pp 4449–4456 (2003)

88. Eisazadeh, H. "Removal of chromium from waste water using poly-aniline". Journal of Applied Polymer Science, 104: 1964–1967, (2007)

89. Guti´errez N., Ramos E., and Contreras C. “Removal of chromium (VI) from aqueous solutions by hydrotalcite-like compounds: kinetic and equilibrium studies ” Revista Mexicana De F´ISICA S 55 (1) 135–138, (2009)

90. Sharma, Y. C., Srivastava, V., Weng, C. H. and Upadhyay, S. “Removal of Cr(VI) from wastewater by adsorption on iron nanoparticles” The Canadian Journal of Chemical Engineering, Volume 87, Issue 6, pages 921–929, (2009)

91. Carnizello A. P., Marcal L., Calefi P. S., Nassar E. J., Ciuffi K. J., Trujillano R., Vicente M. A., Korili S. A. and Gil A. “Takovite−Aluminosilicate Nanocomposite as Adsorbent for Removal of Cr(III) and Pb(II) from Aqueous Solutions” *J. Chem. Eng. Data*, 54 (2), pp 241–247 (2009)

92. Langkam, Johny “Removal of Chromium (VI) from water by using Lanthanum based Hybrid Materials” *MSc thesis by*, National Institute of Technology, Rourkela (2011)

93. Santhana Krishna Kumer A., Kalidhasan S., Vidya Rajesh and Rajesh N., “ Application of Cellulose-Clay Composite Biosorbent toward the effective Adsorption and Removal of Chromium from Industrial Wastewater”, *Ind. Eng. Chem. Res.*, 2012, 51(1),pp58-69

94. Alejandra Pérez-Fonseca A., Cesar Gómez, Haydeé Dávila, and Rubén González-Núñez, “ Chitosen Supported onto gave Fiber—Postconsumer HDPE Composites for Cr(VI) Adsorption”, *Ind. Eng. Chem. Res.*,: October 13, 2011

95. M. Cieslak-Golonka, “ Toxic and mutagenic effects of Chromium (VI) , A review”, Polyhedron , Vol.15, page 3667-3675, Aug.1996

96. Piccaluga G., Corrias A., Ennas G., Musinu A., “ The Sol-Gel Method: Choice of the experimental conditions”, Materials Science Foundations, Vol.13

97. Ahmed,O.,Biswas,P.,and Mollah,M.Y.A., “ Electrochemical Degradation Of Malachite Green(MG) in an Electrocoagulation (EC) cell using iron as sacrificial electrode”, Dhaka Univ.J.Sci.,52(2),249(2003)

98. SMEW, 1985: Standard Methods for the Examination of water and wastewater, A.M. Public Health Association, 15th Ed. P426-429, 1985

99. Lenza. R.F.S., Vasconcelos W.L. " FT-IR of Silicon (IV) oxide" Mat. Res.4(3) (2001)

100. (a) Schwertmann U., and Cornell R.M., Iron oxides in the laboratory. VCH, Publ., Weinheim-New York-Basel-Cambridge. 1991, 5-60pp

(b) Schwertmann U., and Murad E., Clays clay Min. 1983, 31, 277

101. Keiser J.T., Brown C.W.,Heidersbach R.H.,J.Electrochem Soc., 129,2686 (1982)

102. Mohammed Jasim uddin, Muhammed Shah Miran and Mohammad Yousuf Ali Mollah " Electrochemical Synthesis and characterization of iron oxyhydroxide" Journal of the Bangladesh Chemical Society, 20(1),39-45,2007

103. Meera Basa, "Synthesis & Characterization of Silica Coated Iron oxide Nanoparticles by Sol-Gel Technique" M.Sc. Thesis, National institute of Technology, Rourkela (2007)

104. Tabatabaei,S., Shukohfar, A.,Aghababazadeh,R.,Mirhabibi,A., "Experimental study of the synthesis and characterisation of silica nanoparticles via the sol-gel method" Journal of Physics: Conference Series 26 (2006) 371–374

105. Raileanu, M., Crisan, Petrache C., Crisan D., Zaharescu M. "Fe_2O_3-SiO_2 Nanocomposites obtained by different sol-gel routes" Journal of Optoelectronics and Advanced Materials Vol. 5, No. 3, p. 693 – 698 (2003)

106. Qingyin Wu, "Preparation and proton-conductibility of silica gel containing 64 wt.% undecatungstocobaltoaluminic heteropoly acid", Materials Letters , 56 , 19– 23 (2002)

107. Balek,V.,Subrt,J., " Thermal behaviour of iron (III) oxy hydroxide", Pure&App. Chem., Vol. 67, No. 11, pp. 1839-1842, 1995.

108. Guido Ennas, Maria F. Casula, SergioMarras, Gabriele Navarra, Alessandra Scano, and GiaimeMarongiu "Characterisation of FeOOH Nanoparticles and Amorphous Silica Matrix in an FeOOH-SiO_2 Nanocomposite" Journal of Nanomaterials Volume 2008, Article ID 361816

109. Palomares, S.A. , Anchez, S., Ponce-Castaneda, S. , Mart_ınez, J.R., Facundo Ruiz ,Yurii Chumakov, Dom_ınguez, O. , "Quantitative analysis of iron oxide particles Embedded in an amorphous xerogel matrix" Journal of Non-Crystalline Solids 325 251–257 (2003)

110. Singh,D.B.,Prasad,G.,Rupainwar,D.C.,and Singh,V.N. "As(III) removal from aqueous solution by adsorption" Water,Air Soil Pollut.,42,373-86

111. Weber,W.J.& Morris,J.C., " Kinetics of adsorption on carbon from solution", J.San. Eng. Div.,ASCE,89(SA2),31-39

112. Singh,A.K.,Singh,D.P.,Panday,K.K., & Singh,V.N., " Wollastonite as adsorbrnt for removal of Fe(II) from water", J.Chem.Tech.Biotechnol.,42,39-49